Indirect Damage Due to High Intensity Beams

John Seeman
SLAC National Accelerator Laboratory
US-PAS
January 25, 2017

U.S. DEPARTMENT OF ENERGY
Office of Science

SLAC NATIONAL ACCELERATOR LABORATORY

Abstract

Past (future) e+e- colliders have (will) operate(d) with many bunches, short bunch lengths, small emittances, high currents, and small interaction point betas. The various beam requirements and techniques will be discussed with using PEP-II observations as a starting point. The stored beam has a lot of power stored and also high power radiated and then replenished.

Indirect Damage: High Intensity Beams

Head load and damage by electromagnetic fields

Mechanisms of heating of components (with examples)

Risks for the RF system

Damage by synchrotron radiation

Damage to undulators (PETRA-III, LCLS, etc)

How to avoid damage

Instrumentation to make the accelerator safe(r)

Thanks for inputs

Inputs from:

A. Fisher

W. Kozanecki

N. Kurita

M. Nordby

A. Novokhatski

M. Sullivan

M. Weaver

U. Wienands

Collider High Power Topics from PEP-II and other Rings

Beam parameter overview:

Beam position (single pass and orbit)

Beam size

Bunch length

IP luminous size

HOM measurements

Bunch transverse instabilities

Bunch longitudinal instabilities

Chamber temperature

Backgrounds (detector)

Beam loss rates

Beam abort timing system

Chamber temperature

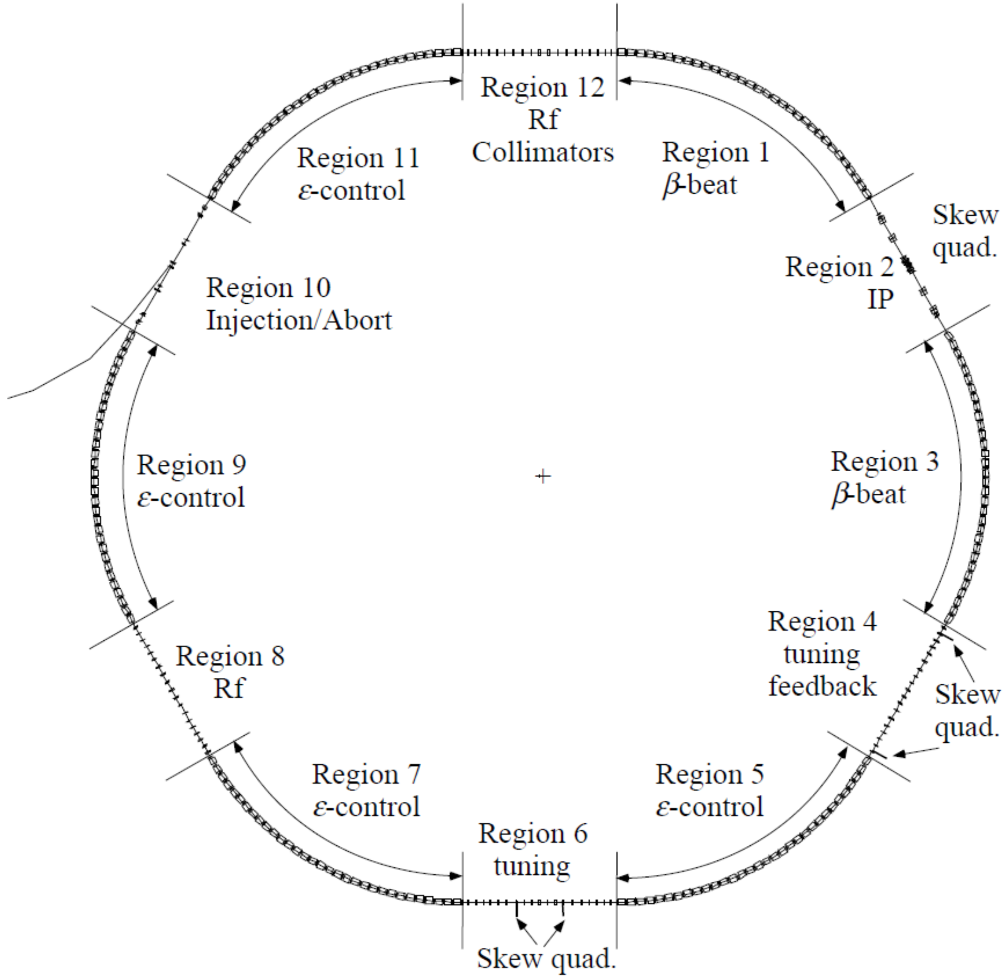

Figure 2. HER Layout

PEP-II Construction and Project Management

PEP-II was constructed by SLAC, LBNL, and LLNL with help from BINP, IHEP, BaBar collaboration.

Many thanks to the
US Department of Energy
and members of the
Machine Advisory Committee.

Design of a collider: Plan for options

SLAC

- For an asymmetric collider

Tune shift

Collision frequency

Bunch charges

With limited vertical tune shift using energy transparency conditions

$$\mathcal{L} = \frac{\gamma_{cm}}{4r_e}\,\xi f_c \left(1+\frac{\sigma_y^*}{\sigma_x^*}\right)\left(\frac{N_L}{\beta_{yL}^*}\frac{N_H}{\beta_{yH}^*}\right)^{1/2} = 2.17\mathrm{x}10^{34}(1+R)\,n\,\xi_y\left(\frac{EI_b}{\beta_y^*}\right)\mathrm{cm}^{-2}\mathrm{s}^{-1}$$

Ratio of beam widths at the interaction point

Beta functions at the interaction point

(cm, A, GeV)

- To get to the required luminosity range:
  - I= several amps
  - β_y* ~ cm
  - ξ ~ .05 or larger
  - Round beams? No! Lattice and IR difficult, high backgrounds

PEP-II Parameters for 3.1 GeV x 9.0 GeV

Parameter	Units	Design	April 2008 Best	2008 Potential
I+	mA	2140	3210	3700
I-	mA	750	2070	2200
Number bunches		1658	1722	1740
β_y*	mm	15-25	9-10	8.5
Bunch length	mm	15	11-12	9
ξ_y		0.03	0.05-0.06	0.07
Luminosity	$x10^{33}$	3	12	20
Int lumi / day	pb^{-1}	130	911	1300

4 times design **7 times design**

KEKB and SuperKEKB Beam Parameters

		KEKB		Nano-beam	
		LER	**HER**	**LER**	**HER**
Energy	GeV	3.5	8	4	7
Beam current	A	1.8	1.4	3.60	2.62
Bunch length	mm	6~7	6~7	6	5
No. bunches		1584		2503	
Energy loss/turn	MV	1.64	3.48	2.15	2.50
Radiation Loss	MW	2.95	4.87	7.74	6.55
Loss factor, assumed	V/pC	-	-	35	40
Parasitic Loss	MW	-	-	1.82	1.10
Total Beam Power	MW	~ 3.5	~ 5.0	9.56	7.65
RF Voltage	MV	8.0	13~15	8.4	6.7

JLEIC Parameters (future)

		strong cooling	
		p	e
Beam energy	GeV	100	5
Collision frequency	MHz	476	
Particles per bunch	10^{10}	0.98	3.7
Beam current	A	0.75	2.82
Polarization		>70%	>70%
Bunch length, rms	cm	1.2	1.2
Norm. emittance, x/y	µm	0.5 / 0.1	70 / 14
x/y β*	cm	6 / 1.2	4 / 0.8
Vert. beam-beam param.		0.015	0.053
Laslett tune shift		0.048	small
Detector space, up/down **For full-acceptance detector**	m	3.6 / 7	2.4 / 1.6
Hourglass (HG) reduction		0.80	
Lumi./IP, w/HG, 10^{33}	**$cm^{-2}s^{-1}$**	**19.5**	

Lumi with weak cooling **4.6 x 10^{33} $cm^{-2}s^{-1}$**

Lumi without bunched beam cooling **~1 x 10^{33} $cm^{-2}s^{-1}$**

Future High Energy e+e- Collider Parameters

SLAC

parameter	FCC-ee (100 km)			CEPC (54 km)	LEP2 (27 km)
energy/beam [GeV]	**45**	**120**	**175**	**120**	105
bunches/beam	90000	770	78	50	4
beam current [mA]	1450	30	6.6	16.6	3
luminosity/IP x 10^{34} $cm^{-2}s^{-1}$	**70**	**5**	**1.3**	**2.0**	0.0012
energy loss/turn [GeV]	0.03	1.67	7.55	3.1	3.34
synchrotron power [MW]	100			103	22
RF voltage [GV]	0.08	3.0	10	6.9	3.5

FCC-ee: 2 separate rings & 2 IPs

CEPC: single beam pipe version

Synchrotron Radiation Monitor

Extraction of SR light

Size measurements

Bunch length measurements

The PEP-II Collider

PEP-II: Exit for synchrotron light to measurement table

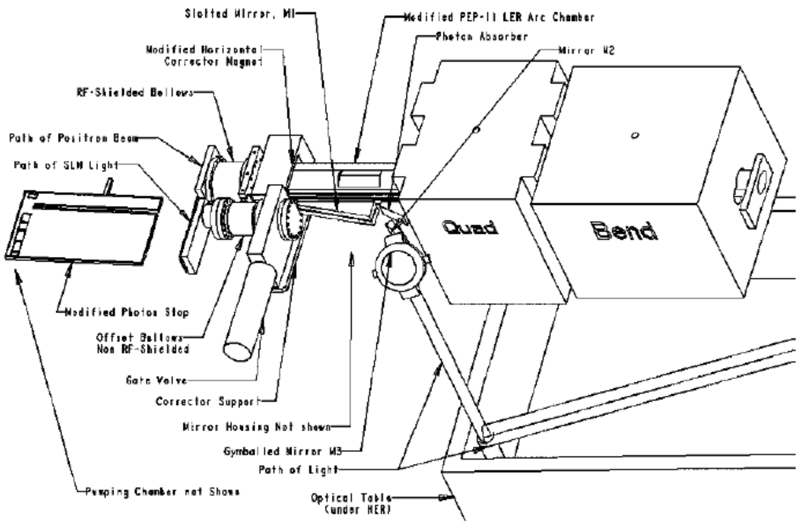

Figure 3. The LER synchrotron-light monitor, showing the modified photon stop and the slotted first mirror.

Parameter	HER	LER
Circumference [m]	2199.318	
Revolution time [µs]	7.336	
RF frequency [MHz]	476	
Harmonic number	3492	
Number of full buckets	1658	
Bunch separation [ns]	4.20	
Nominal current [A]	0.99	2.16
Maximum current [A]	3	3
Nominal energy [GeV]	9.01	3.10
Maximum energy [GeV]	12 (at 1 A)	3.5
Bend radius in arc dipoles [m]	165	13.75
Critical energy in dipoles [keV]	9.80	4.83

PEP-II Synchrotron Light Optics for Beam Size Measurements

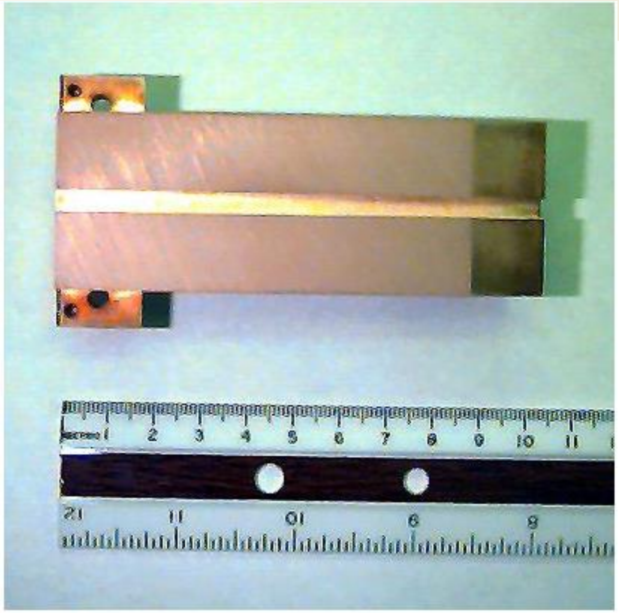

af_007 Synechroton Light Monitor Optics 8-19-97

JS_141 LER Synchrotron Light Monitor 10/26/98

AF_005 Synchtotron Light Monitor Optics 8-19-97

Synchrotron light monitor

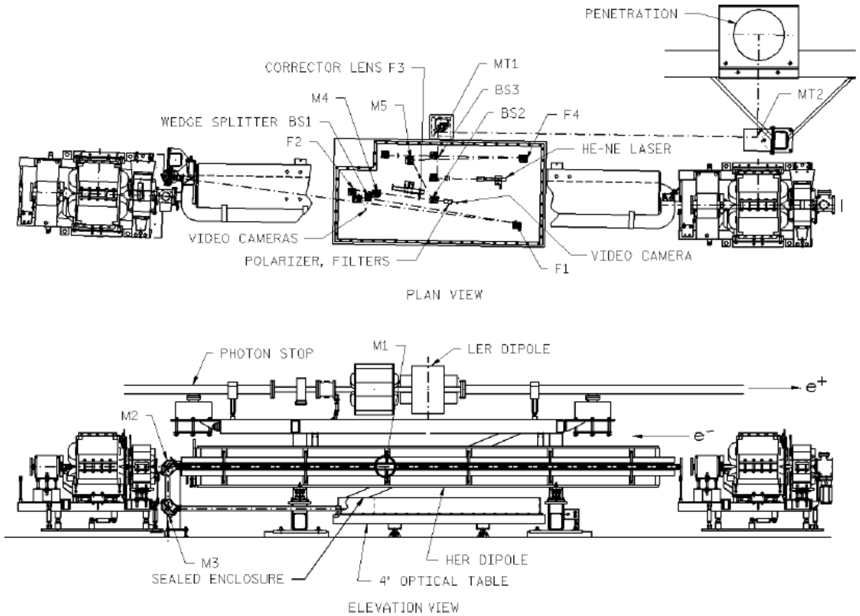

Figure 1. HER and LER beamlines in mid-arc, showing path of the HER synchrotron light and the optical table under the HER dipole.

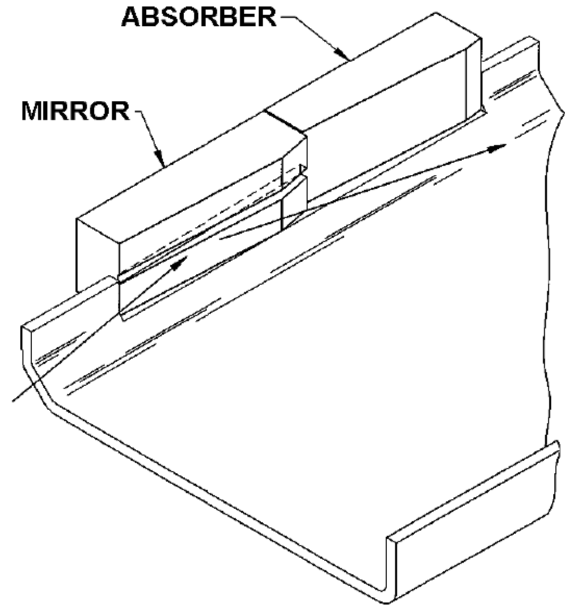

Figure 2. The slotted first mirror and the x-ray absorber, both mounted in the wall

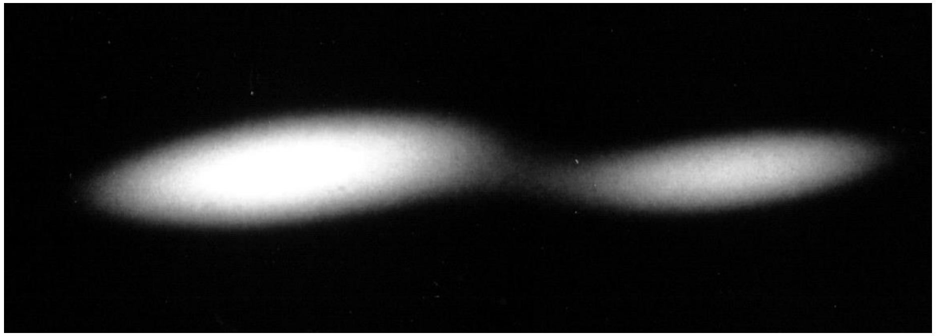

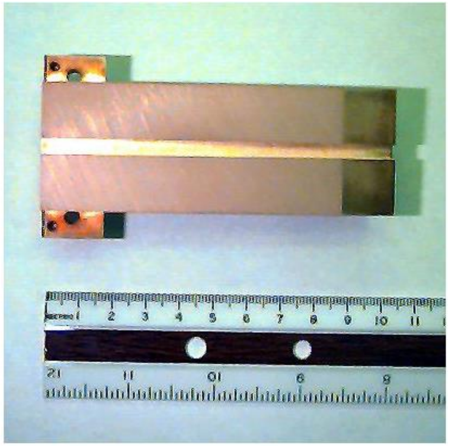

af_007 Synechroton Light Monitor Optics 8-19-97

Streak camera: LER bunch length versus current

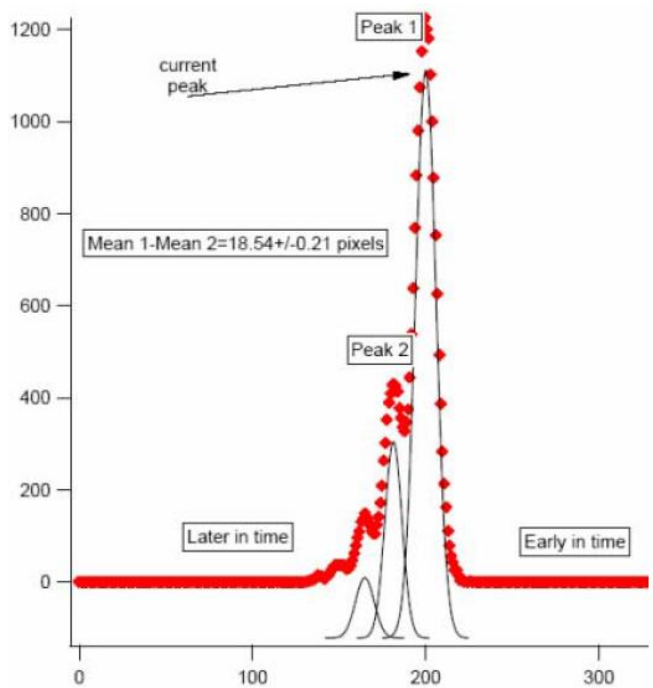

Figure 1: A streak-camera image of a light pulse transmitted through the etalon, projected onto the camera's time axis (intensity vs. pixel number). The distance between reflections provides a calibration.

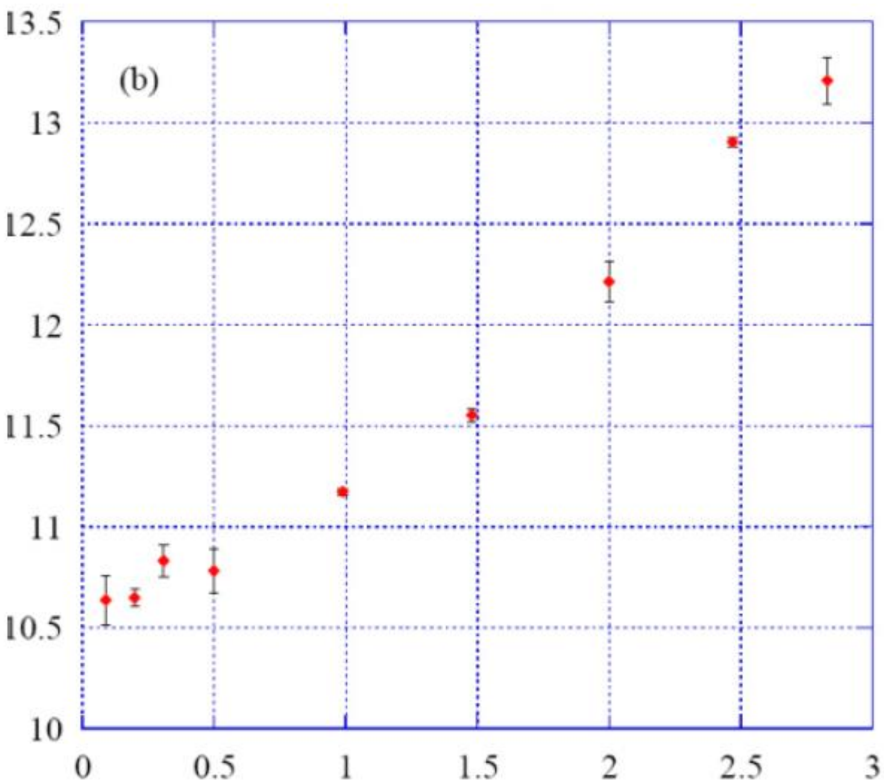

Figure 2: Streak-camera measurements of LER bunch length (mm) vs. current (mA).

LER bunch length versus bunch number in train

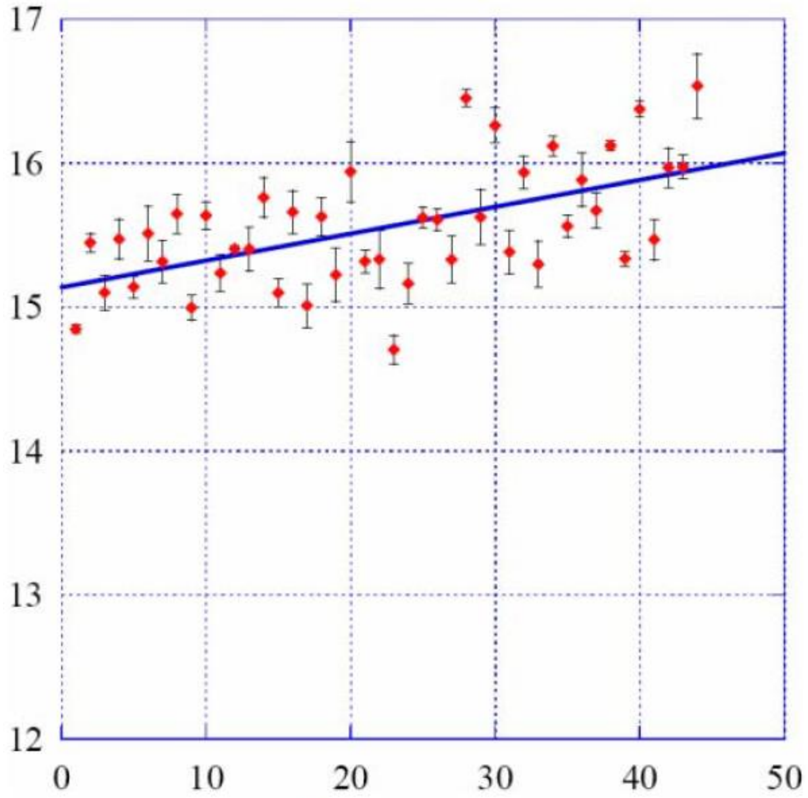

Figure 4: Streak-camera measurements of LER bunch length (mm) vs. bunch number along the 20th bunch train. 1.4 mA/bunch and 3.8 MV.

PEP-II Beam Position Measurements (single pass and orbit)

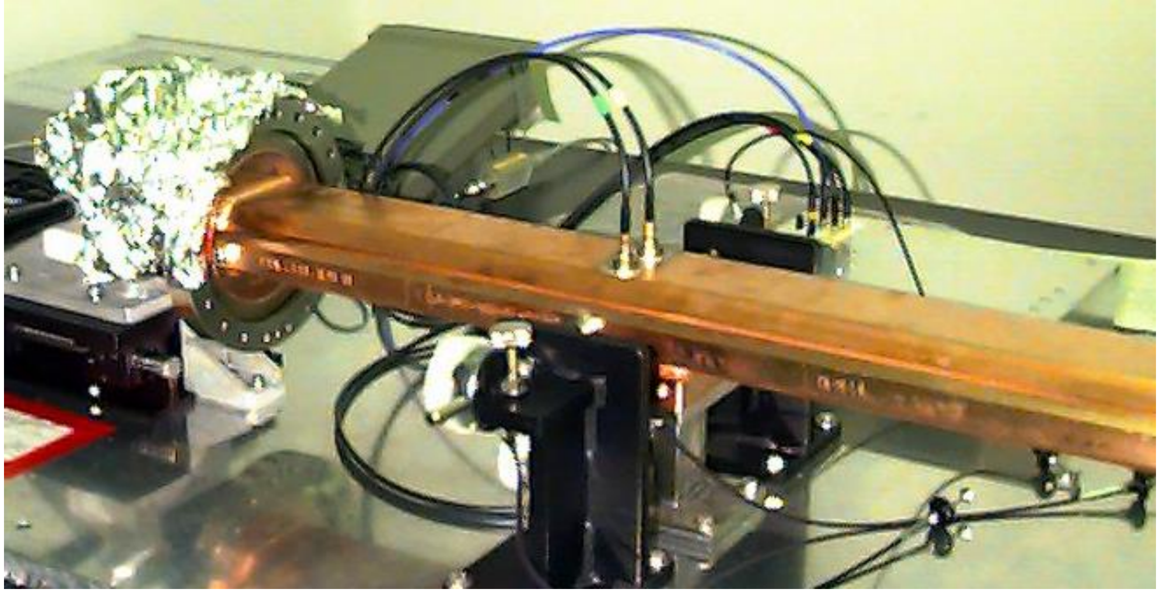

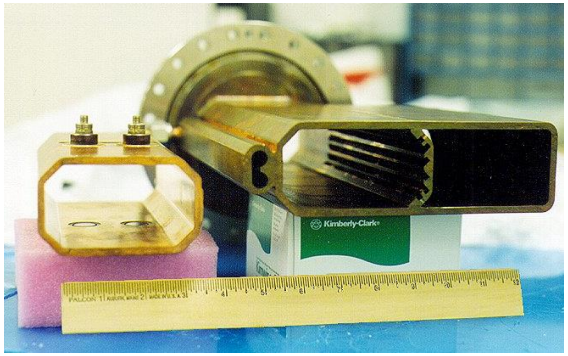

PEP-II BPM buttons and
HER copper vacuum chamber

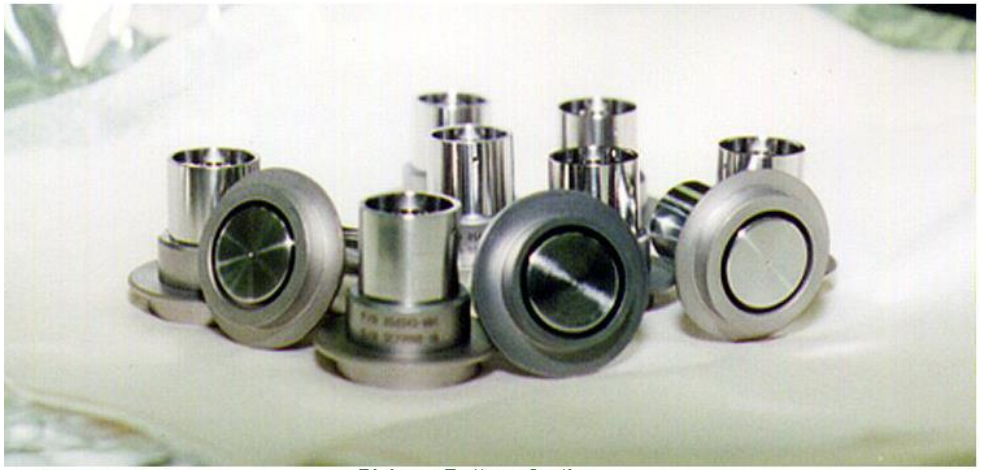

AF_002 Pick-up Buttons for the Beam-Position Monitors 8-19-97

BPM – Complicated design

Thermal models

- Goal
  - Predict acceptable temperatures
  - Power
  - Match experimental measurements
- Difficulties
  - Boundary conditions unclear
    - Where does the power go?
    - Contact between button and housing
    - Radiation calculations

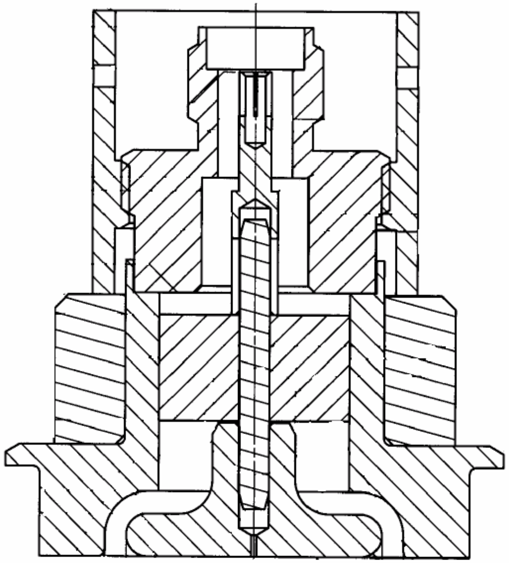

Higher Order Modes (HOM) Heating

Beam interaction with the vacuum chambers

HOM Movie

HOM generation

HOM heating

SLAC

Main HOM sources

RF cavities: narrow band impedance.

Resistive-wall wake fields

Complicated geometry of Interaction Region (IR)

Beam chamber elements: kickers, collimators, bellows, BPMs, distributed pumps, …

HOM Power Consequences

- Heating of the vacuum elements
  - Temperature and vacuum rise
  - Chamber deformations and vacuum leaks
  - Decreasing the pumping speed
  - Outgassing
- Multipacting, sparking and breakdowns
  - Vacuum leaks
  - Melting thin shielded fingers
  - Longitudinal instabilities
  - High backgrounds (high radiation level in the detector)
- Electromagnetic waves outside vacuum chamber
  - Interaction with sensitive electronics

HOM Calculations

Movie of HOMs for PEP-II bellows unit by A. Novokhatski

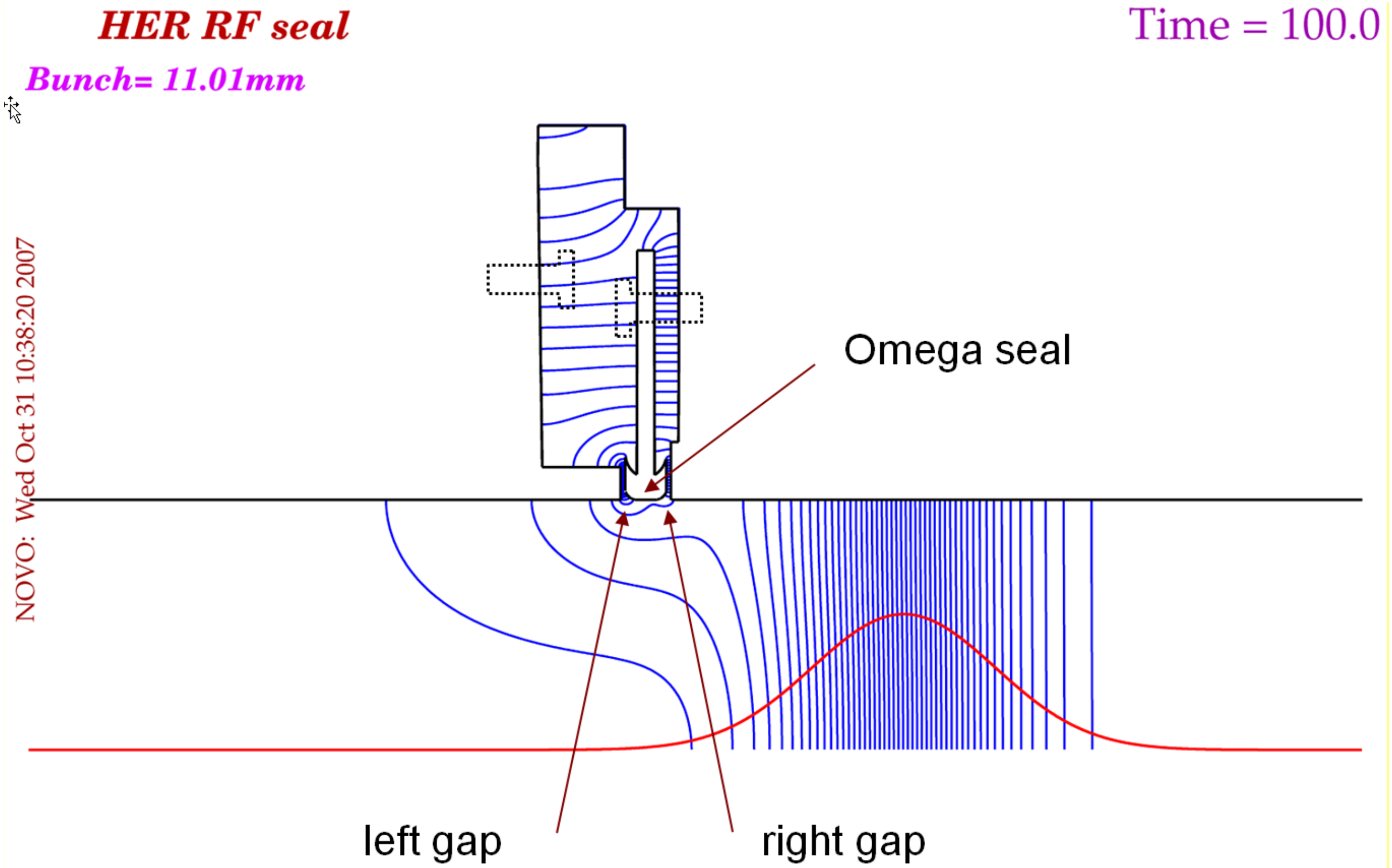

Expected HOM Power

A. Novokhatski

	LER 2900 mA	HER 1800 mA
Vacuum element	**Power [KW]**	**Power [KW]**
RF cavities	63.46	76.16
Collimators	18.11	16.7
Kickers	17.3	6.08
Screens	1.24	5.5
BPMs	9.4	3.6
IR wakes	13.66	5.26
Resistive wall	71.74	36.15
Total power	**195**	**167**
Measured power	**210**	**298**

HER synchrotron and HOM power losses

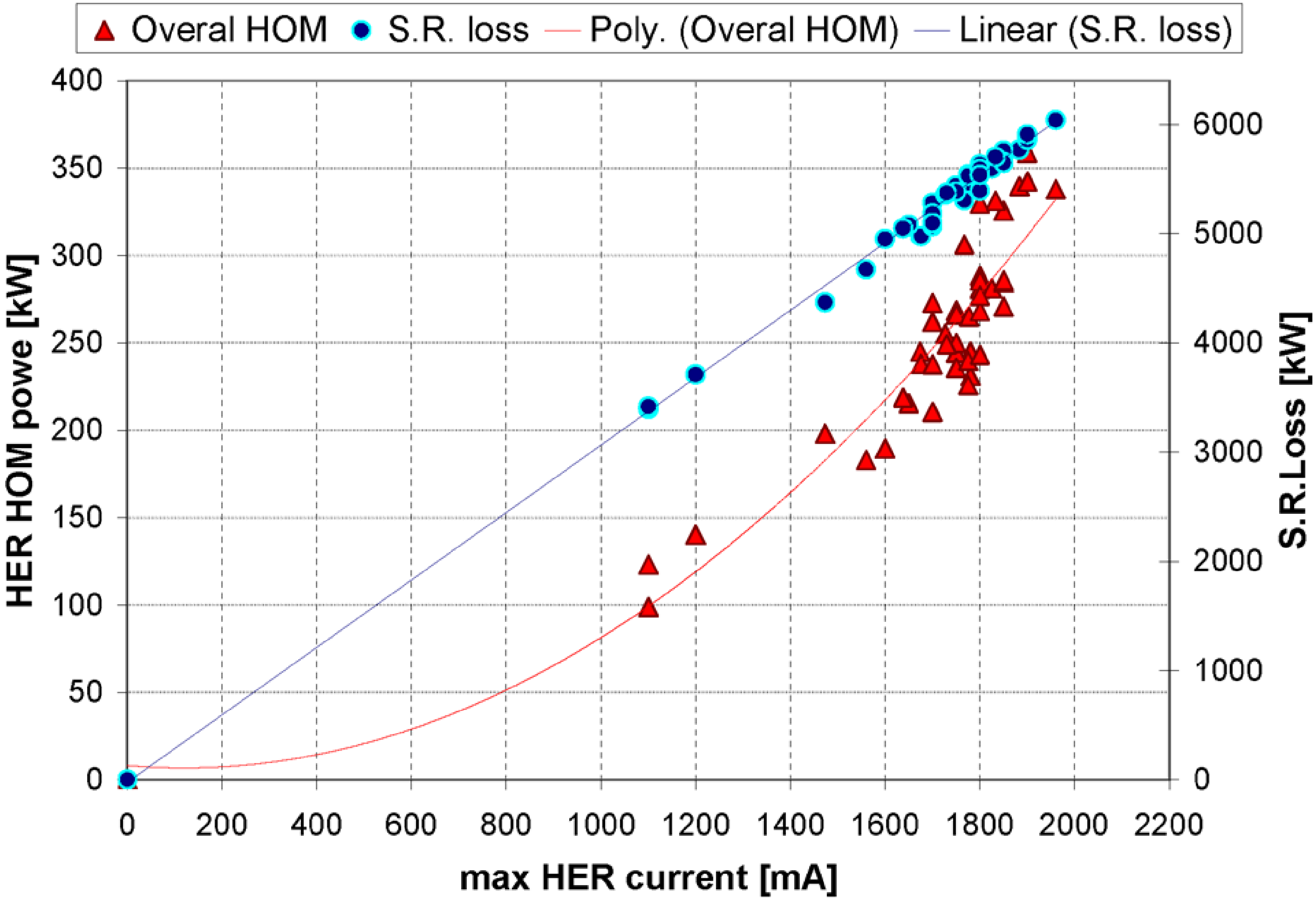

PEP-II first turns in HER : Beam Position Monitors

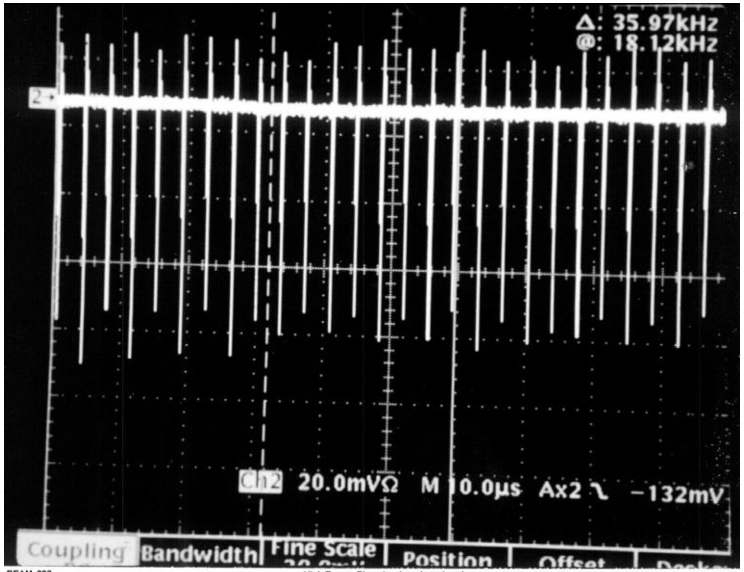

BEAM_003 High Energy Ring - two bunches stored 6-17-97

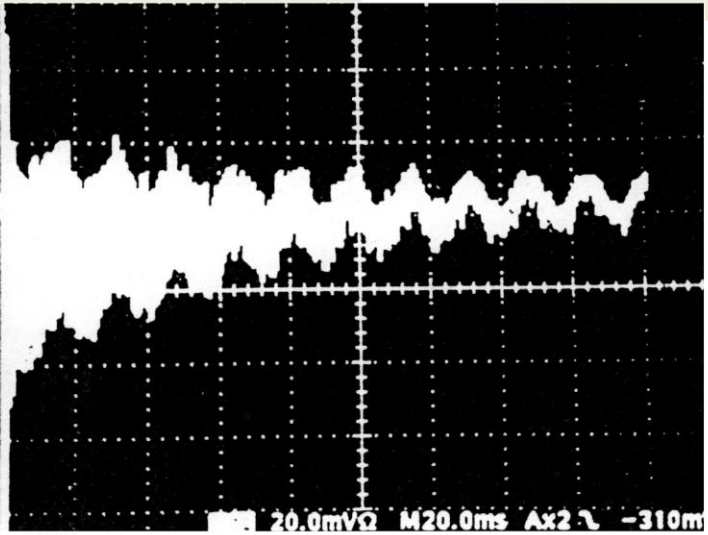

24500trn HER Beam envelope 24500 turns 8-19-97

Two bunches in HER

Injection stacking

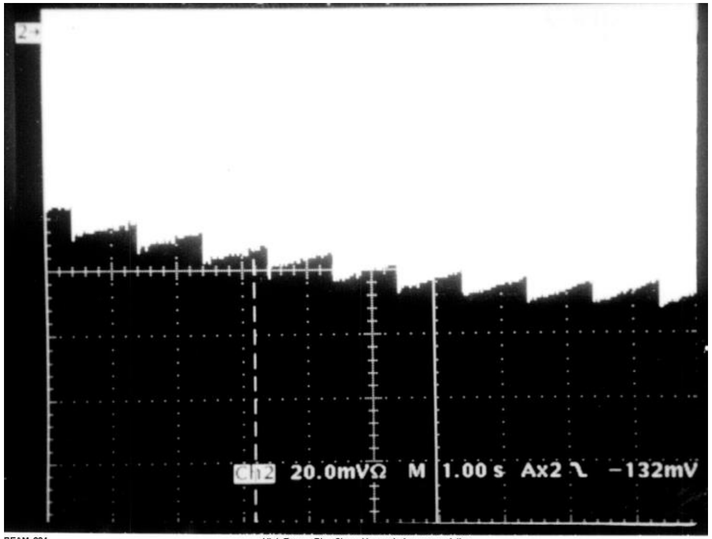

BEAM_004 High Energy Ring Shored beam during accumulation 6-17-97

PEP-II bunch train pattern

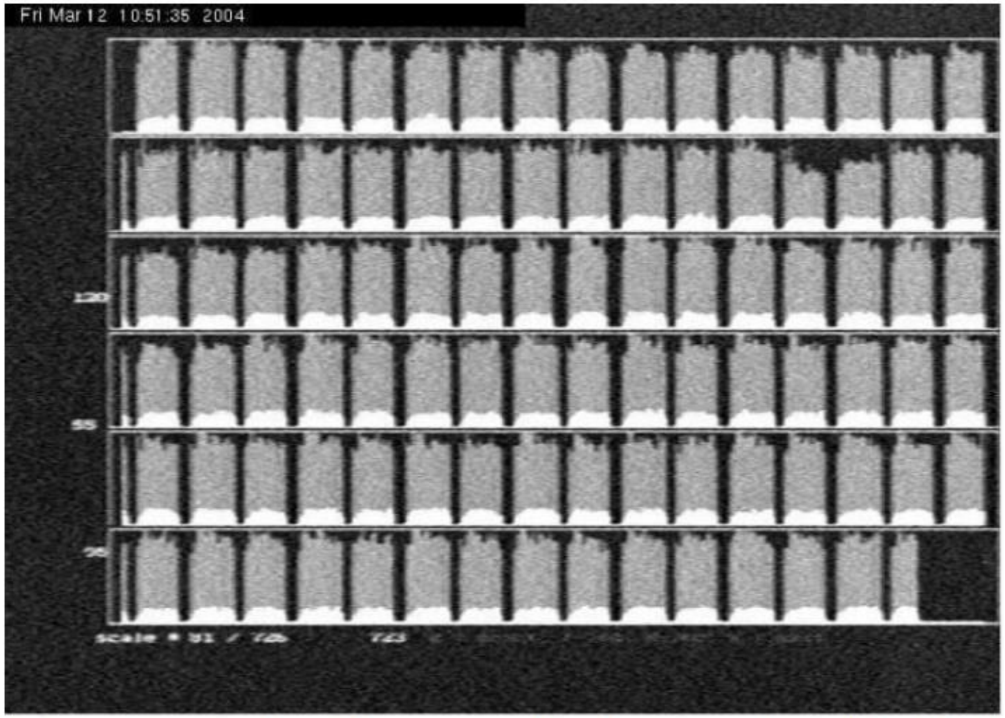

Figure 5: Luminosity versus bucket number. The LER injection non-closure brings the beam out of collisions and causes luminosity dips of up to 30%. The bunch pattern is basically by-2 with 95 trains of 14 or 15 bunches out of 18 places.

PEP-II Line spacings

$$\tau_b = \frac{m}{f_{RF}}, \qquad m = [1, 2, 3, \ldots]\,. \tag{1}$$

The integer number m determines the bunch pattern and measures the distance between two bunches in the wavelength of the main RF harmonic. The minimum distance between bunches corresponds to one wavelength. The spectrum lines corresponding to the bunch spacing are

$$f_n = \frac{n}{\tau_b} = \frac{n}{m} f_{RF}. \tag{2}$$

The bandwidth of the spectrum is determined by the bunch length and becomes larger for shorter bunches. A typical positron beam spectrum measured at the LER of PEP-II is shown in Fig. 1. The bunch pattern was "by two" ($m = 2$). The Fourier spectrum was taken from the signal of a button Beam Position Monitor (BPM). The bunch length was 12 mm and the spectrum goes up to 13 GHz.

Frequency spectrum versus bunch length

Then we fit the envelope of the main lines, with their logarithmic power scale, to a quadratic

$$y(f) = 10(\log_{10} e)\left[y_0 - \left(\frac{2\pi f}{c} \sigma_z \right)^2 \right] \qquad (4)$$

by varying two parameters, the amplitude y_0 and the bunch length σ_z .

Spectrum of Positron LER Beam

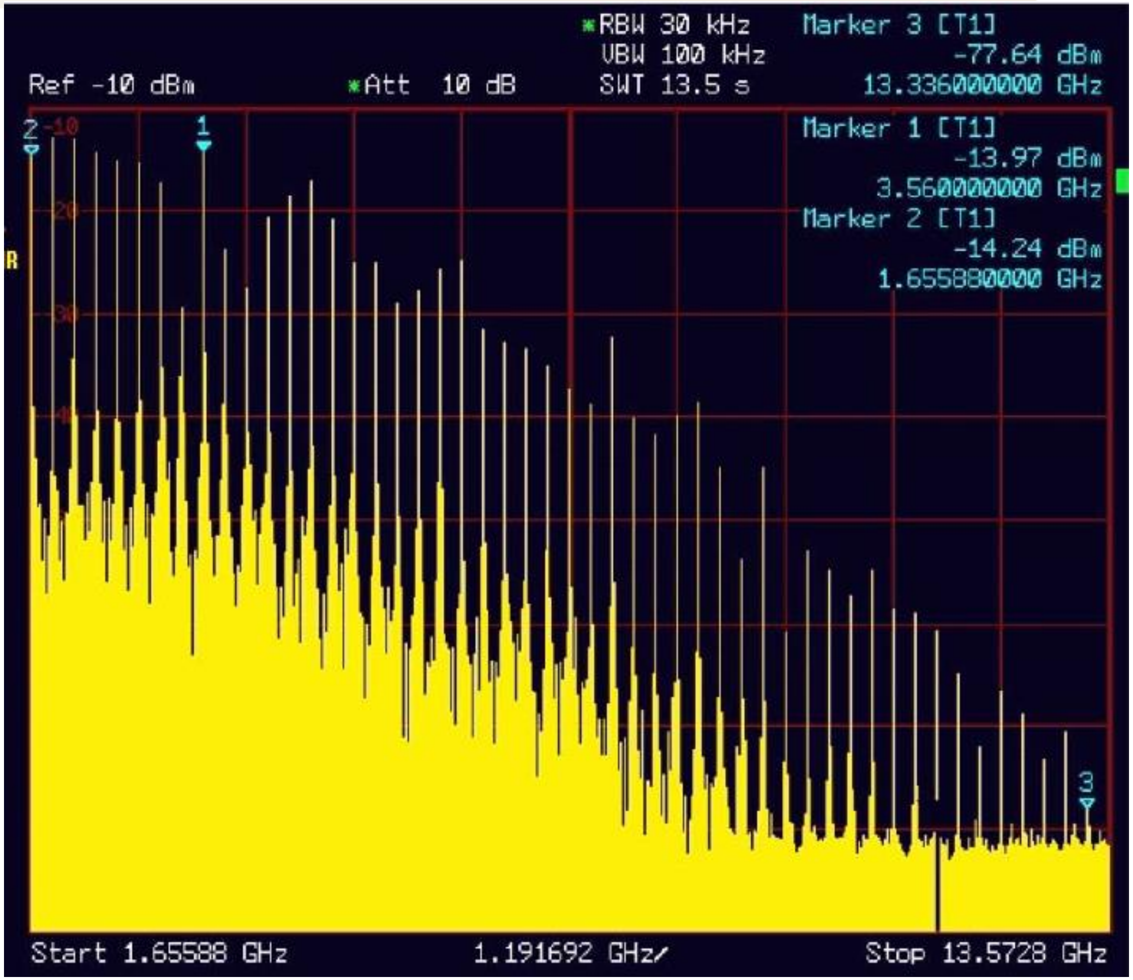

Fig. 1. Spectrum of the positron beam for the bunch pattern by two and a bunch length of 12 mm. The horizontal scale is 1.191692 GHz per division.

LER bunch length from RF spectrum

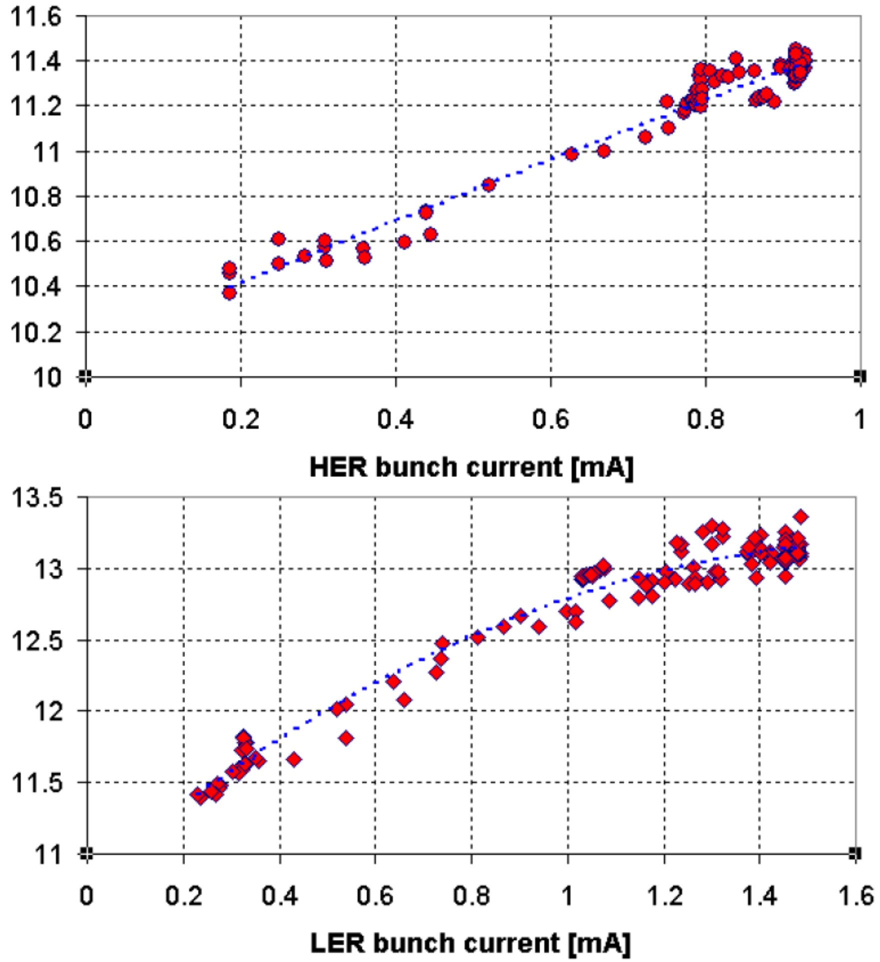

Figure 8: Bunch length (mm) measured from the RF spectrum, for (a) HER at 16.5 MV and (b) LER at 3.8 MV, as a function of bunch current (mA). Colliding multibunch fill.

Novokhatski

Resistive-Wall Wake (bunch lengthening)

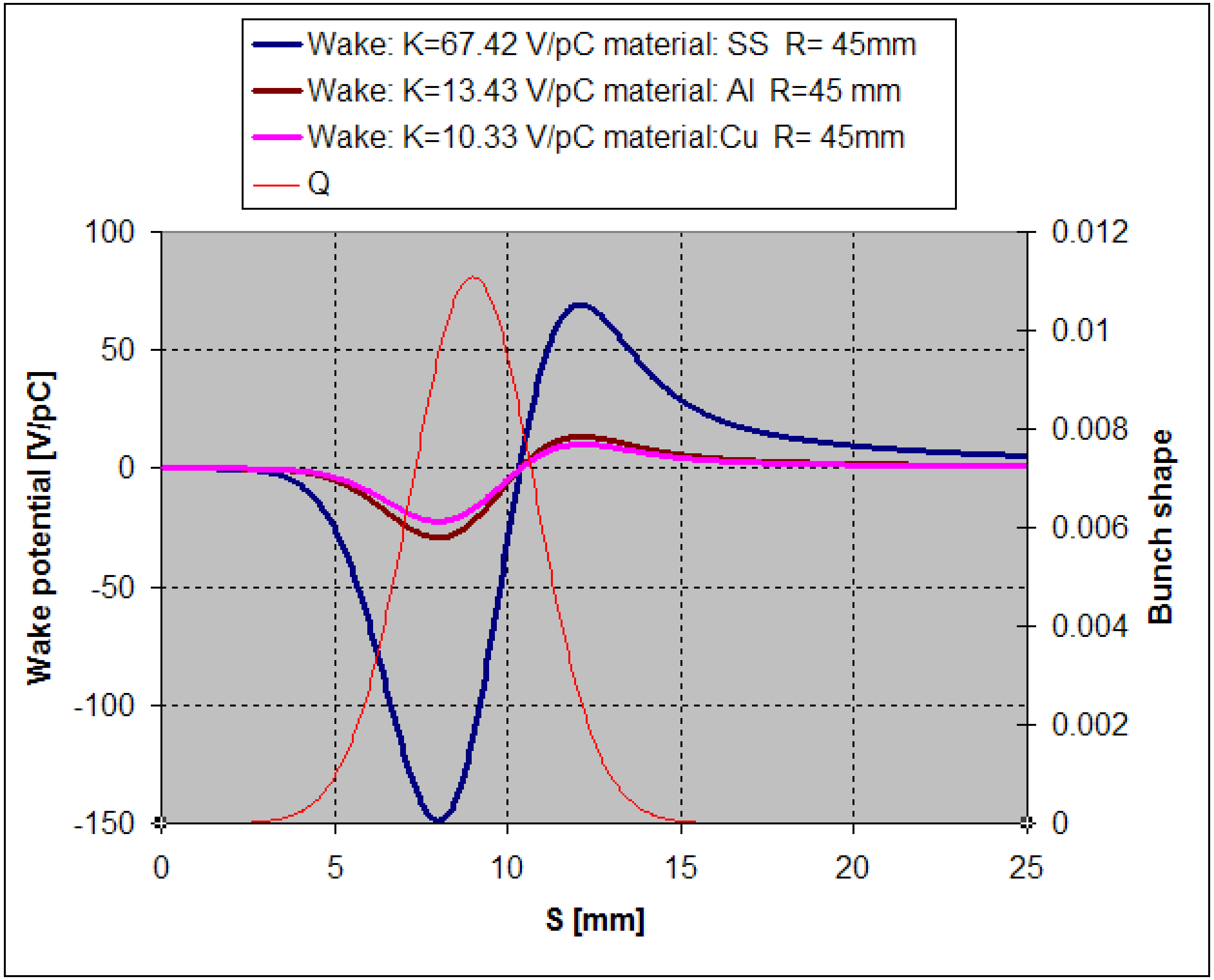

Power
SS: 45 MW
Al: 9 MW
Cu: 7 MW

SR: 18 MW

HOM power versus beam current in HER and LER

$$P_{[W]} = 146.2 \times Q_{[gpm]} \Delta T_{[^\circ F]}$$

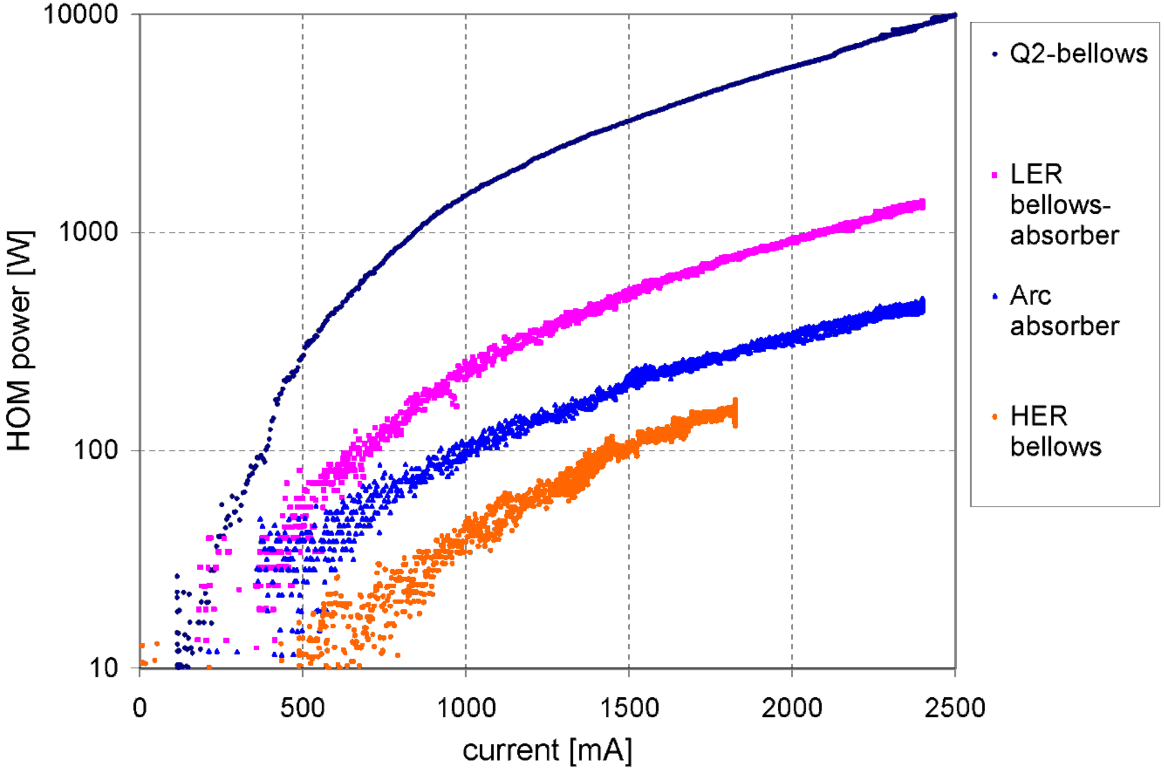

Measured HOM power captured in different absorbers at the level of several kilowatts; however the total power may be much higher.

Novokhatski

Beam Abort Spoiler (increase dumped beam emittance)

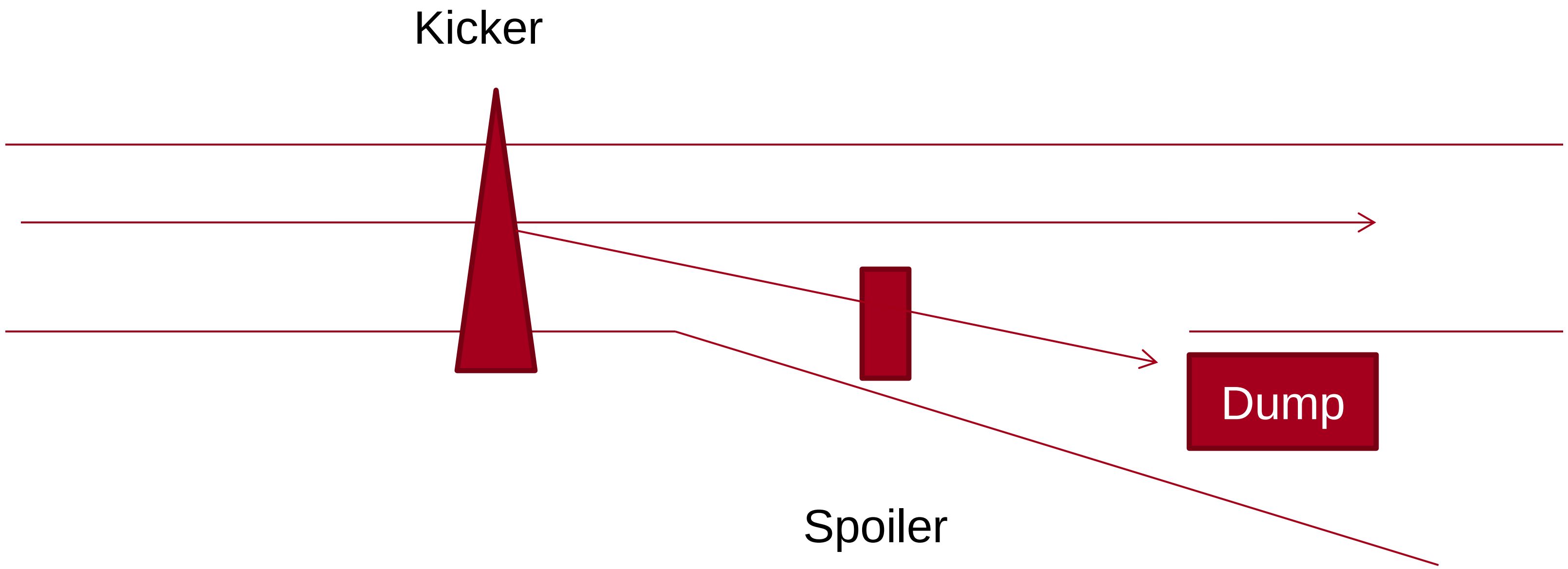

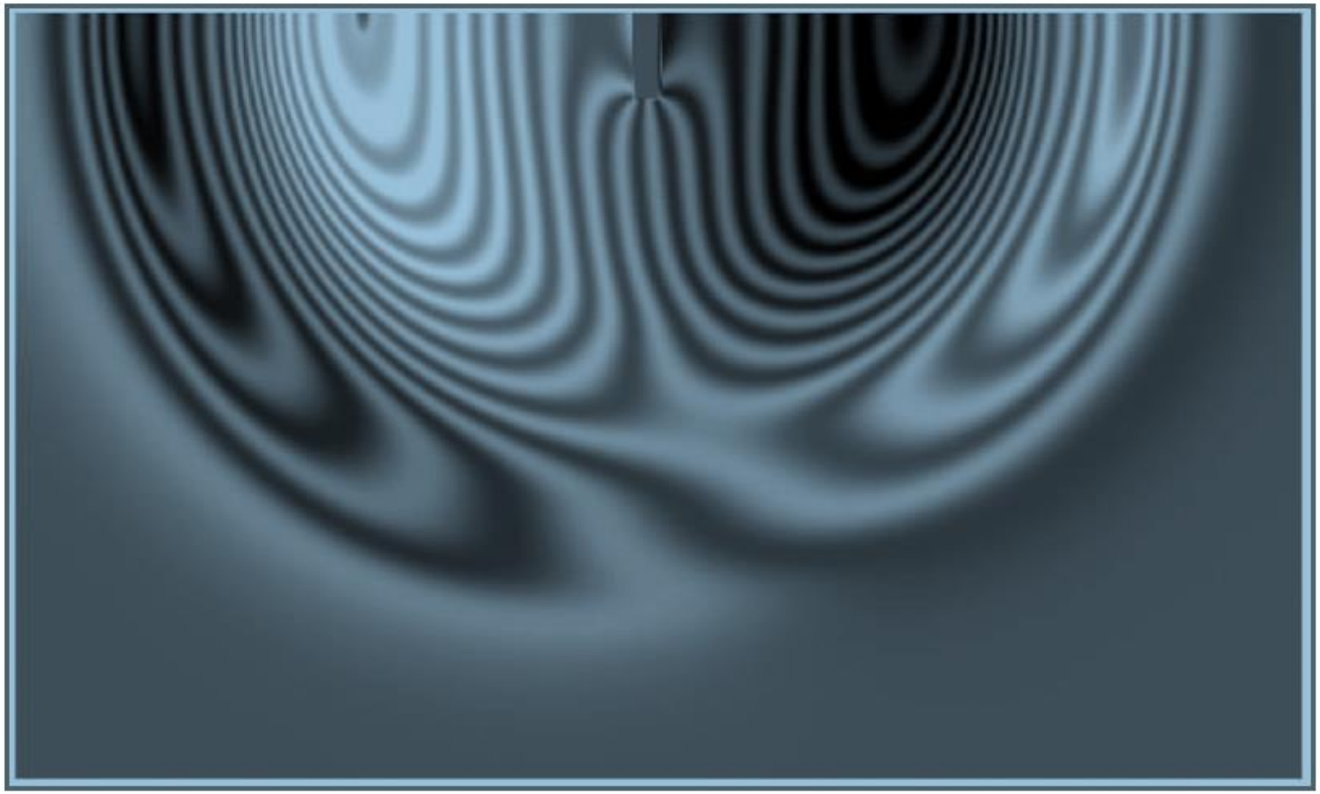

Fig. 7. Electric field lines in a beam pipe after a bunch has passed a small bump. The electric field is concentrated at the edge of a bump.

PEP-IOI

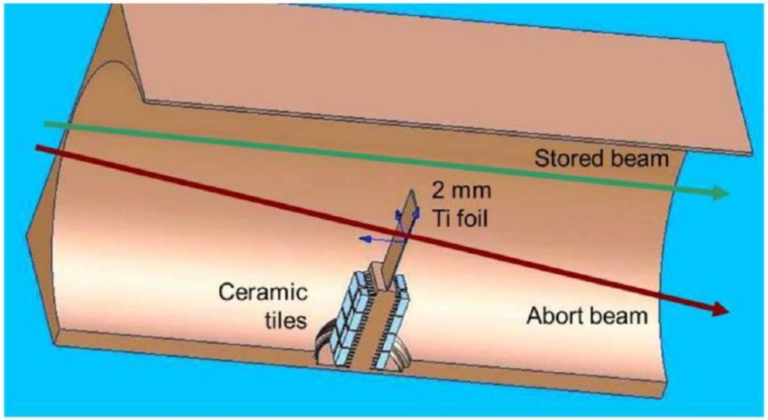

Fig. 10. Scatch of the emittance spoiler for the aborted beam. The beam goes through the titanium foil only if it is aborted.

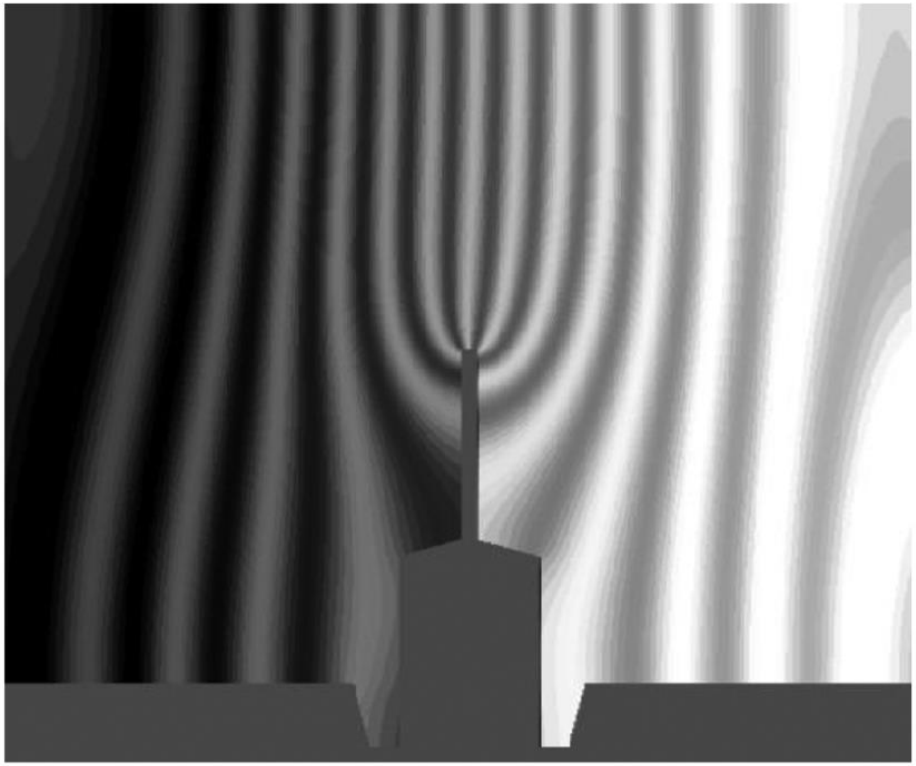

Fig. 11. Electric field lines near the spoiler after a bunch has passed by.

PEP-II Abort beam spoiler

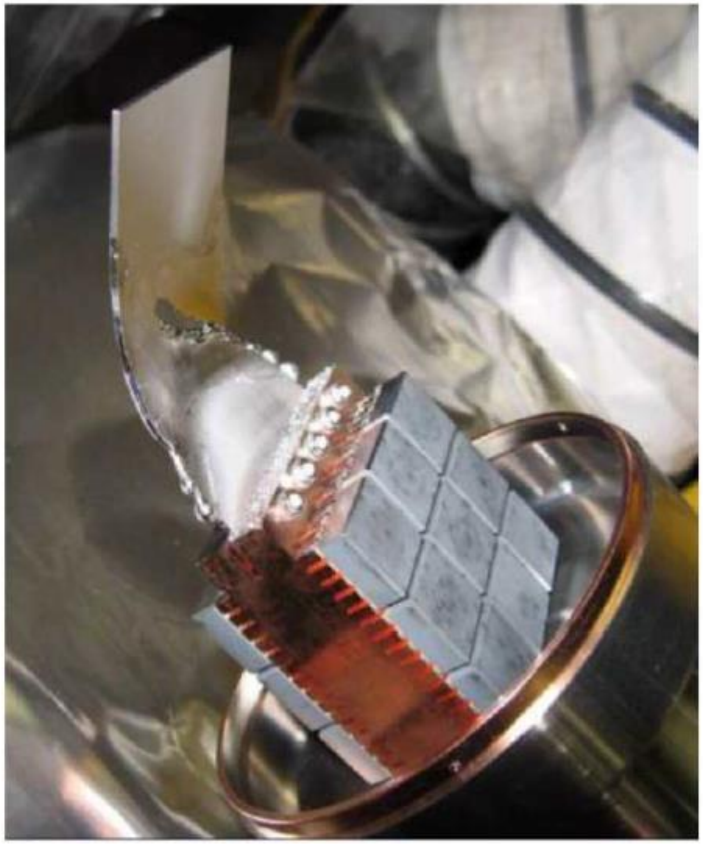

Fig. 13. Beam emittance spoiler with a melted titanium foil.

Unshielded beamline bellow → High HOMs

PEP-II HOMs for Bellow Seals (Omega)

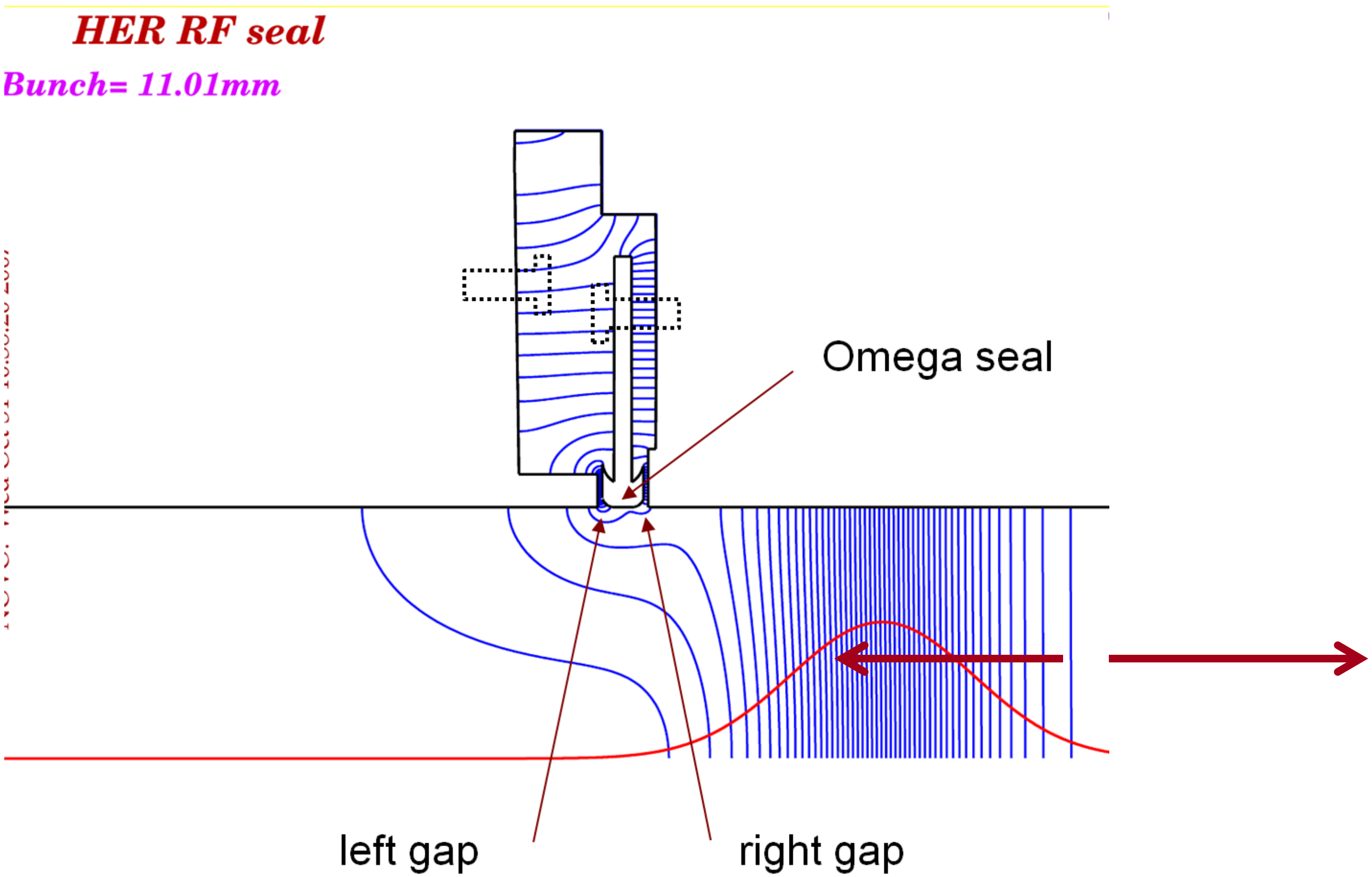

PEP-II bunch wake in a chamber RF gap

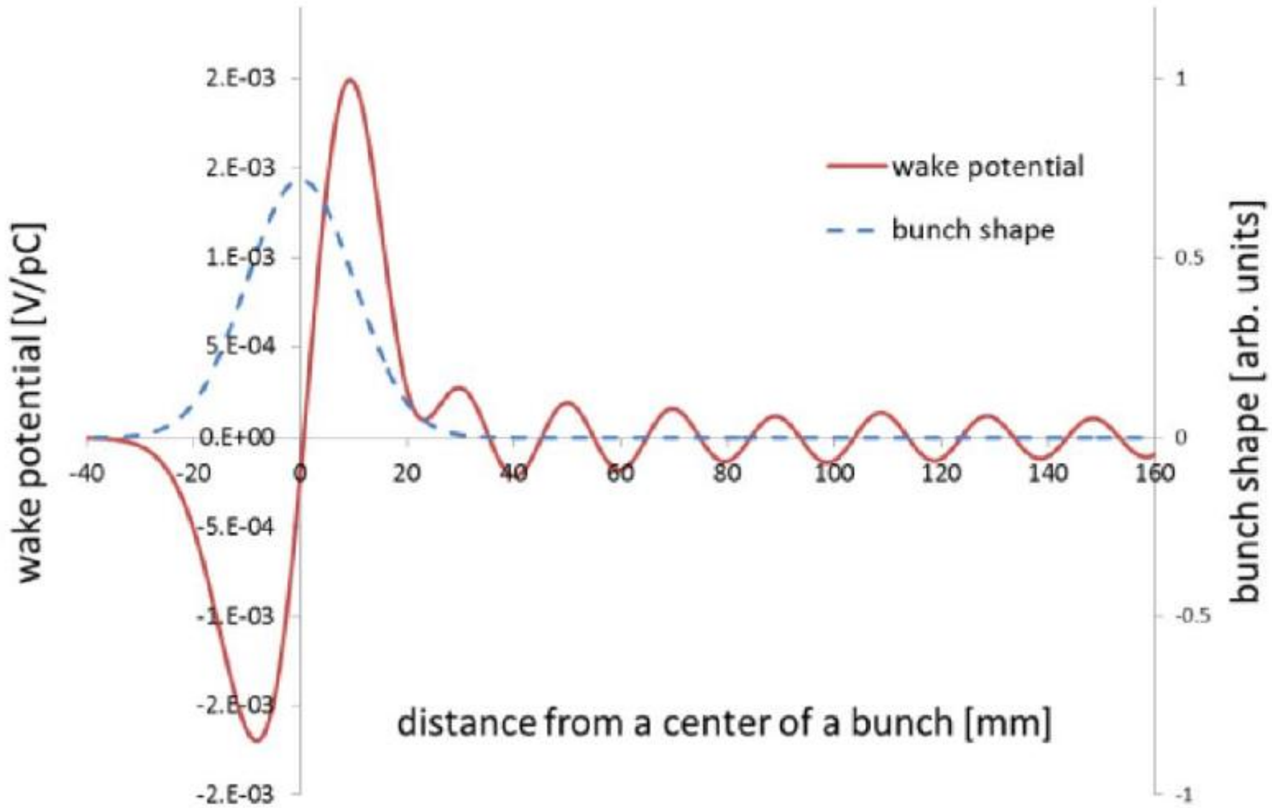

Fig. 2. Wake potential of a small gap (0.5 mm) in the beam pipe. The transverse size of the gap is 5 mm.

Novokhatski

PEP-II

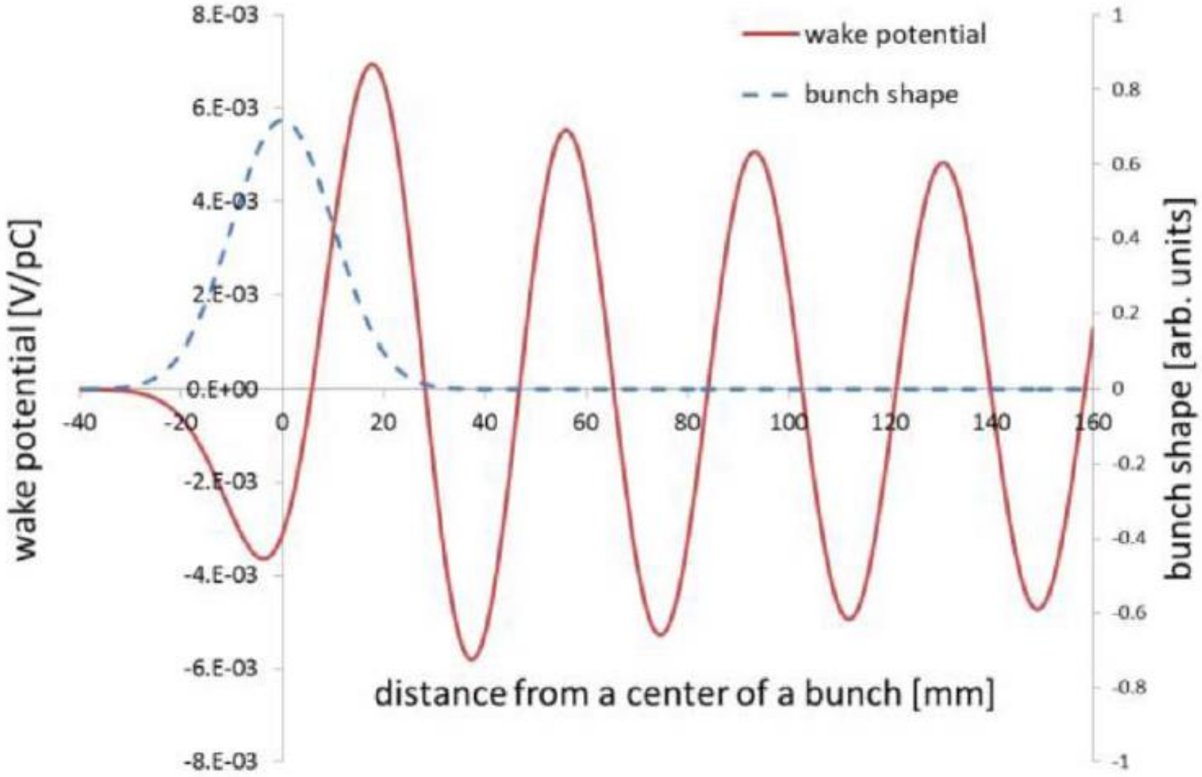

Fig. 3. Wake potential of a small gap (0.5 mm) in the beam pipe. The transverse size of the gap is 10 mm.

LER vacuum valve RF gap overheated from HOMs

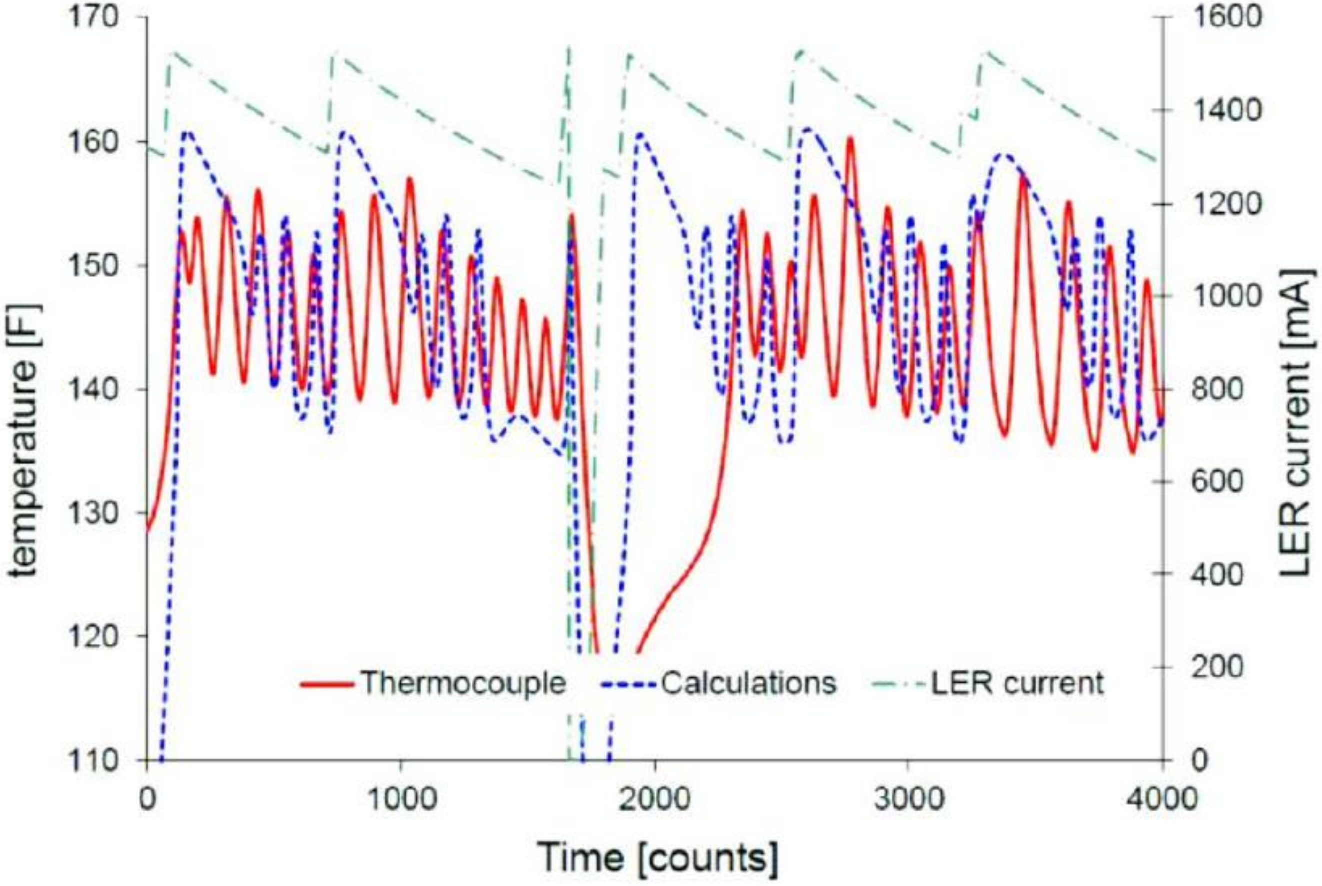

Fig. 5. Comparison of the measured temperature on the valve's body (a red solid line) and a simulated temperature (a blue dotted line). A green dot-dashed line shows the positron current. There was a beam abort loss in the middle of the plot and the LER beam was refilled.

Arcing omega seal

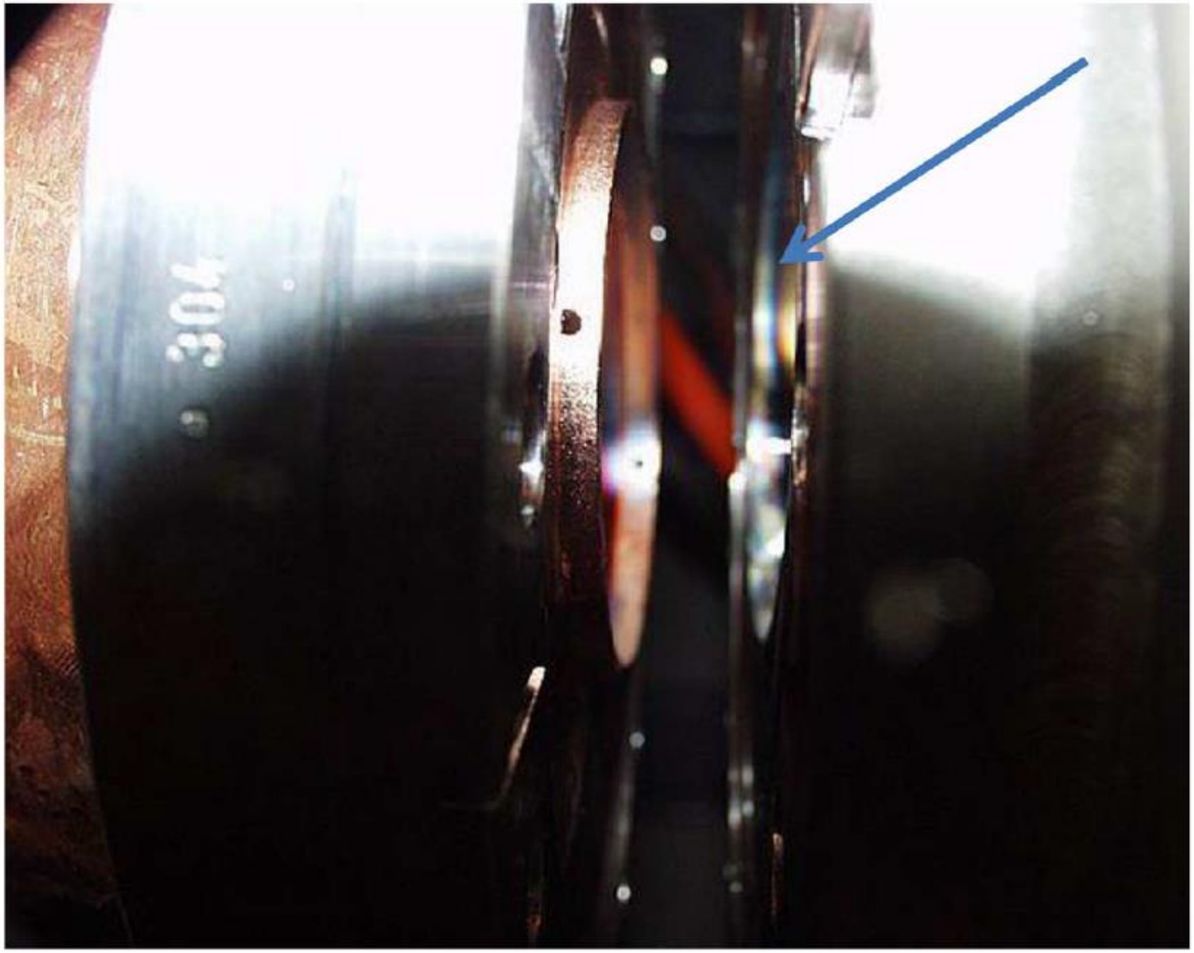

Fig. 4. Disconnected flanges and an RF seal (gap ring). Traces of arcing are on the right stainless still flange.

HER arc 5 RF seal at 6122 other side

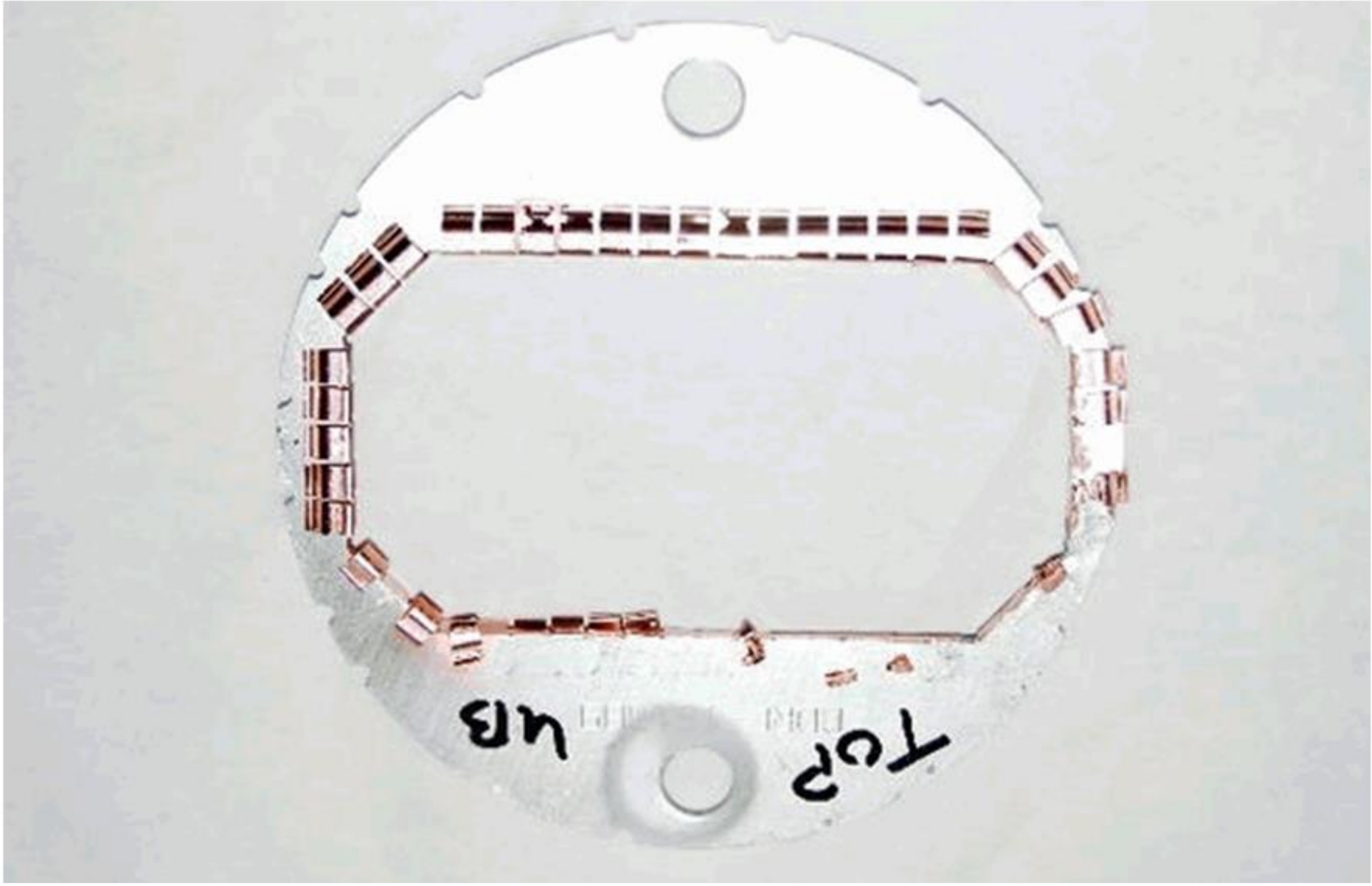

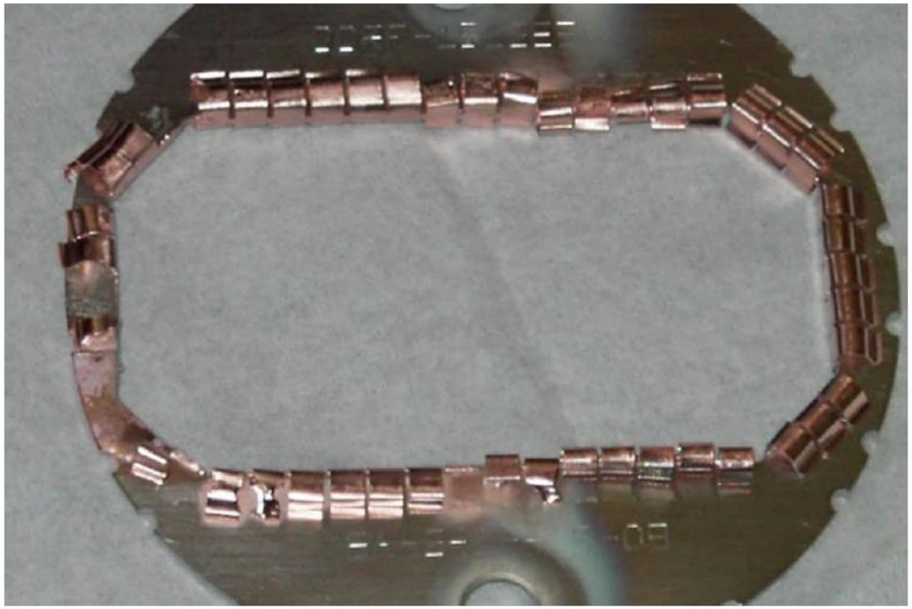

Figure 6. Picture of a damaged HER flex flange RF seal. HOM power getting behind the GlidCop (dispersion strengthened Cu) fingers heated up the stainless steel frame to the melting point of Cu (left side of picture). In addition, one can see signs of arcing where there is Cu deposition on the stainless steel frame top and bottom. The right hand side of the picture shows undamaged fingers.

HOM Absorbing Bellows (Version 1)

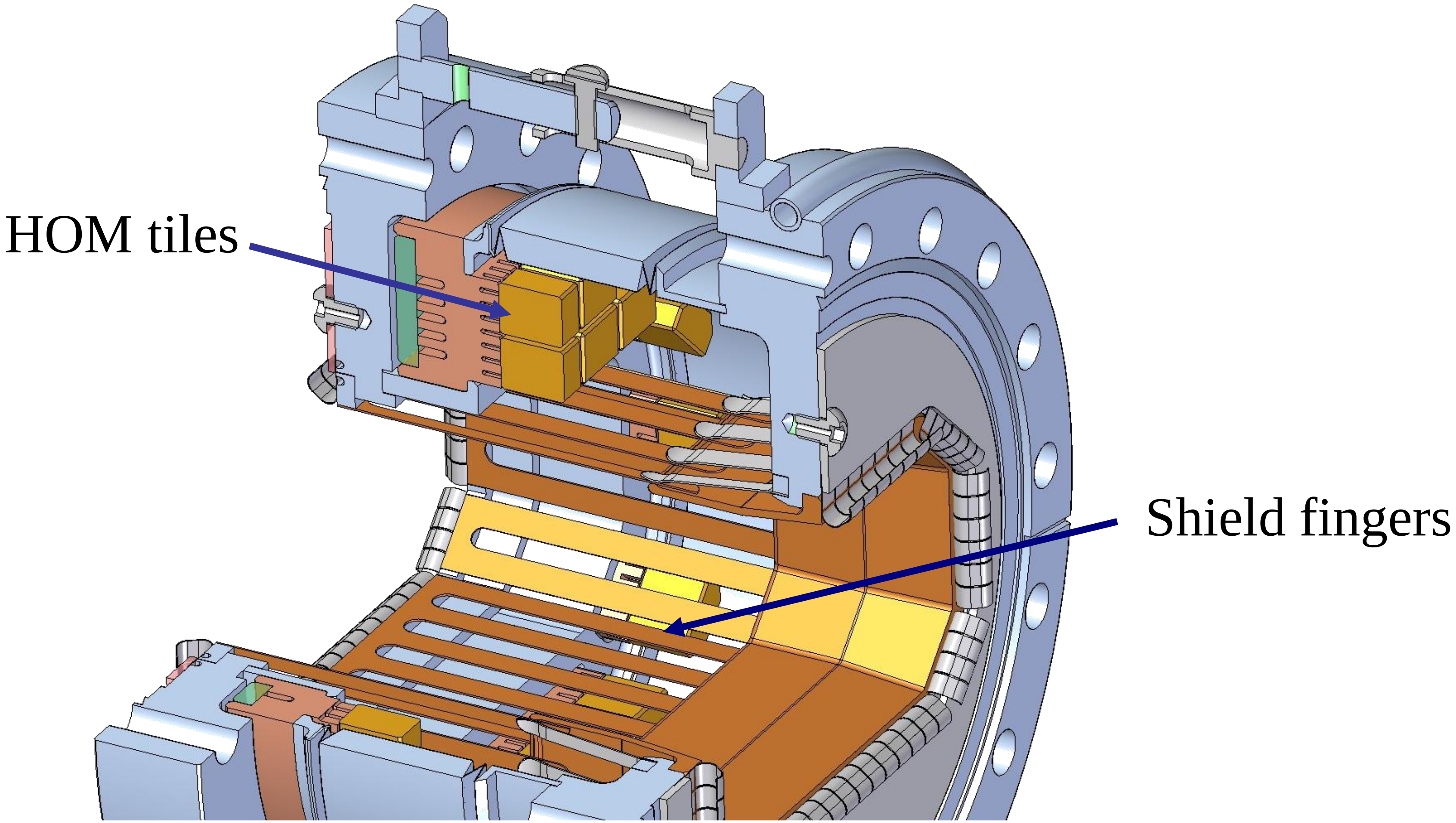

PEP-II bellow in a Very High HOM region → Need better design

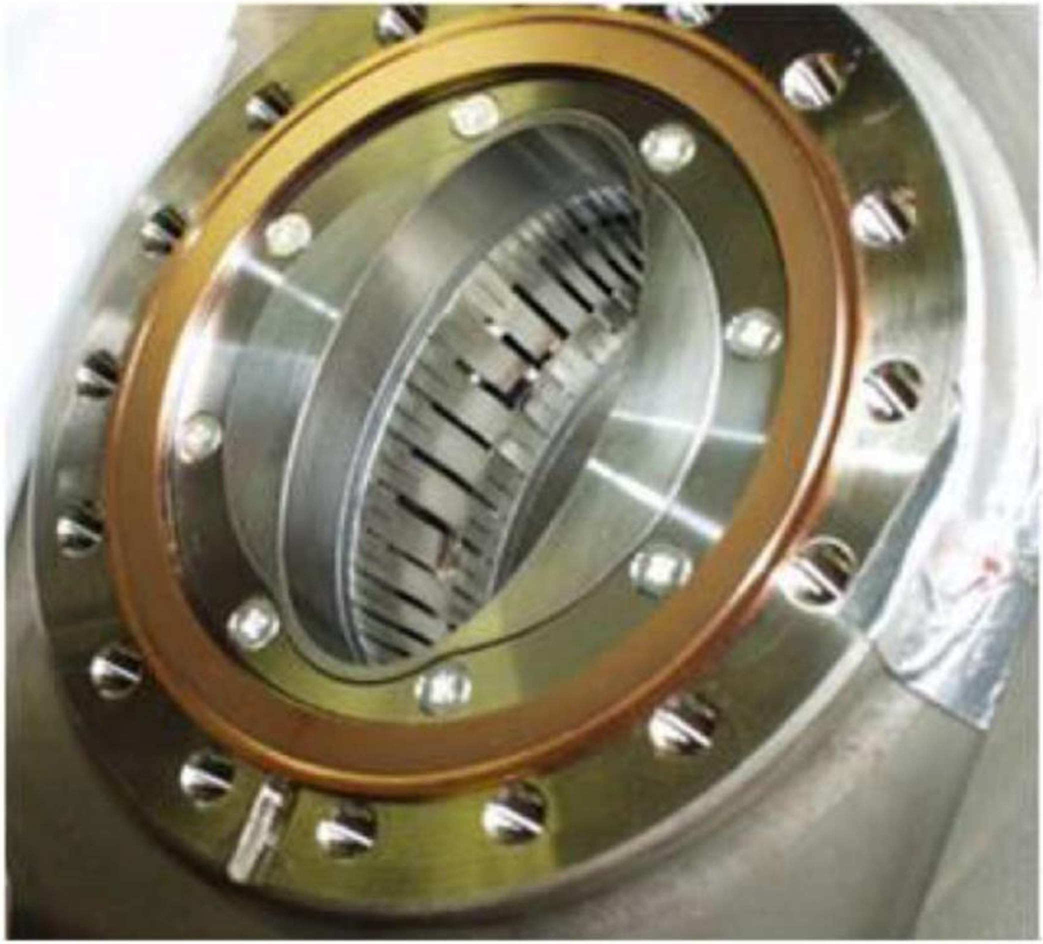

Fig. 6. Shielded vacuum valve with a vacuum copper gasket. Discharges were so strong that they damaged the RF shielding fingers.

Q2 bellow version 21

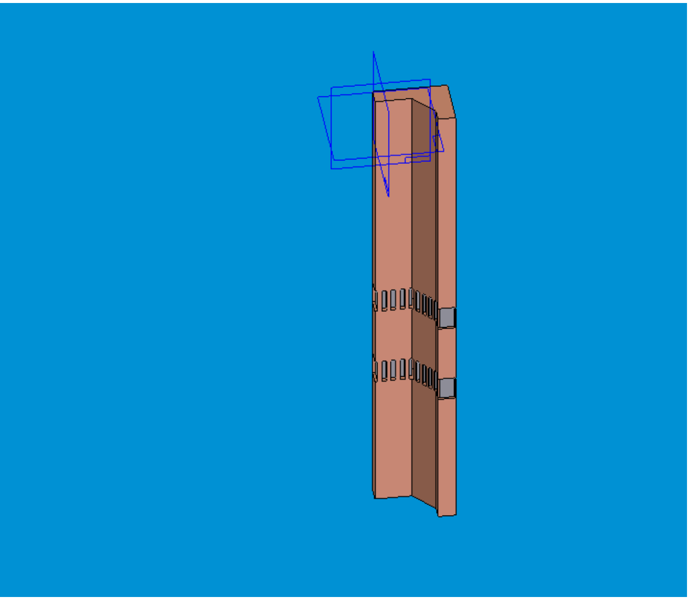

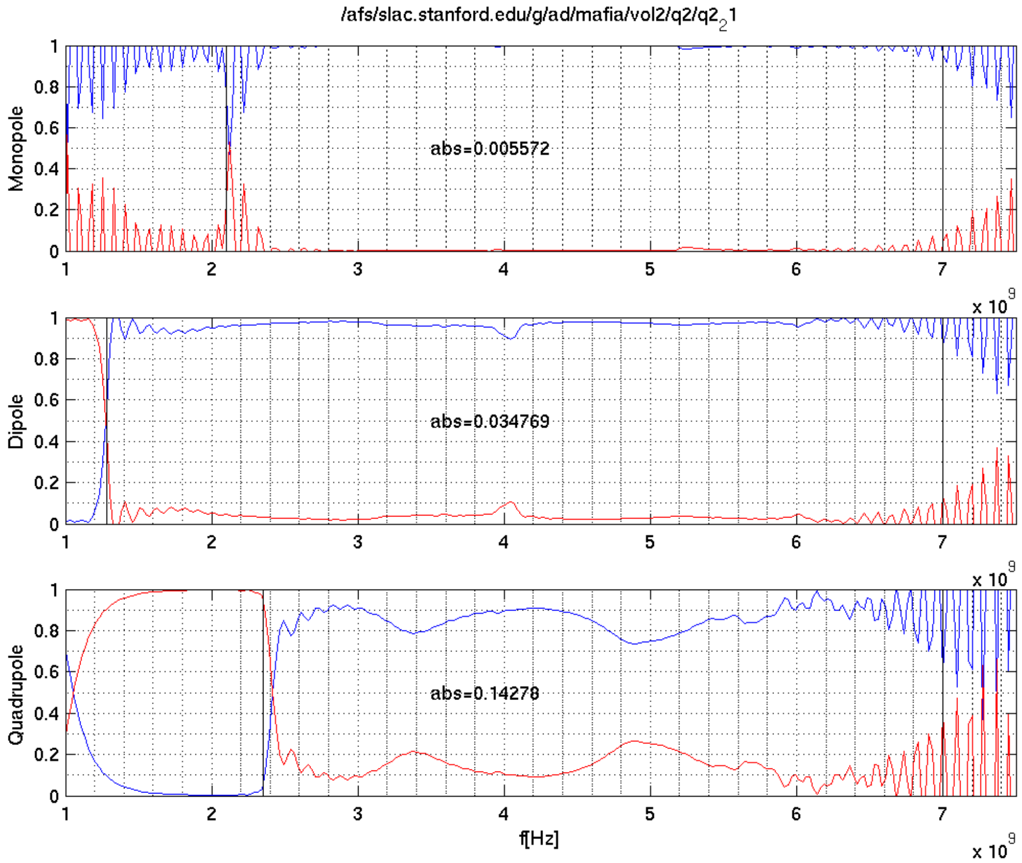

Q2 bellow version 22

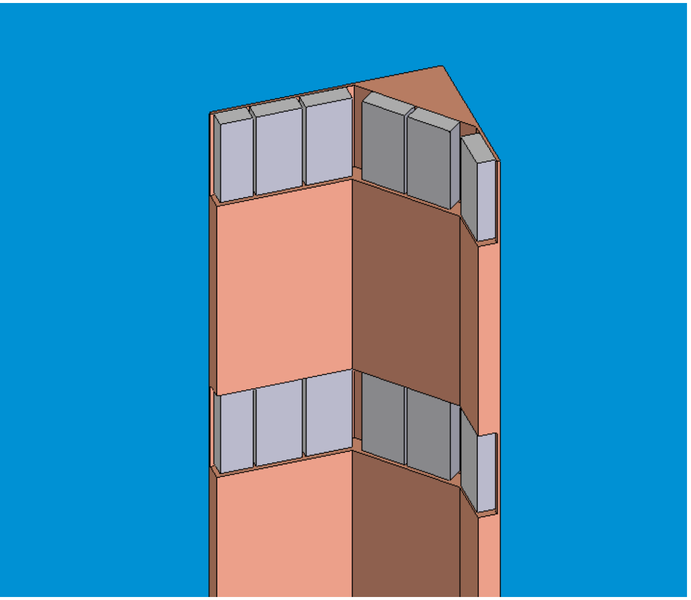

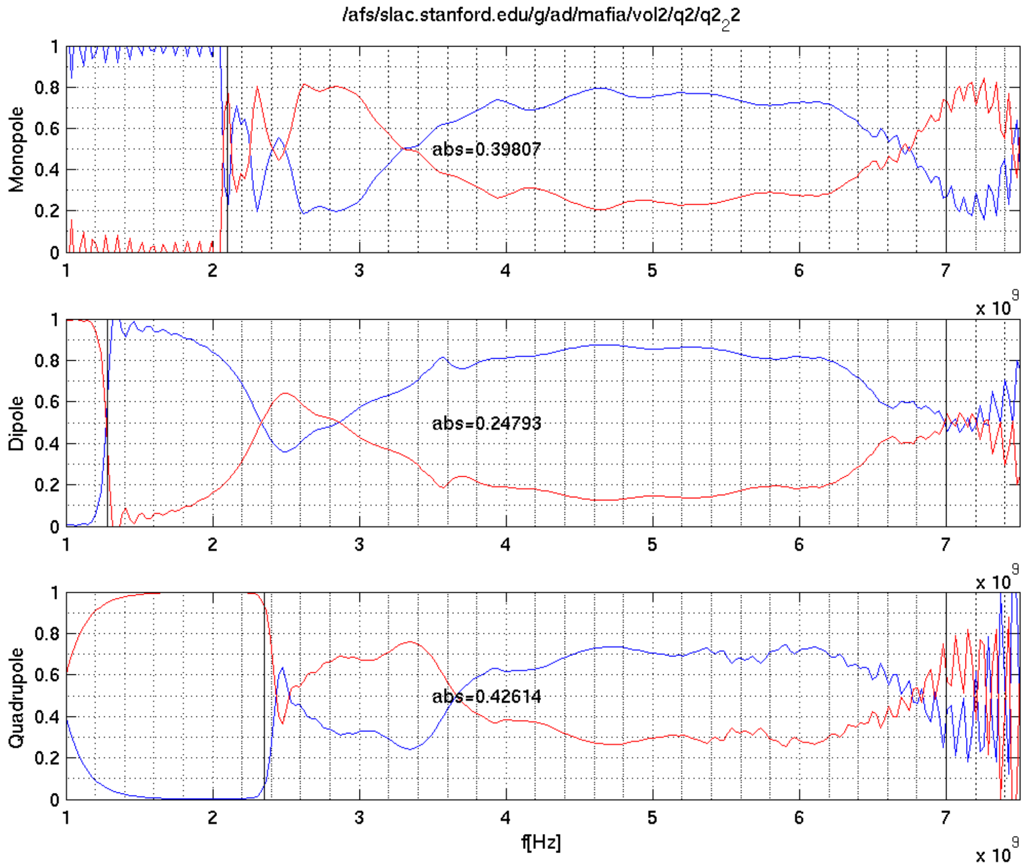

Q2 bellows version 30

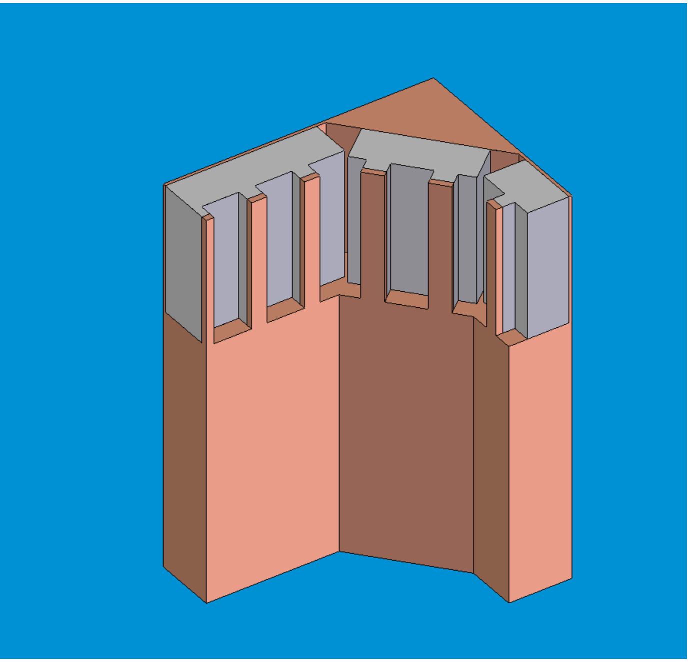

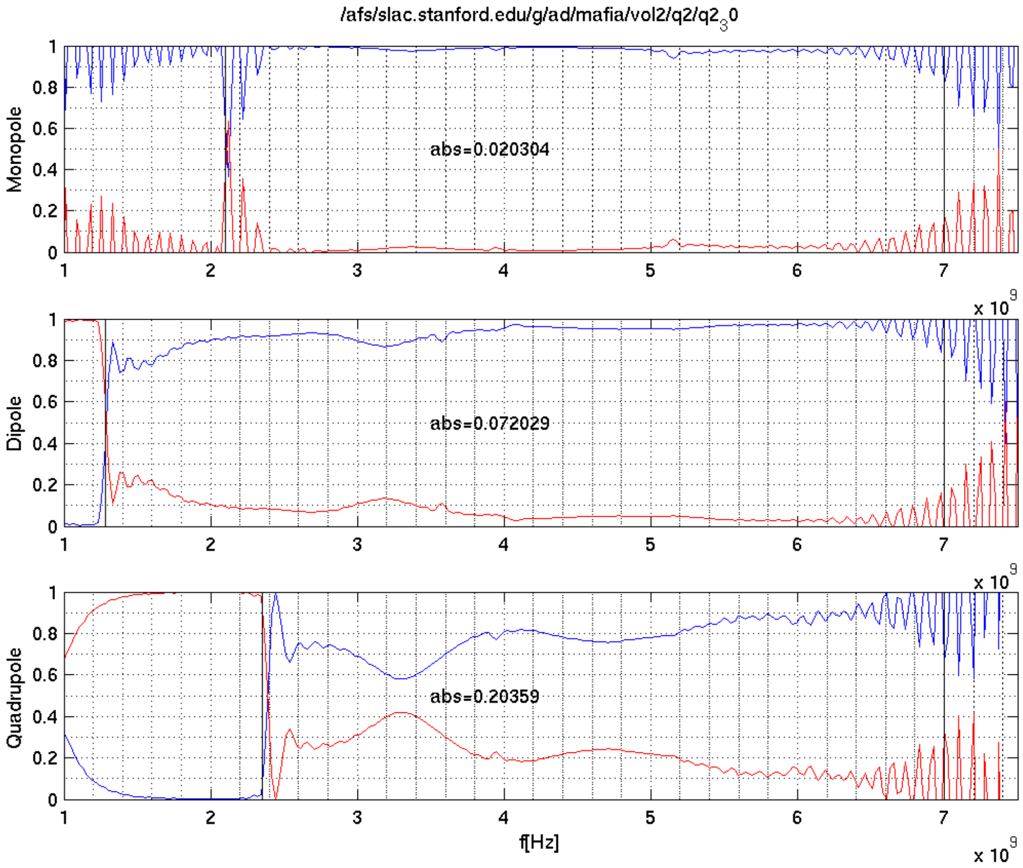

Q1/Q2 Bellows Thermo Model at 10 KW (N. Kurita)

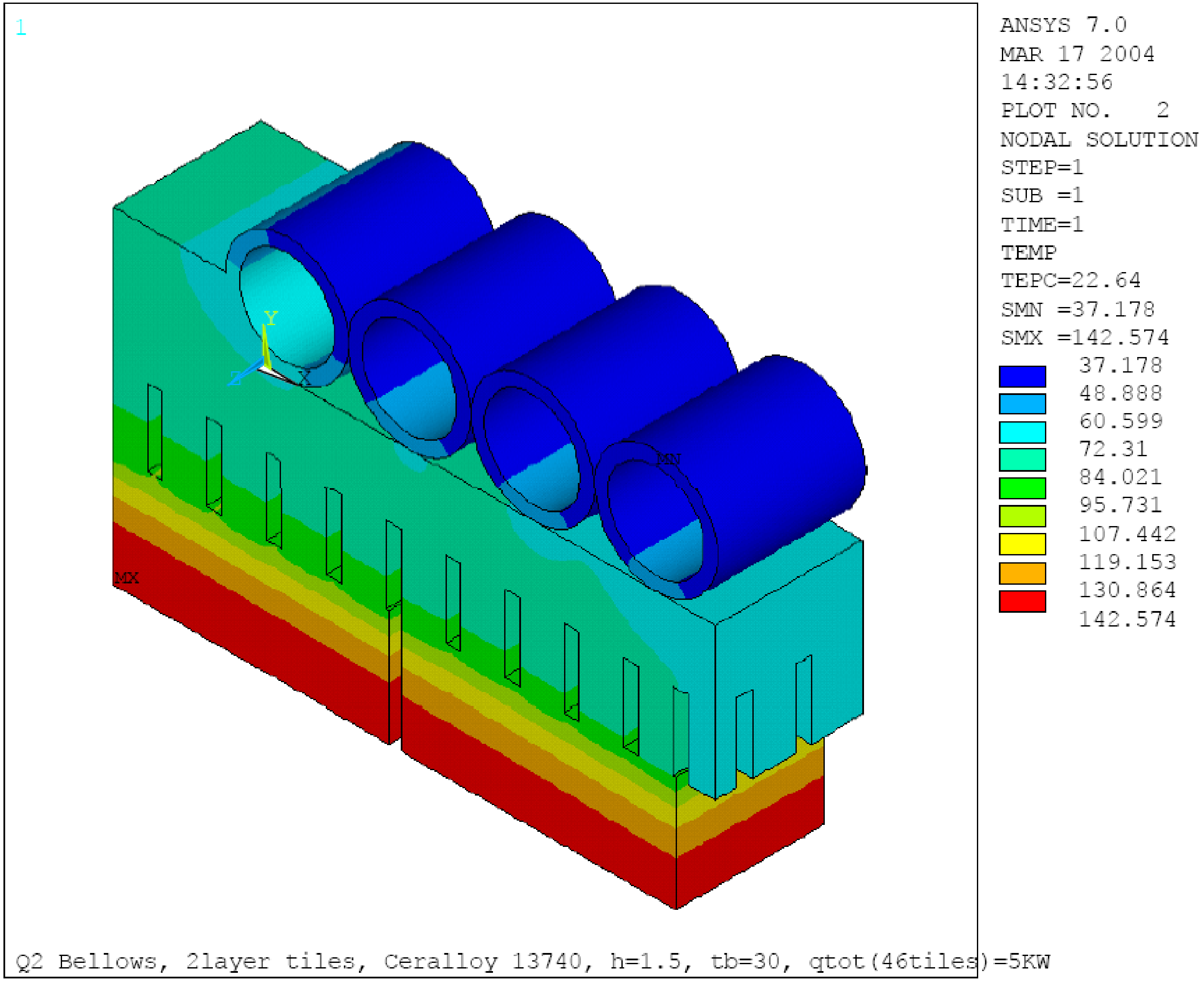

A new Q2-bellows

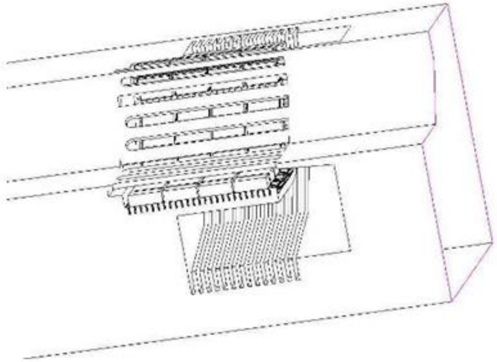

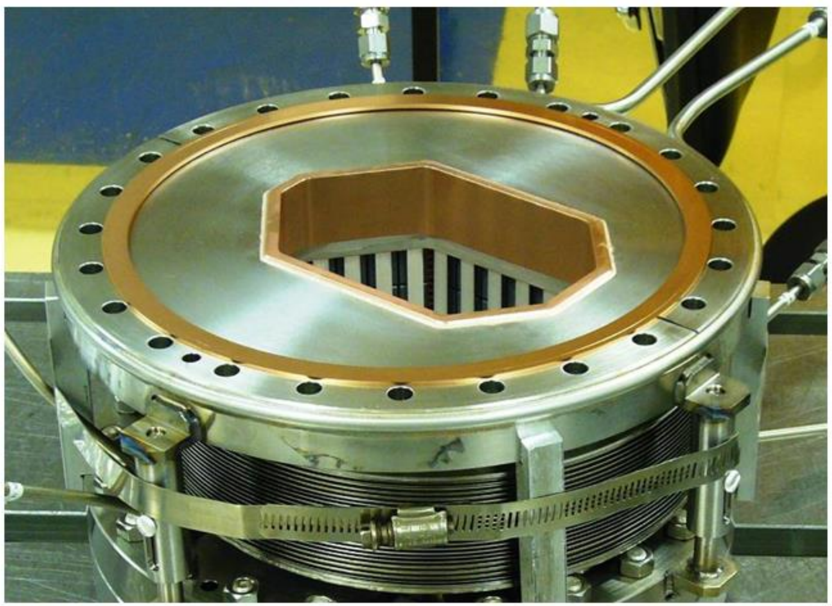

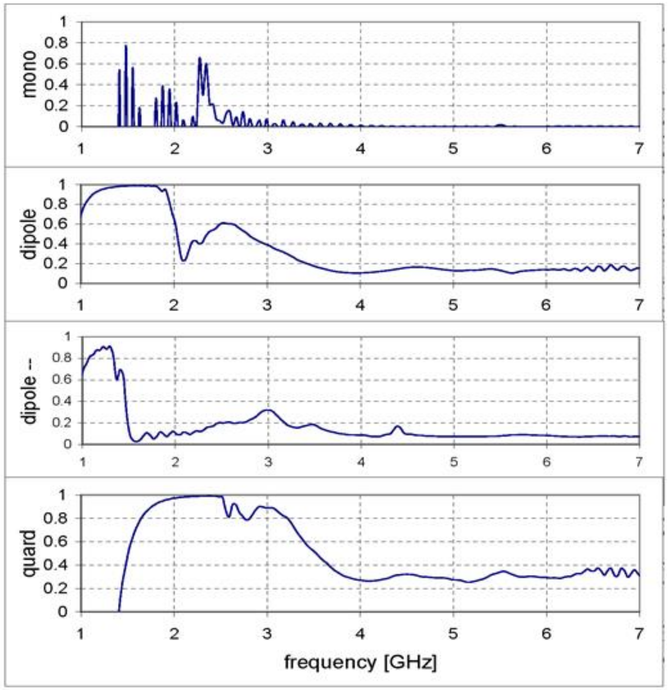

Absorbing parameters of a new Q2 absorber

Final sliding bellows solution with Many Cooling Loops

The new MKIII bellows

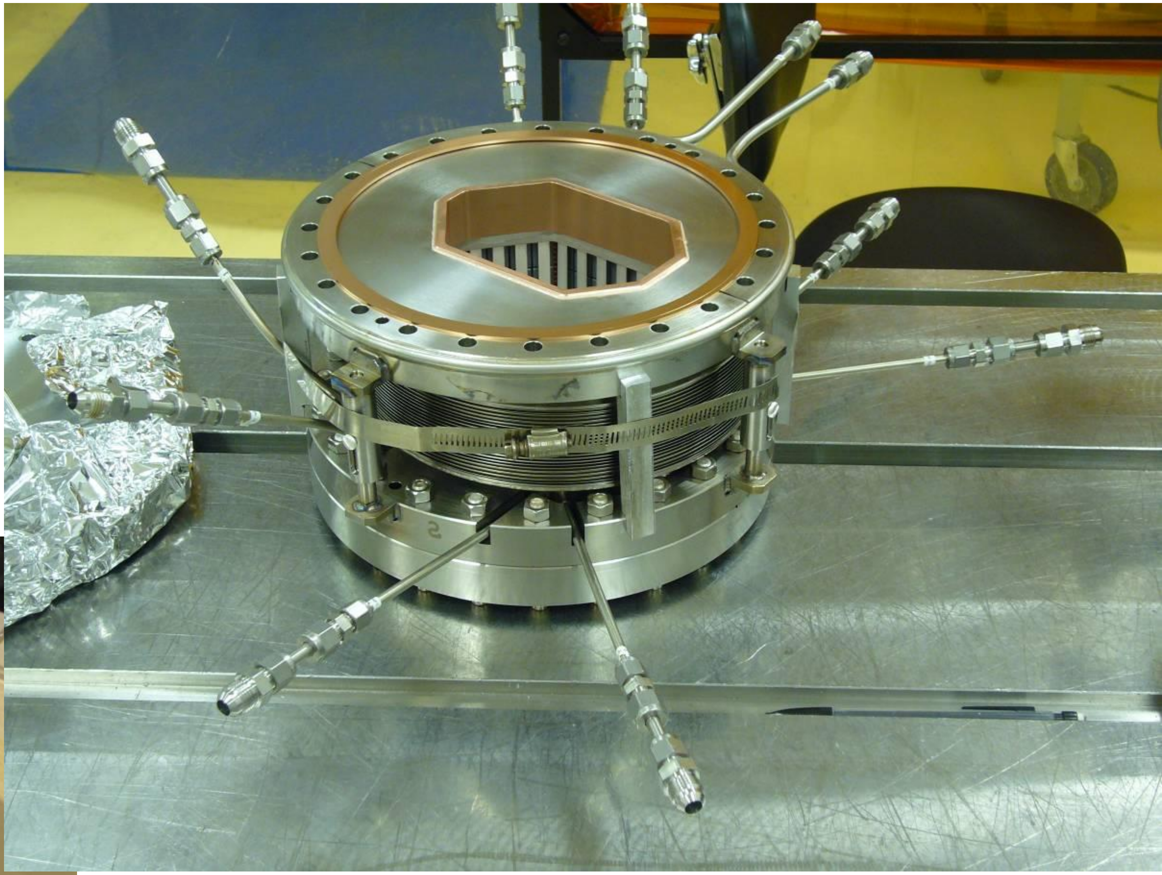

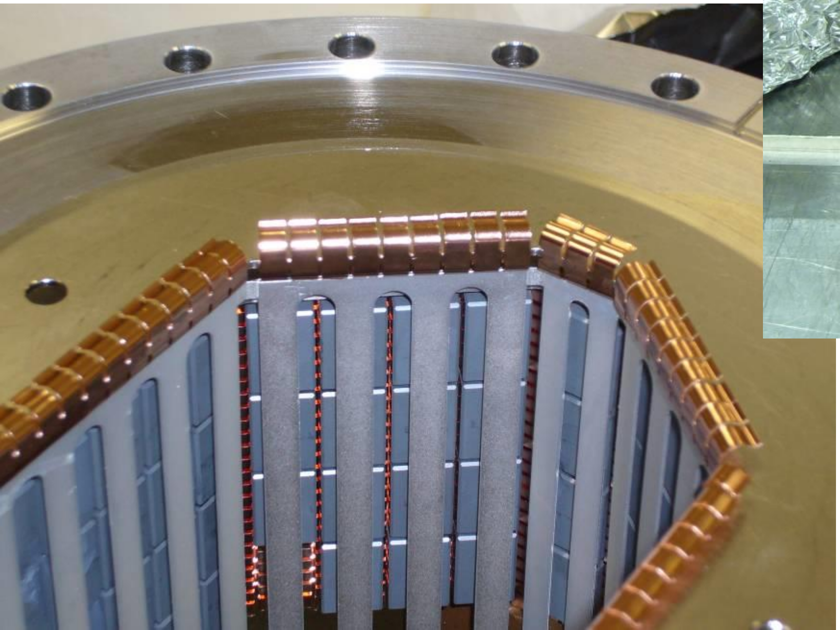

Beam Line Q2 HOM absorbers

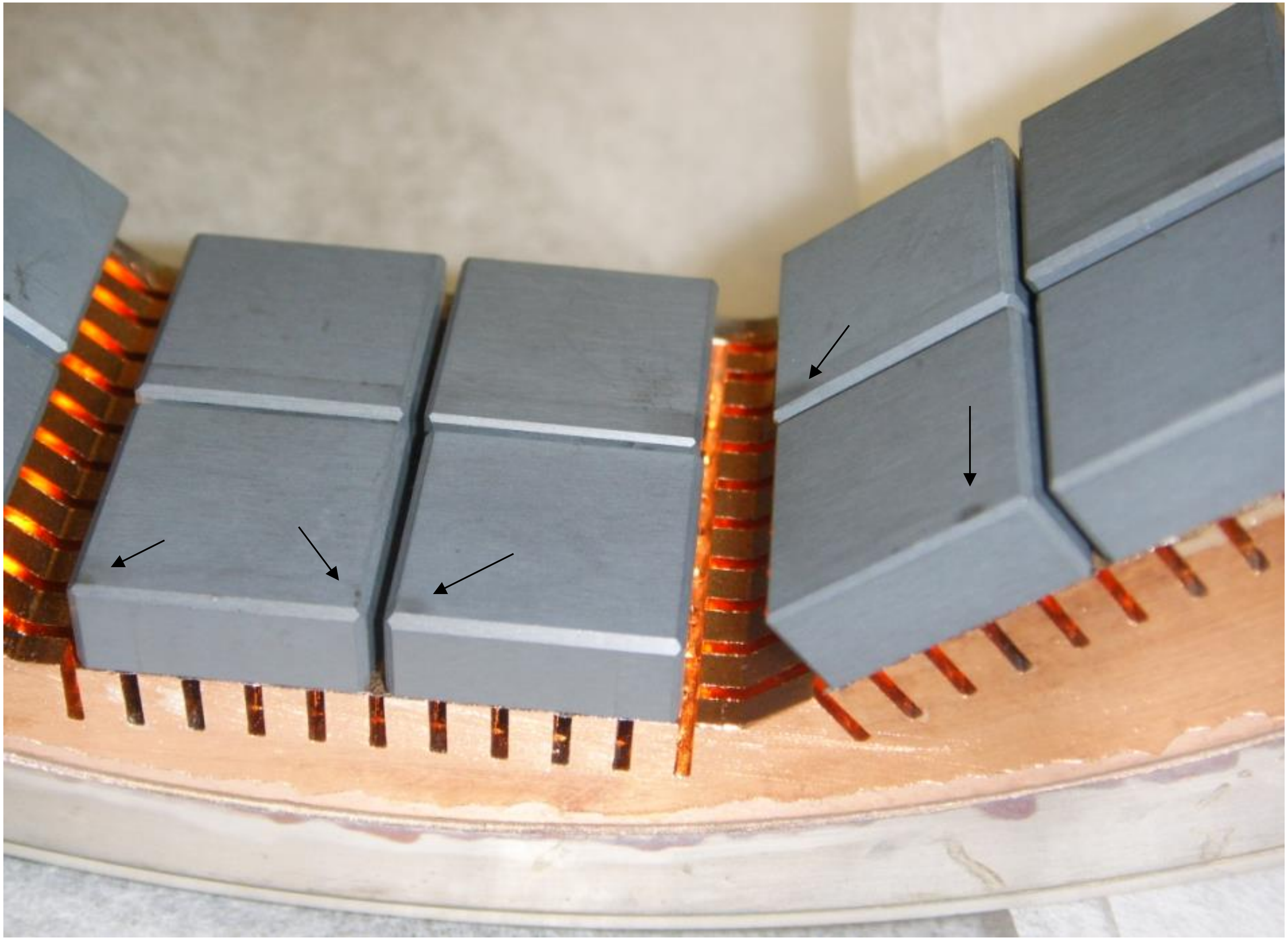

Fast Vacuum Pressure Rise in IR due to Arcing SiC

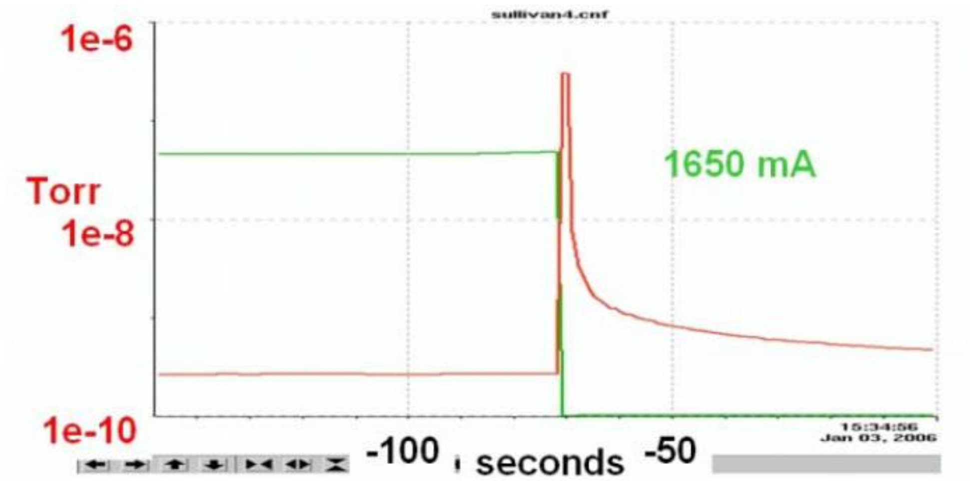

Figure 2: Time plot of a fast pressure spike and radiation abort event. The green curve is the LER beam current.

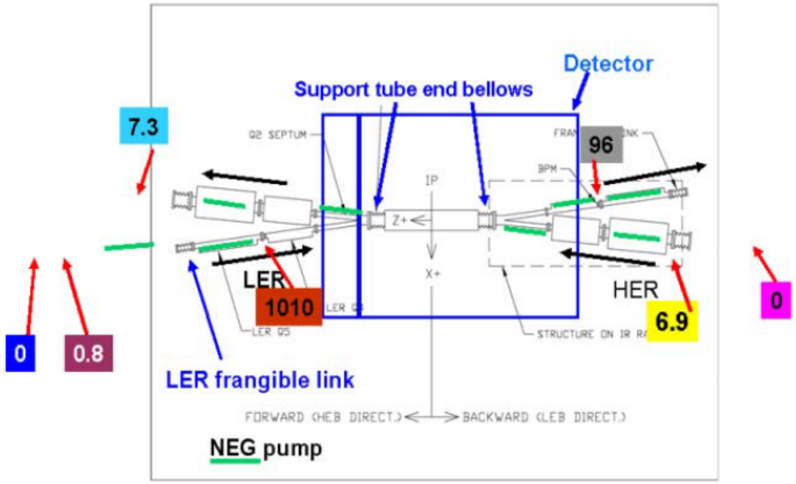

Figure 1: Layout of the Interaction Region. The numbers are typical peak pressure readings in nTorr for one of these fast pressure spike events. The green bars indicate the location of NEG pumps in this area. The layout is pictorial. The total z length of this region is about ±10 m.

IR Q2 Bellows and Vertex Chamber Bellows

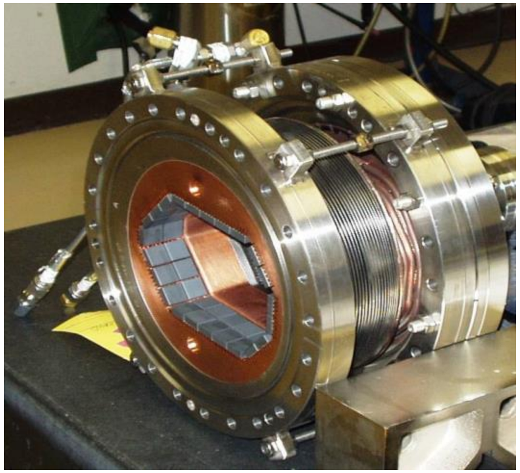

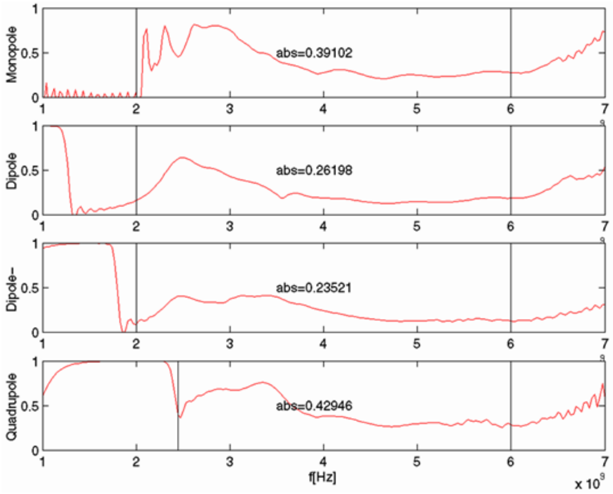

$$\kappa \approx \frac{cZ_0}{4\pi^{3/2}a} \cdot \frac{L}{\sigma\sqrt{\varepsilon}}$$

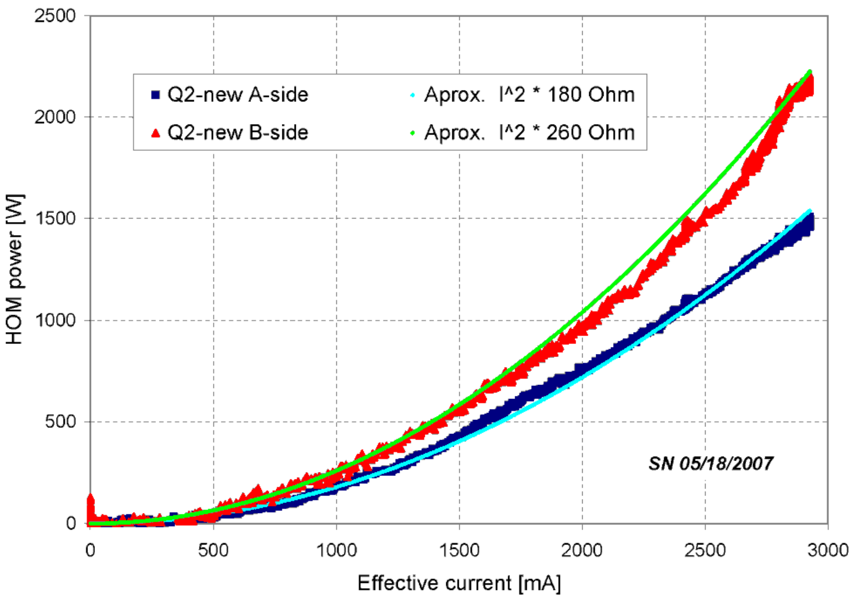

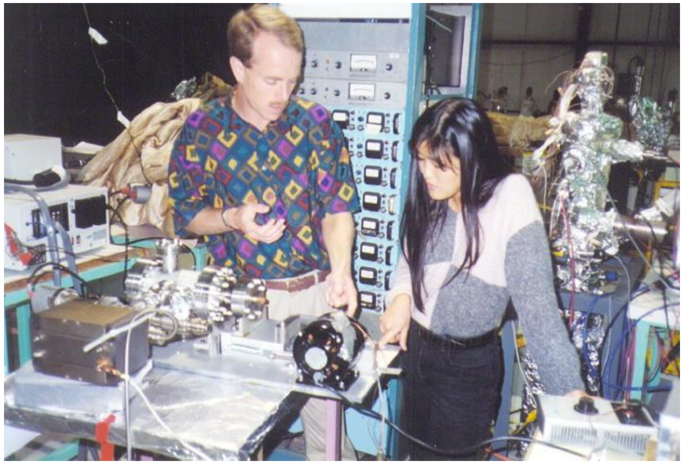

Dark spots on tiles (~3 spots total)

The cause of the dark spots is not known.
Manufacturing? Arcing? Vacuum leaching?

Dark spot on tile corner (1 mm^2)

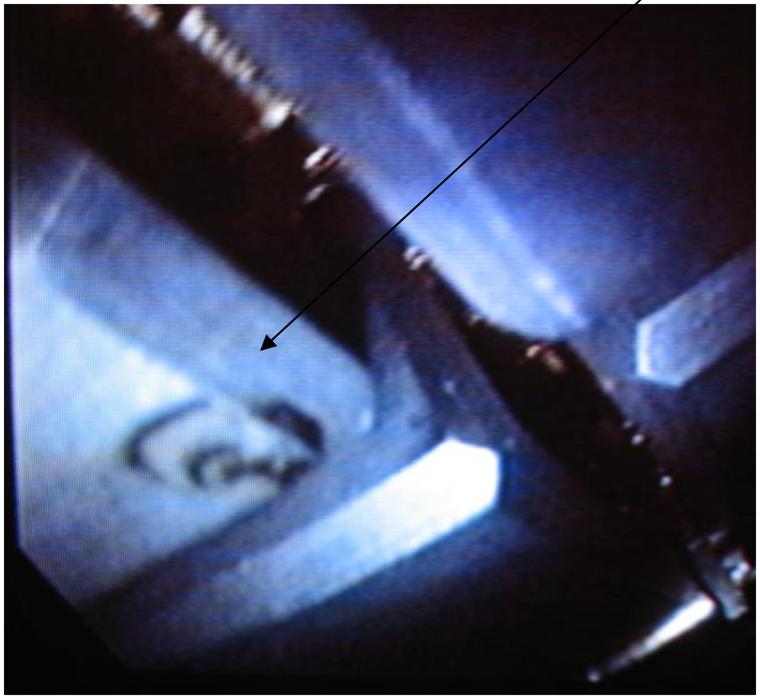

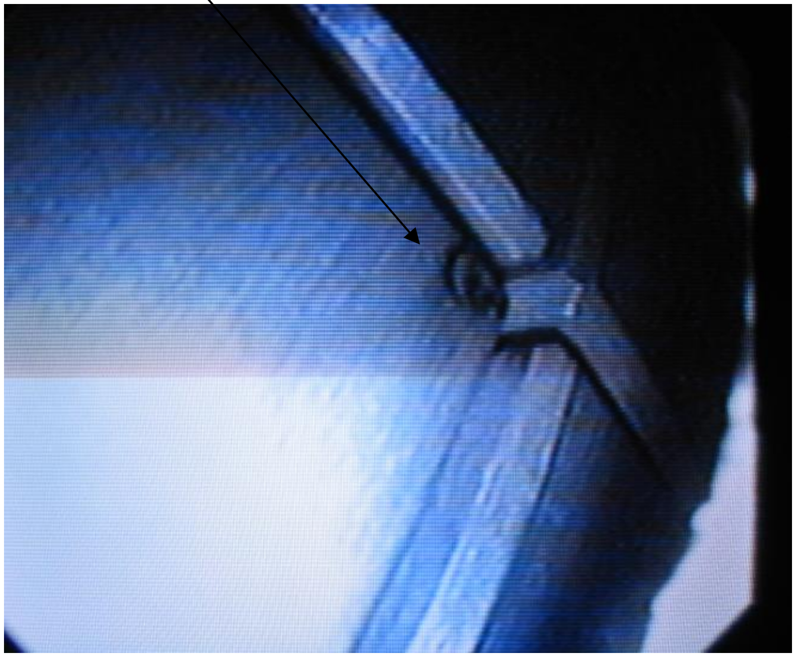

Tile Brazing

All bottom half tiles probed. No loose tiles!
Checked 39 tiles on the bottom and sides.

Probe moved to push on tiles.

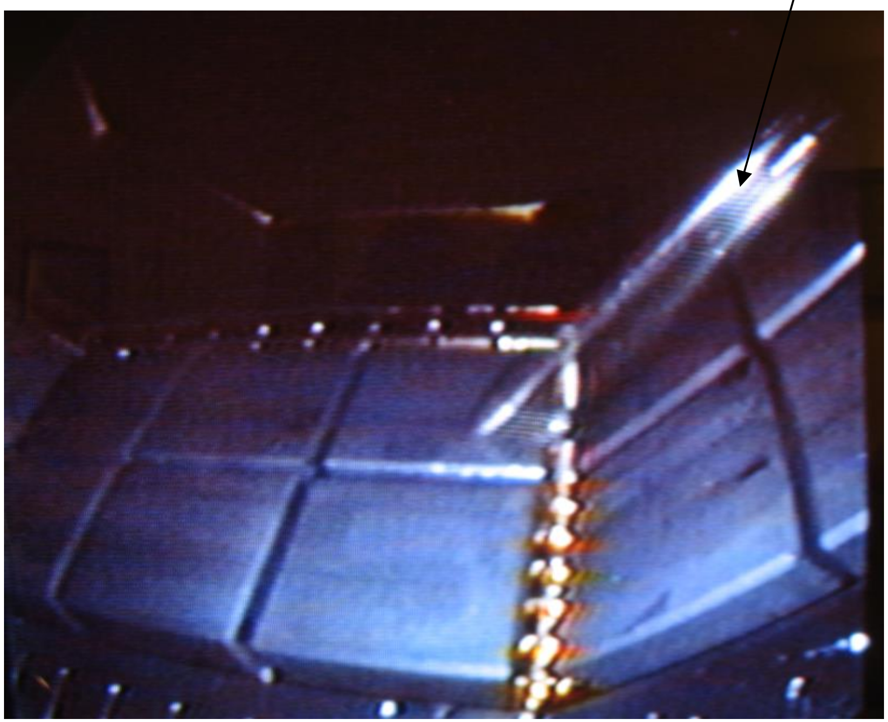

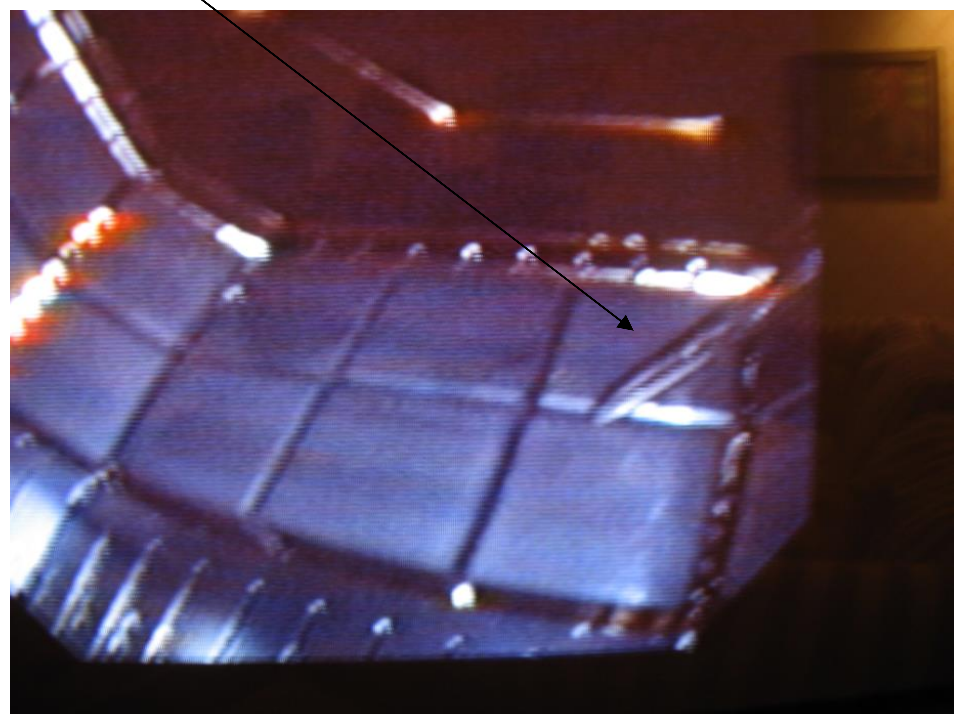

Beam induced burn marks

Tile Thermal Model

Closest match to Stan's in air measurements.

- 250 C at button
- 25 C body

Will do an in air analysis

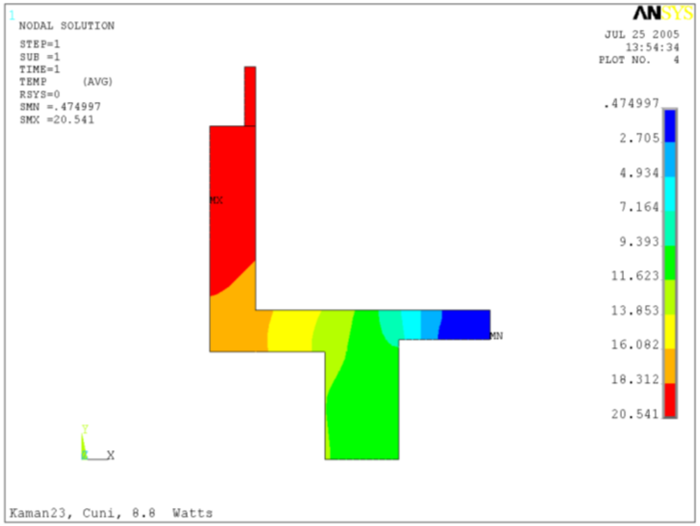

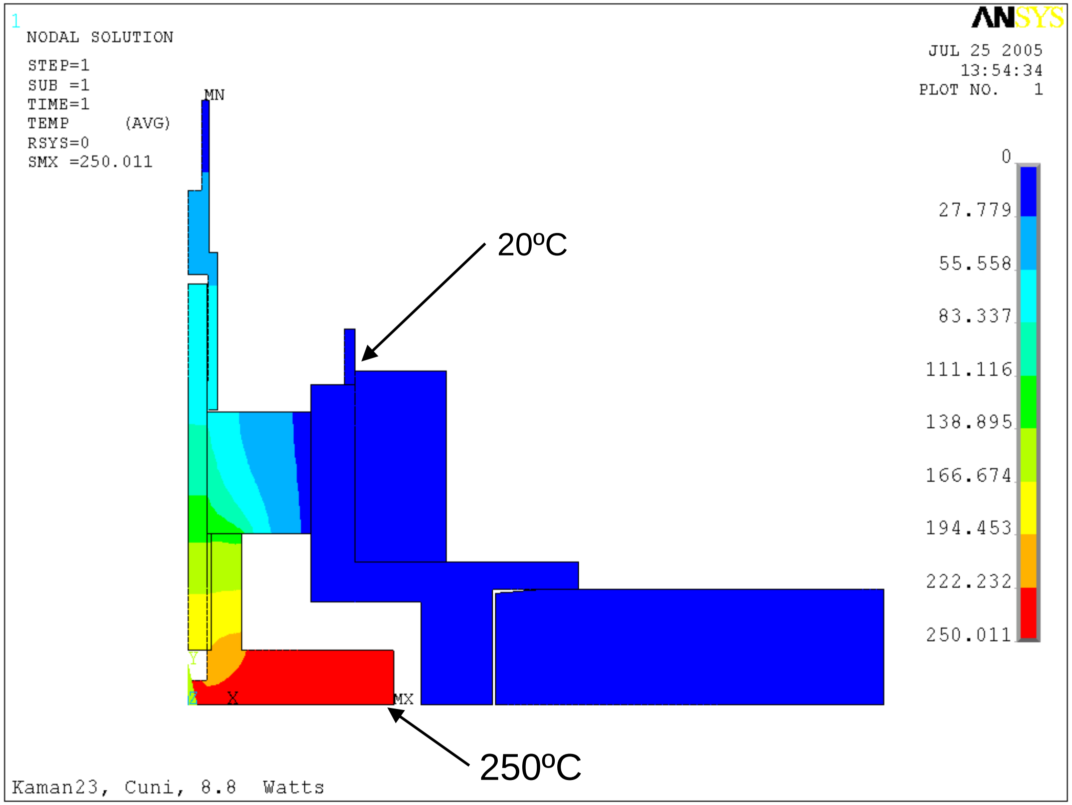

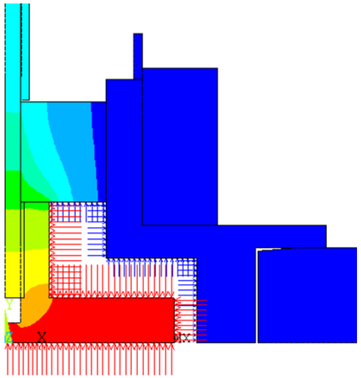

RF System

RF system layout

High power RF

Calculation and measurements of ring-wide HOMs

A Typical PEP-II RF System

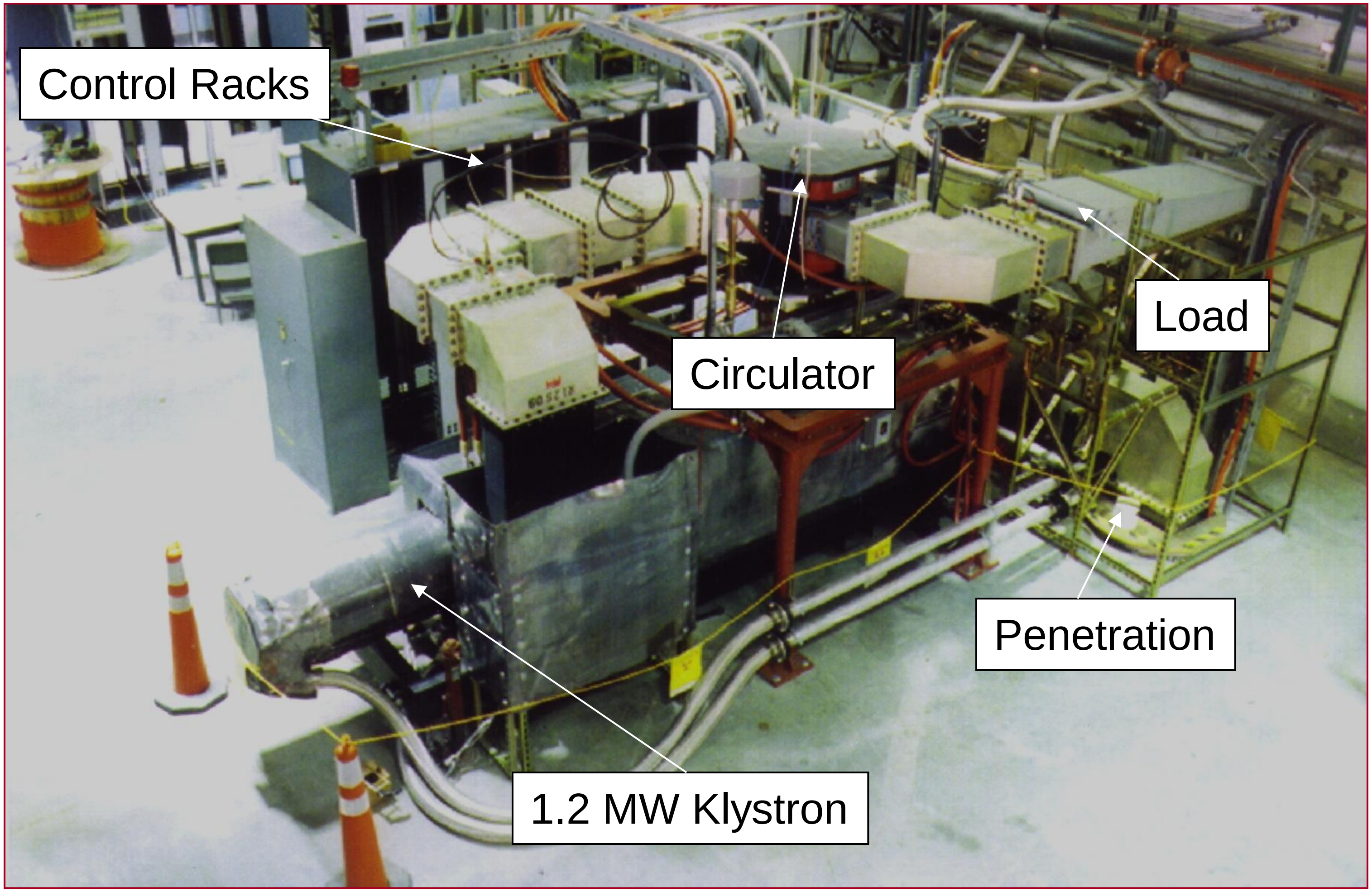

PEP-II RF Cavity

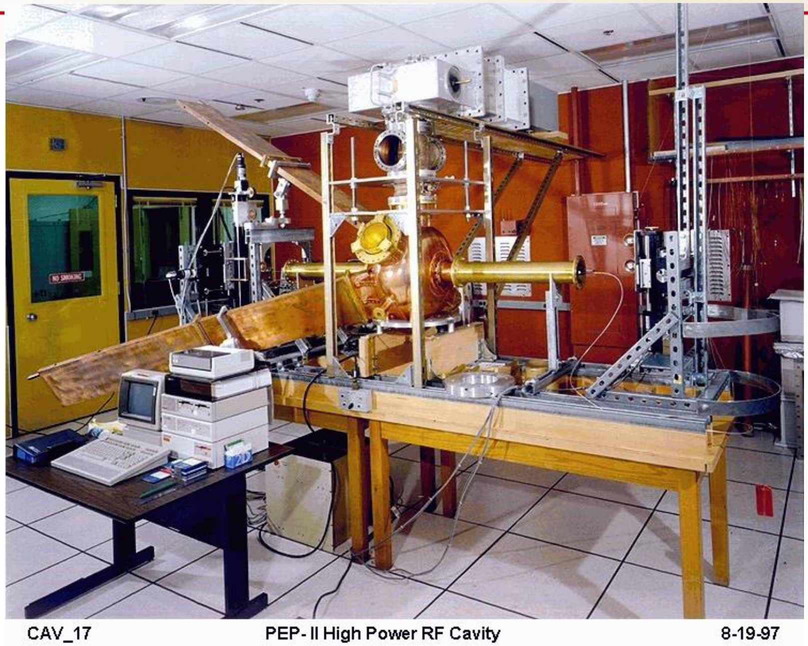

Early design and testing at LBL.

High power production cells.

Fully fitted cavity units with HOM dampers.

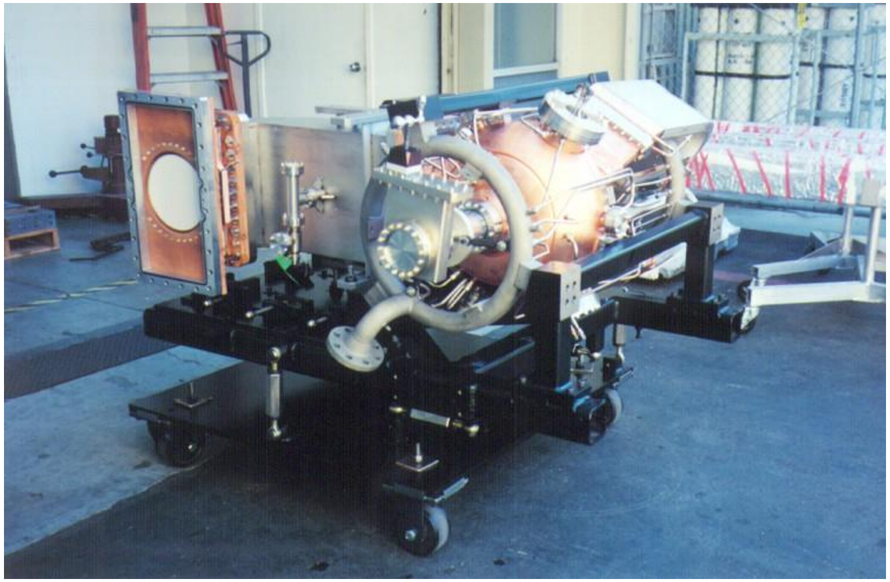

RF System Upgrades – HER 12-2

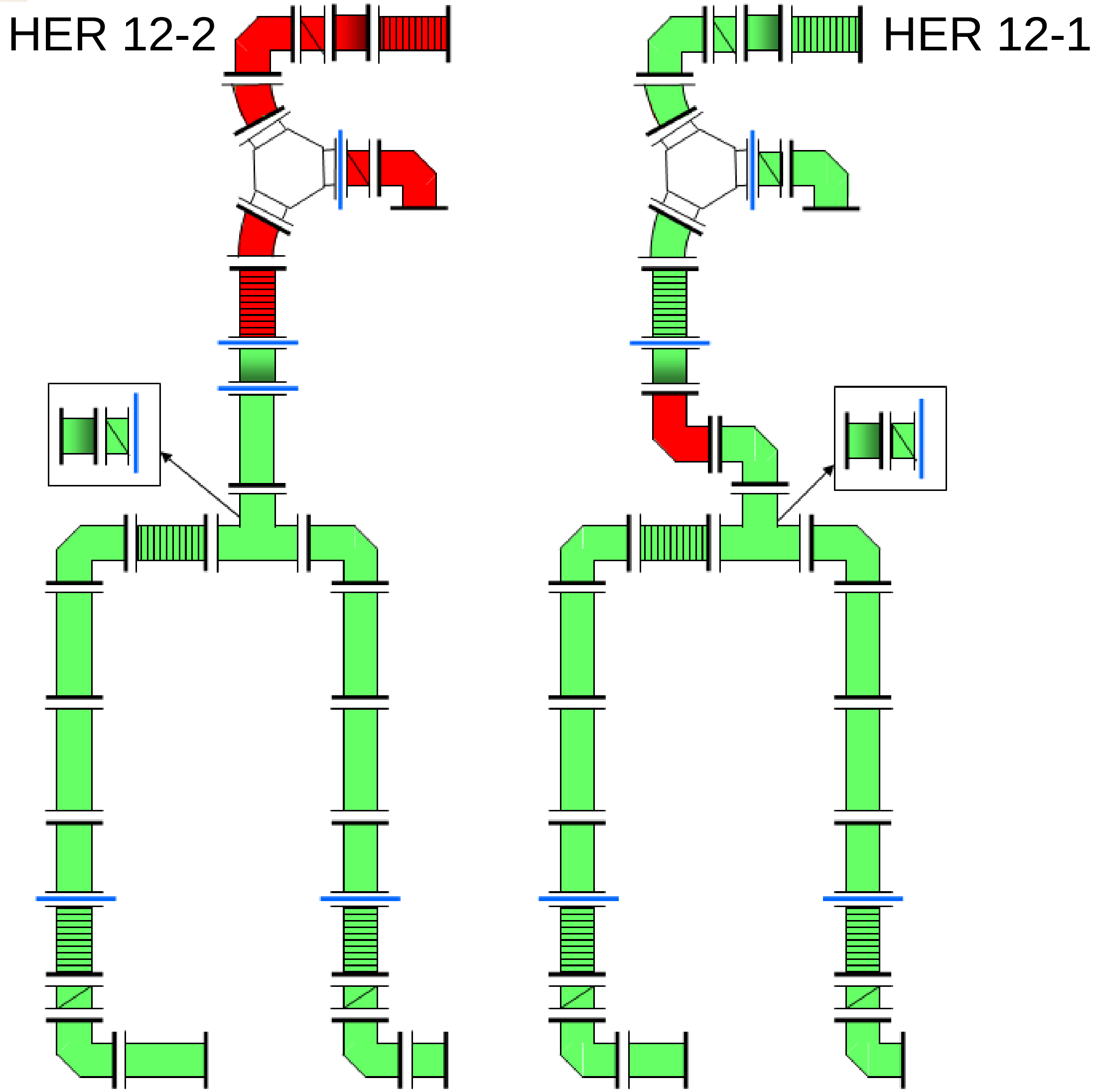

PEP-II RF Parameters (ca 2006) (P. McIntosh)

Table 1: PEP-II RF System Characteristics

RF Parameters	HER					LER				
	Jul 2001	**Jul 2004**	**Jul 2005**	**Jul 2006**	**Optimum 2006**	**Jul 2001**	**Jul 2004**	**Jul 2005**	**Jul 2006**	**Optimum 2006**
RF Voltage/Ring (MV)	10.6	16	16.7	17.5	**19.5**	3.5	3.8	5.05	6.8	**8.5**
Number of Klystrons	5	8	9	10	**10**	3	3	4	5	**5**
Number of Cavities	20	26	26	26	**26**	6	6	8	10	**10**
Average Gap Voltage/Cavity (kV)	530	615	642	673	**750**	583	633	631	680	**850**
Average Dissipated Power/Cavity (kW)	38	51	55	61	**75**	46	54	53	62	**97**
Average Beam Power/Cavity (kW)	161	215	222	233	**279**	186	289	270	264	**340**
Average Total RF Power/Cavity (kW)	199	266	277	294	**354**	231	343	323	326	**437**
Average Klystron Power (kW)	847	918	848	805	**966**	490	757	706	695	**914**
Beam Current (A)	0.9	1.55	1.6	1.68	**2**	1.62	2.45	3	3.6	**4.5**
Luminosity (10^{33} cm^{-2} s^{-1})	3.399	9.213	12.5	15.8	**23.5**	3.399	9.213	12.5	15.8	**23.5**

July 2006 optimum projections were unrealized.

Main mode. Electric Field Distribution

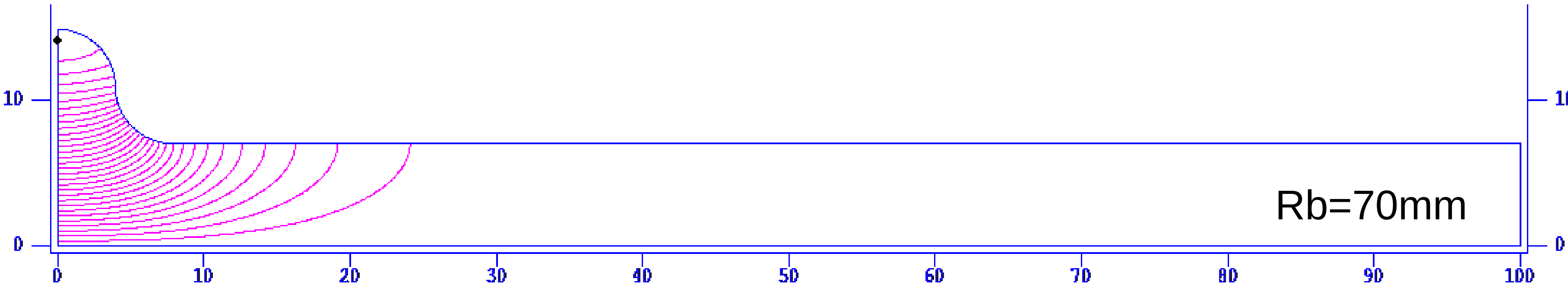

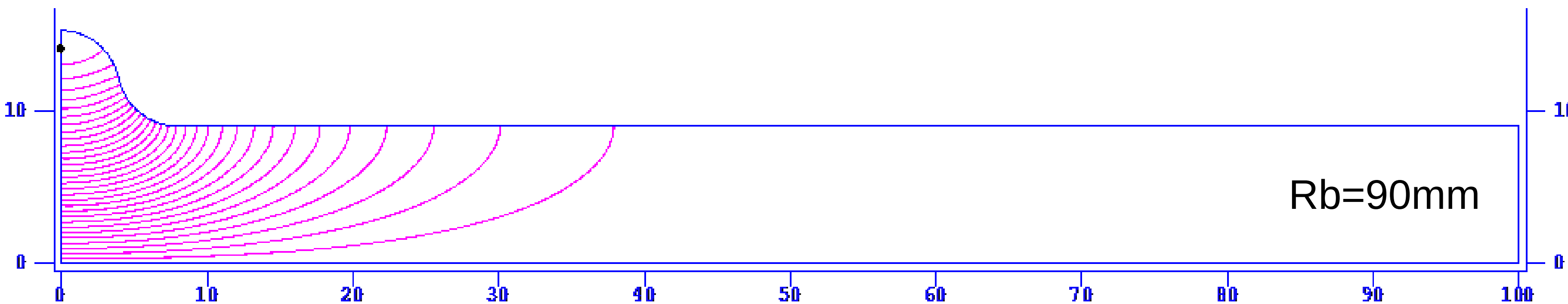

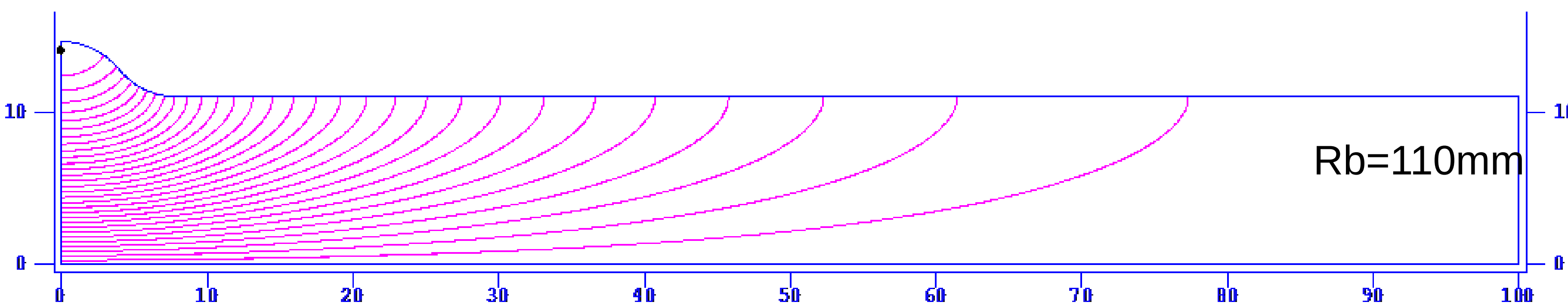

A bump does not decrease R/Q

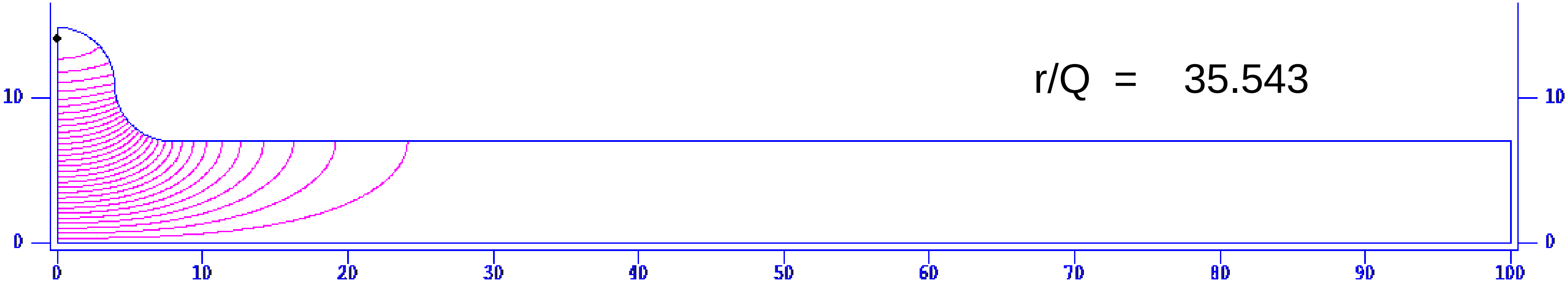

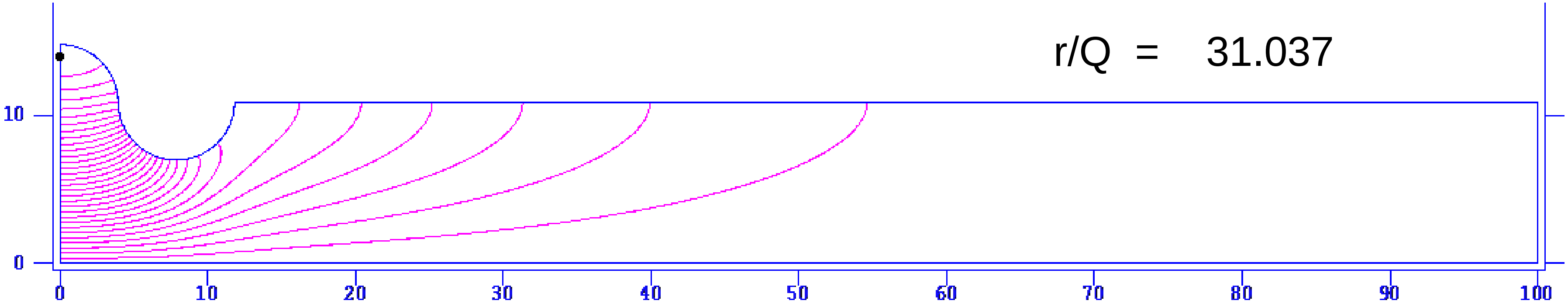

Checking dependence from bore radius
Two-radiuses cavity: λ/2

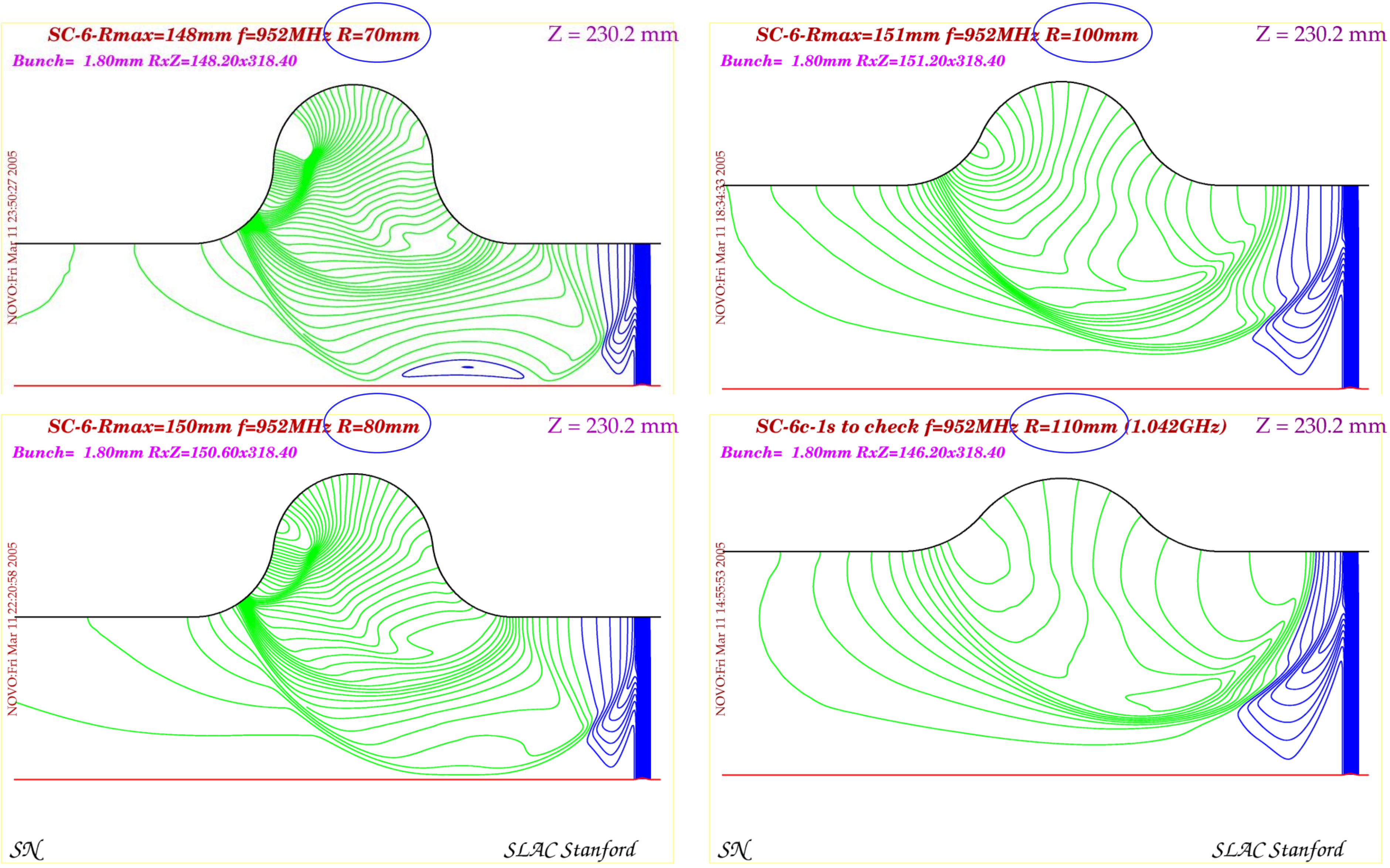

λ/2   Cavity length   λ/4

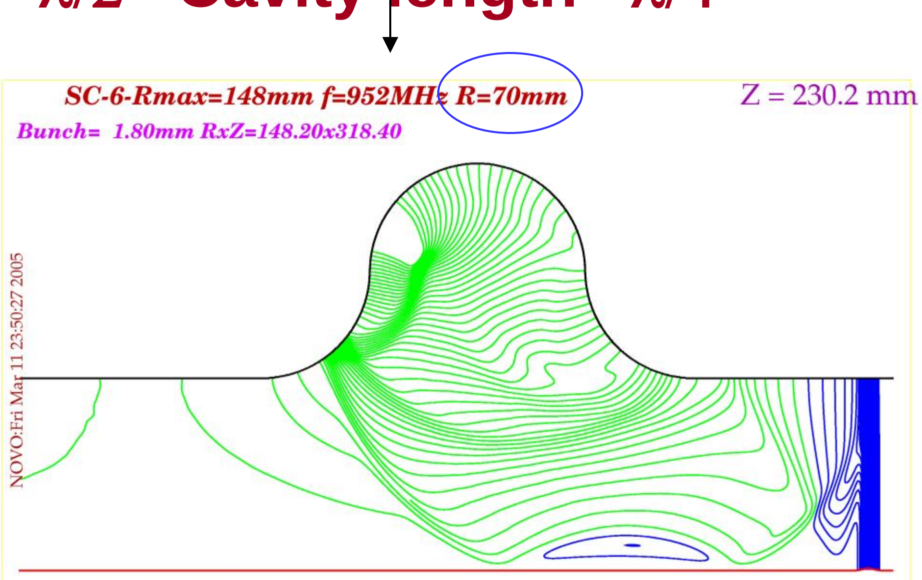

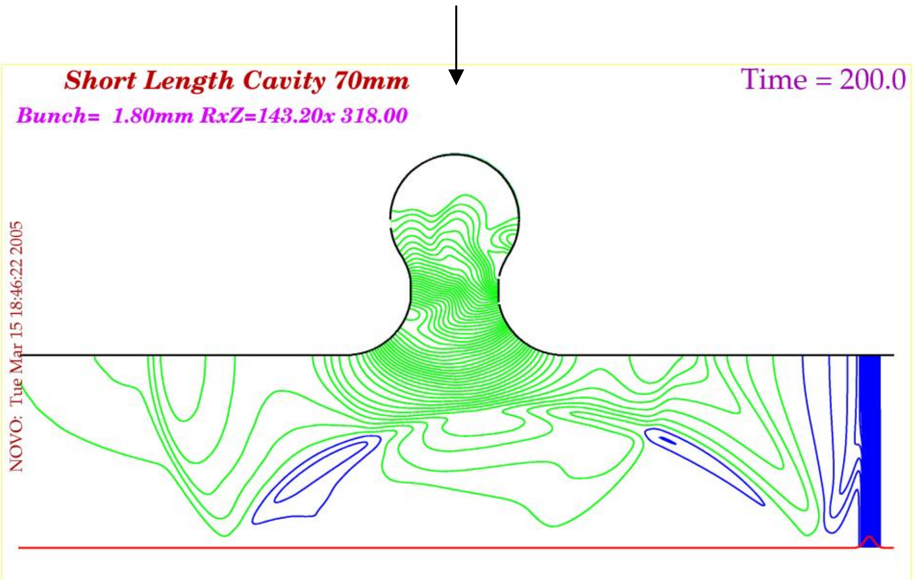

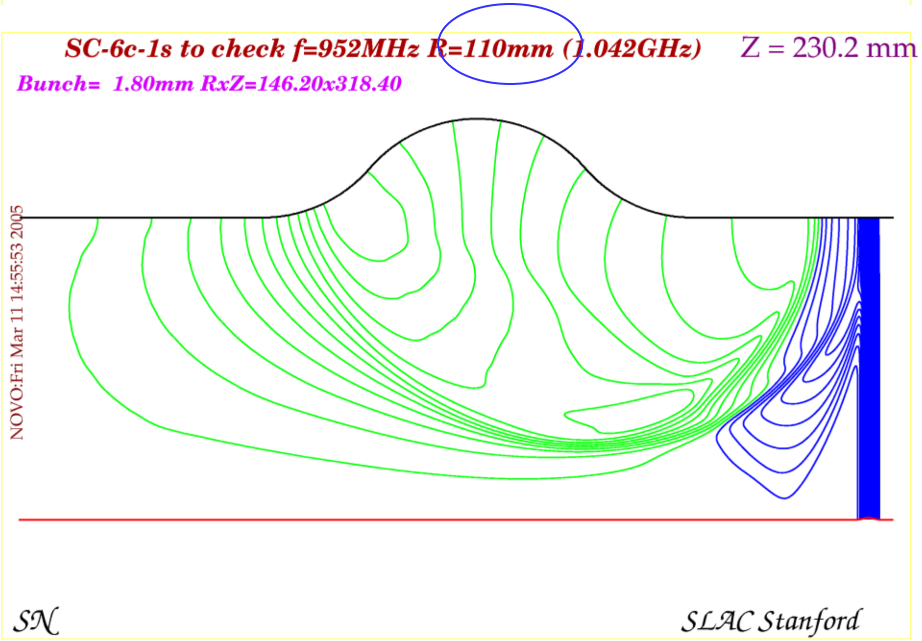

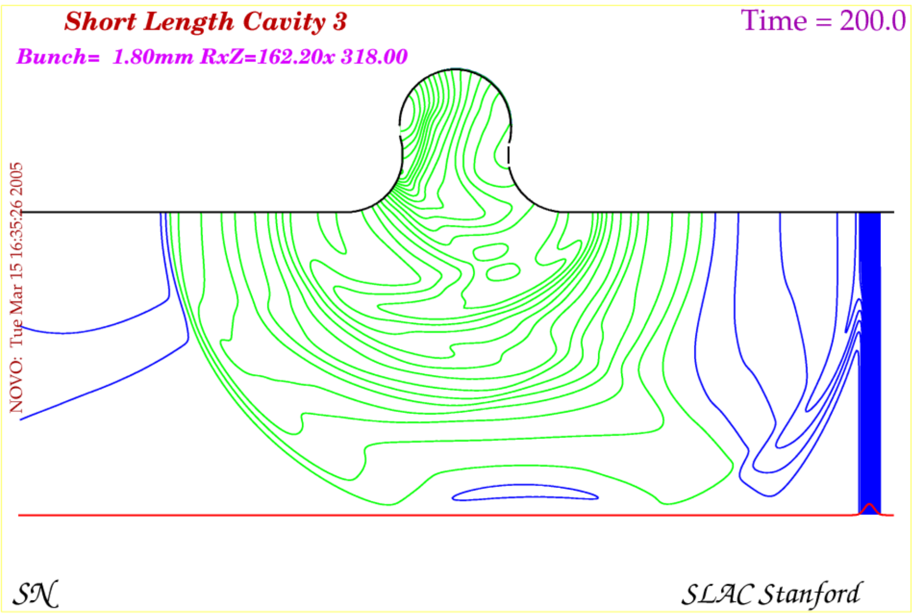

How cavity shape changes impedance for fixed bore radius

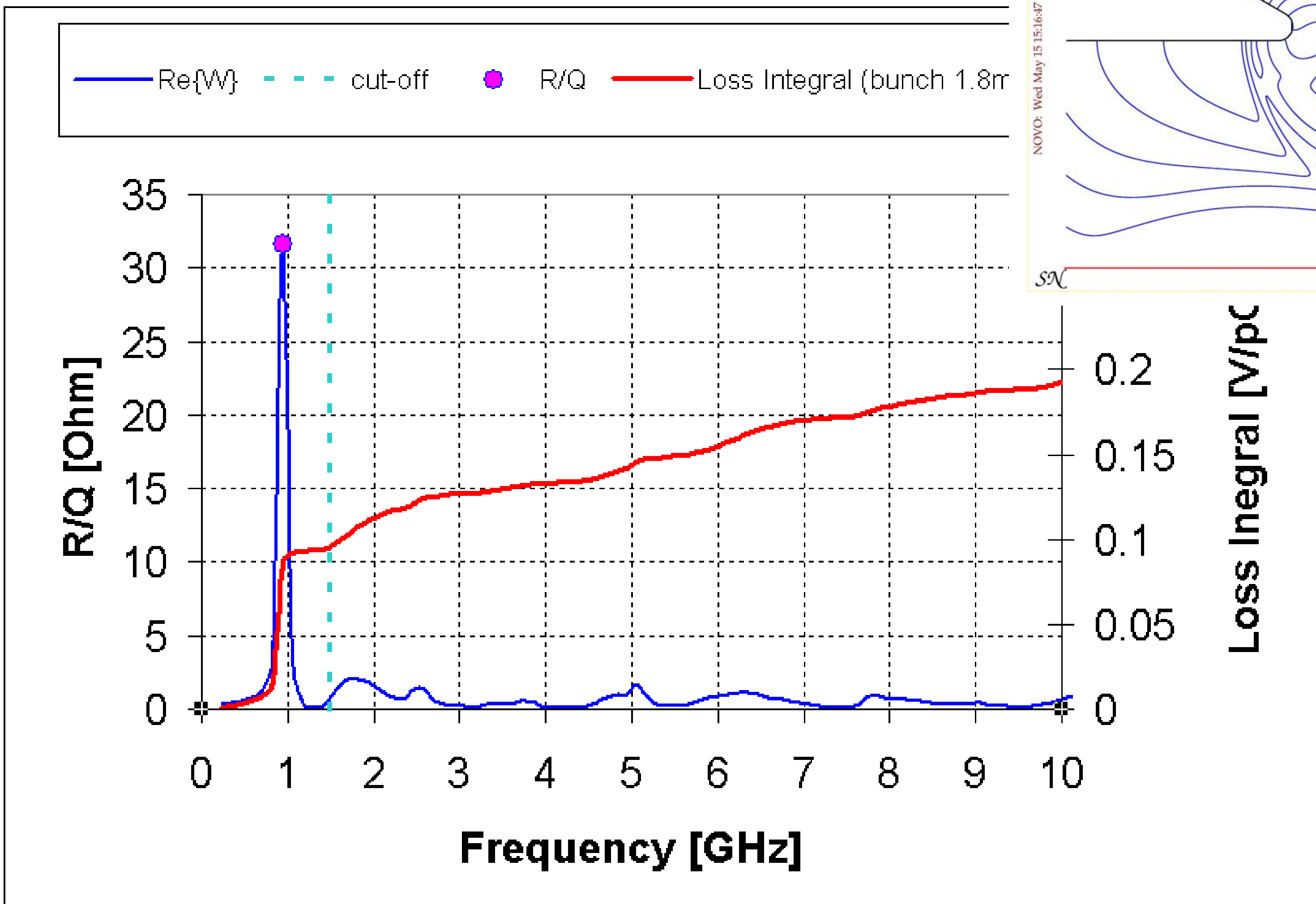

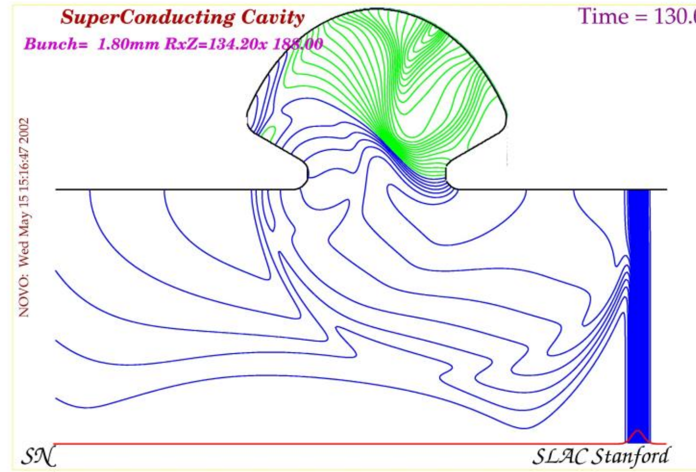

PEP-II (Novokhatski)

Power balance

$$\sum_{cav} P_{cav}^{forward} = \sum_{cav} P_{cav}^{reflected} + \sum_{cav} P_{cav}^{loss} + P_{beam}$$

Cavity loss
$$P_{cav}^{loss} = P_{cav}^{loss}(0)\left(\frac{U_{cav}(I)}{U_{cav}(0)}\right)^2$$

$$P_{beam} = U_{S.R.} \times I + Z_{HOMs} \times I^2$$

incoherent radiation — coherent radiation

Total forward power

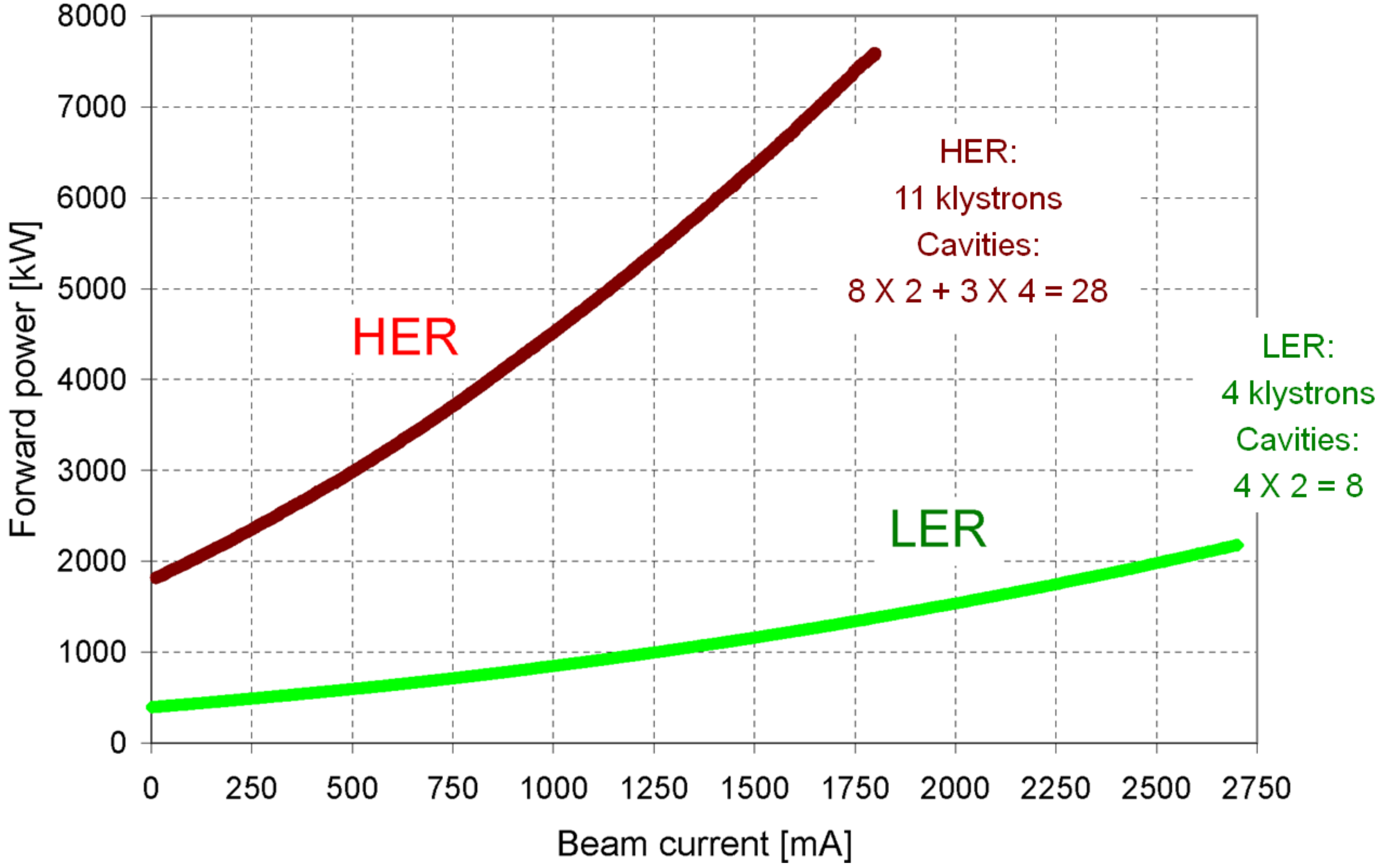

PEP-II

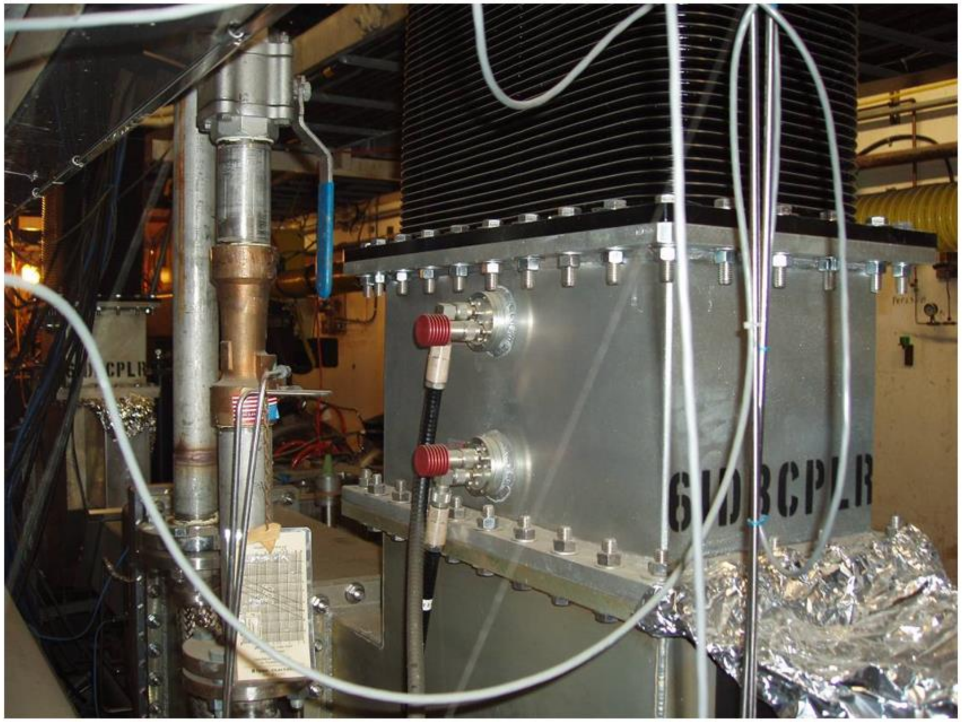

- SLAC directional couplers provide accurate data for a cavity incident and reflected power.
- HOM power is a part of RF power balance.

Beam power

(Forward power minus reflected minus cavity loss)

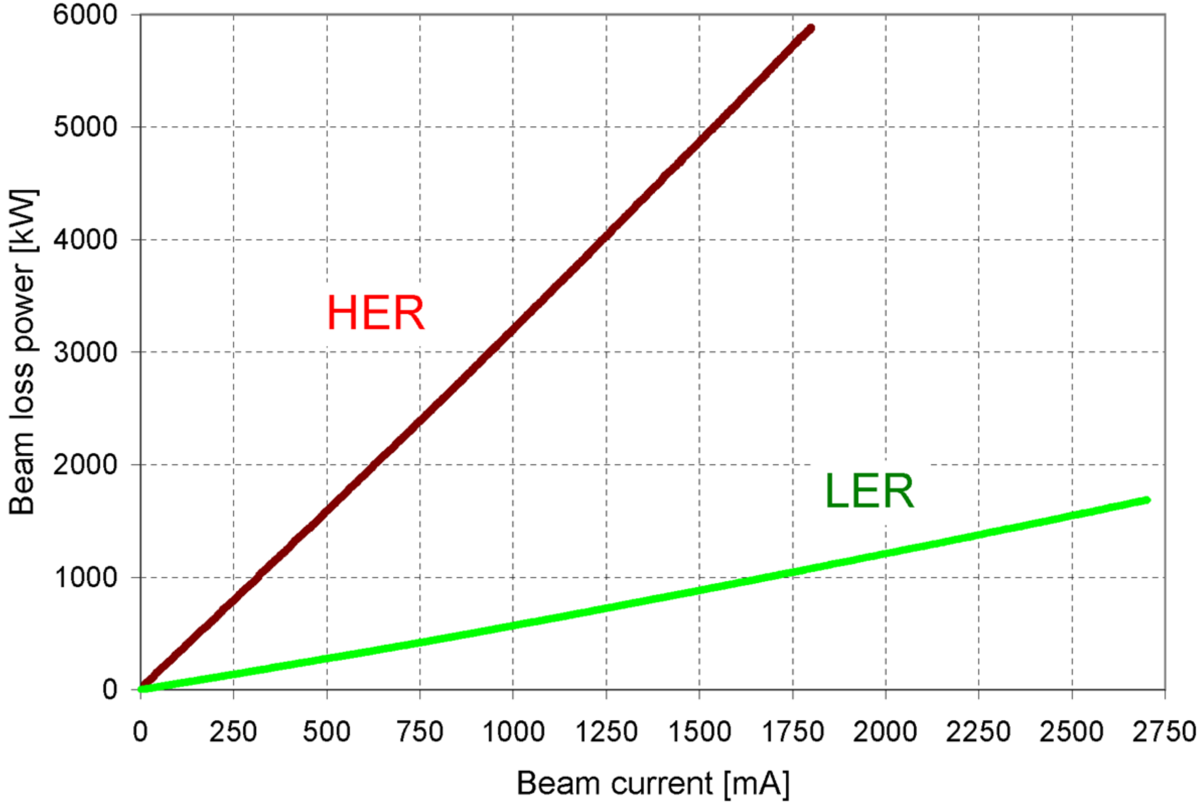

SLAC

Total reflected power

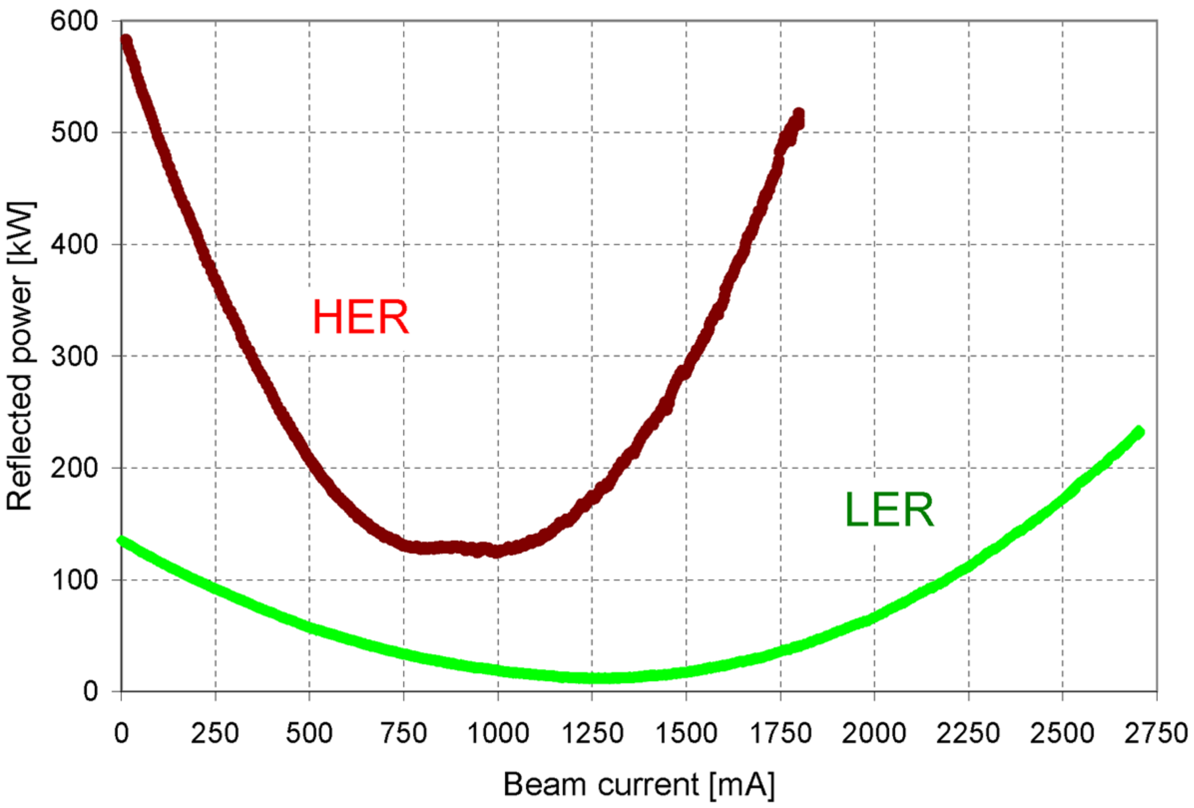

SLAC

HOM power

(Subtracting linear term form the beam power)

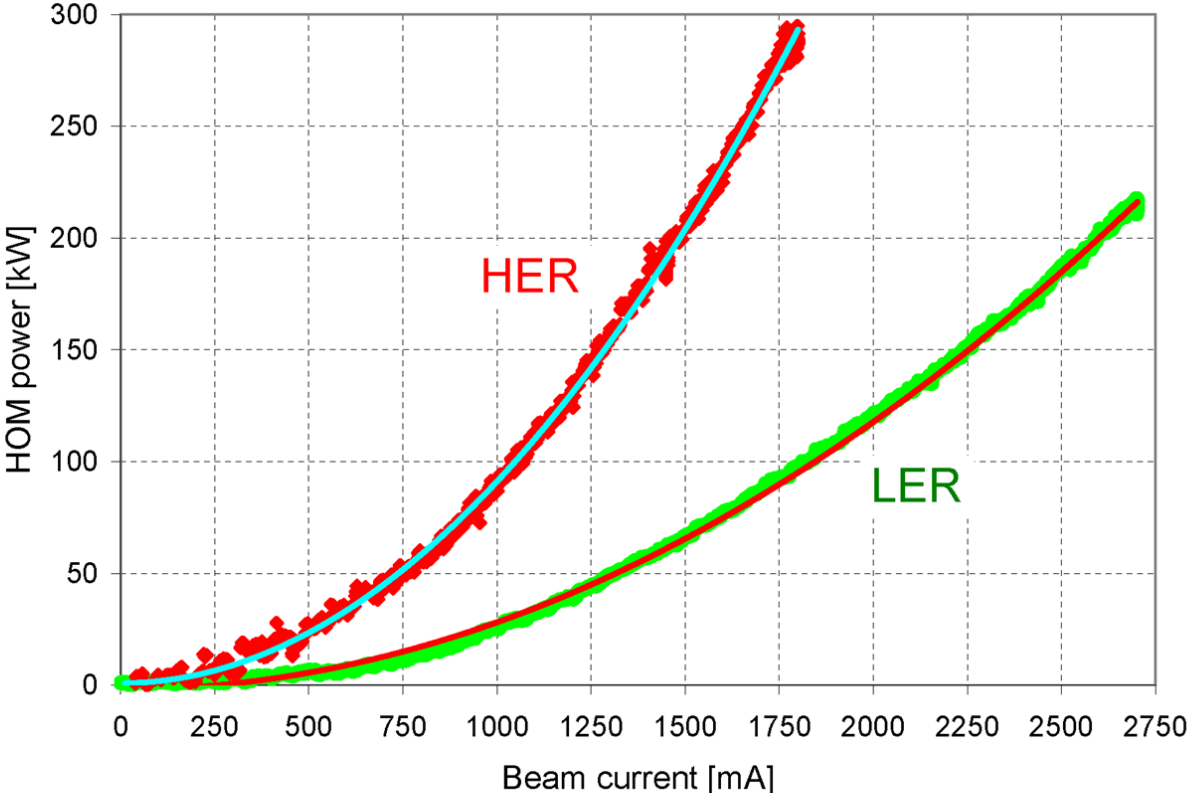

RF Power Measurements to Find HOM Power

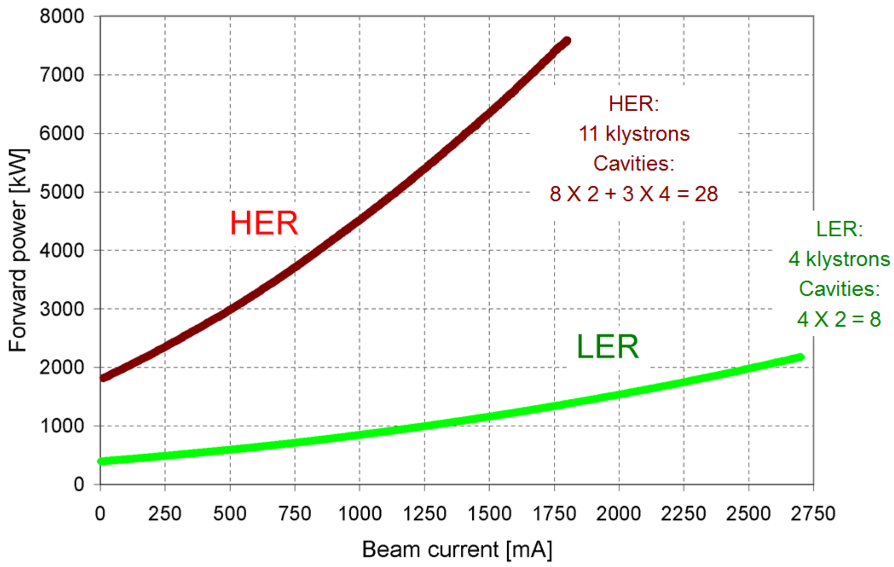

(Forward power minus reflected minus cavity loss)

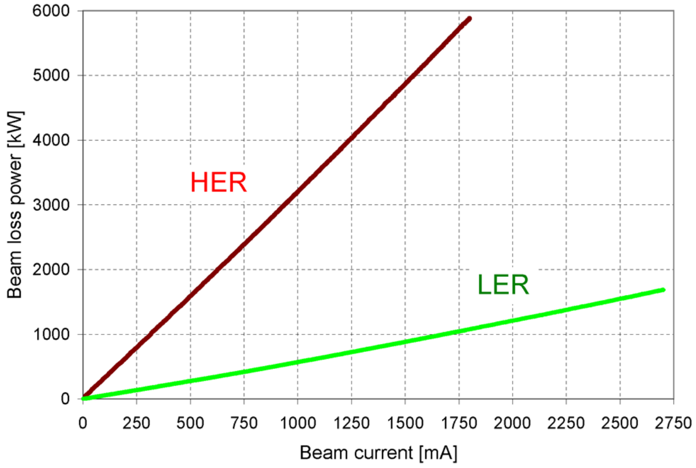

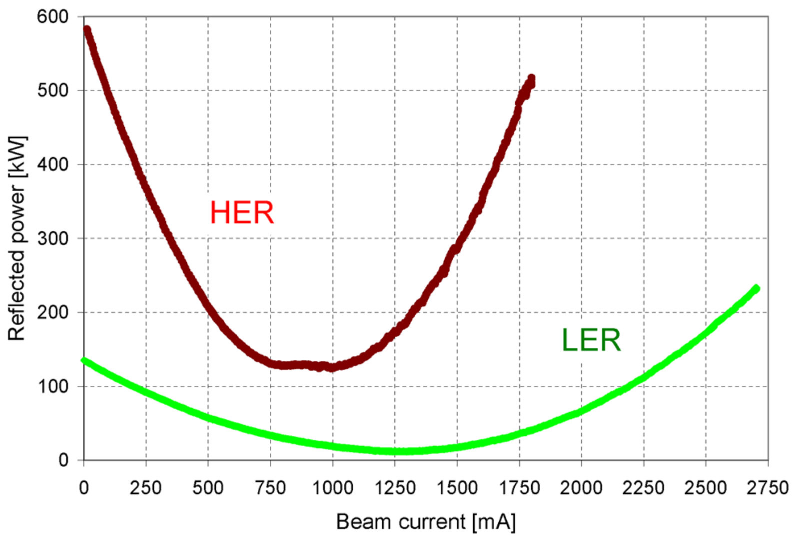

(Subtracting linear term form the beam power)

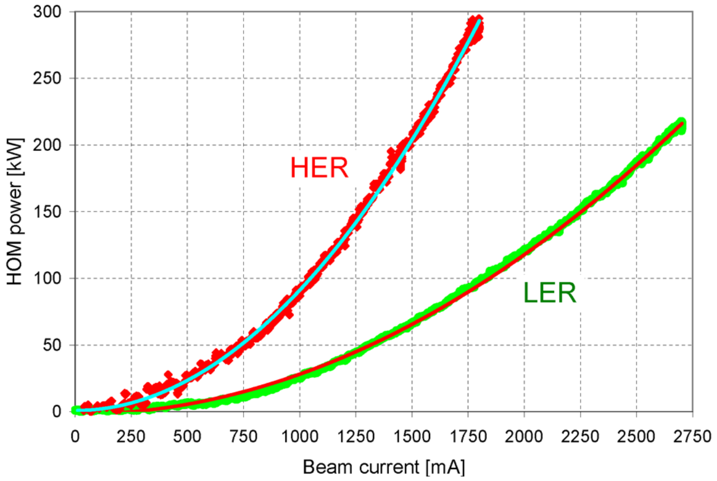

HOM Power in Q-2s

$$P_{[W]} = 146.2 \times Q_{[gpm]} \Delta T_{[^\circ F]}$$

Old

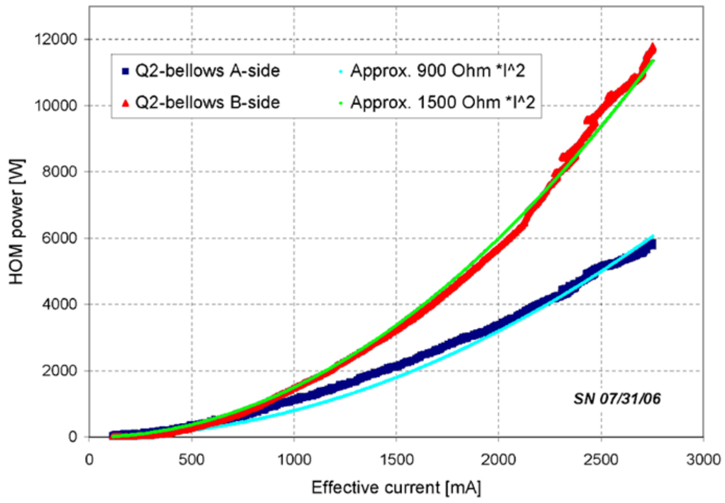

New

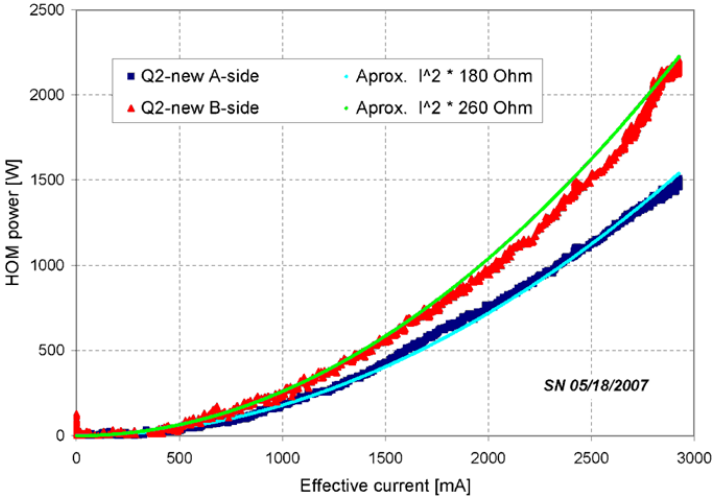

Effect: five times less power

HOM Loss Power versus Time

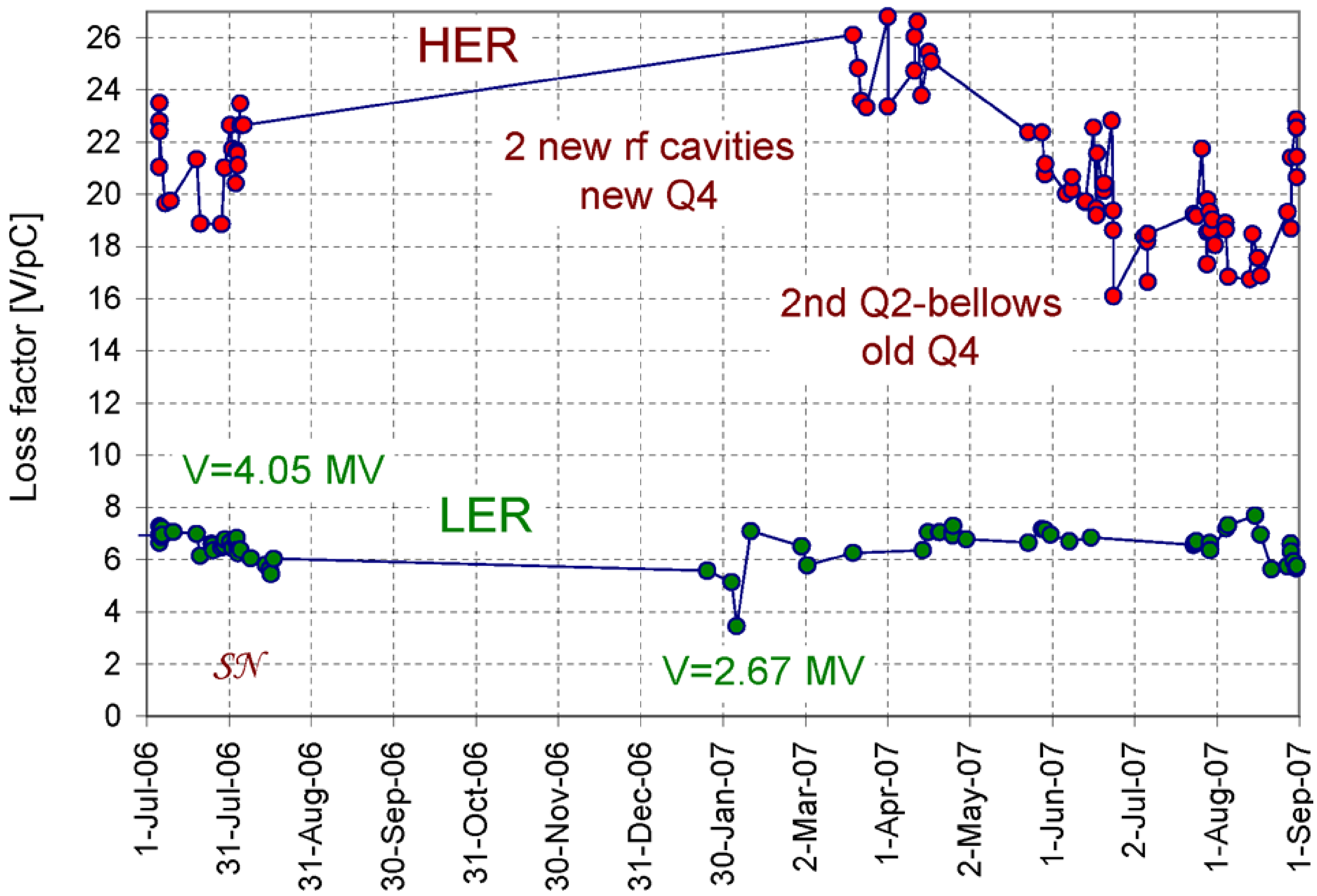

Moderate-fast real-time vacuum pressure monitoring from LER beam instability and loss

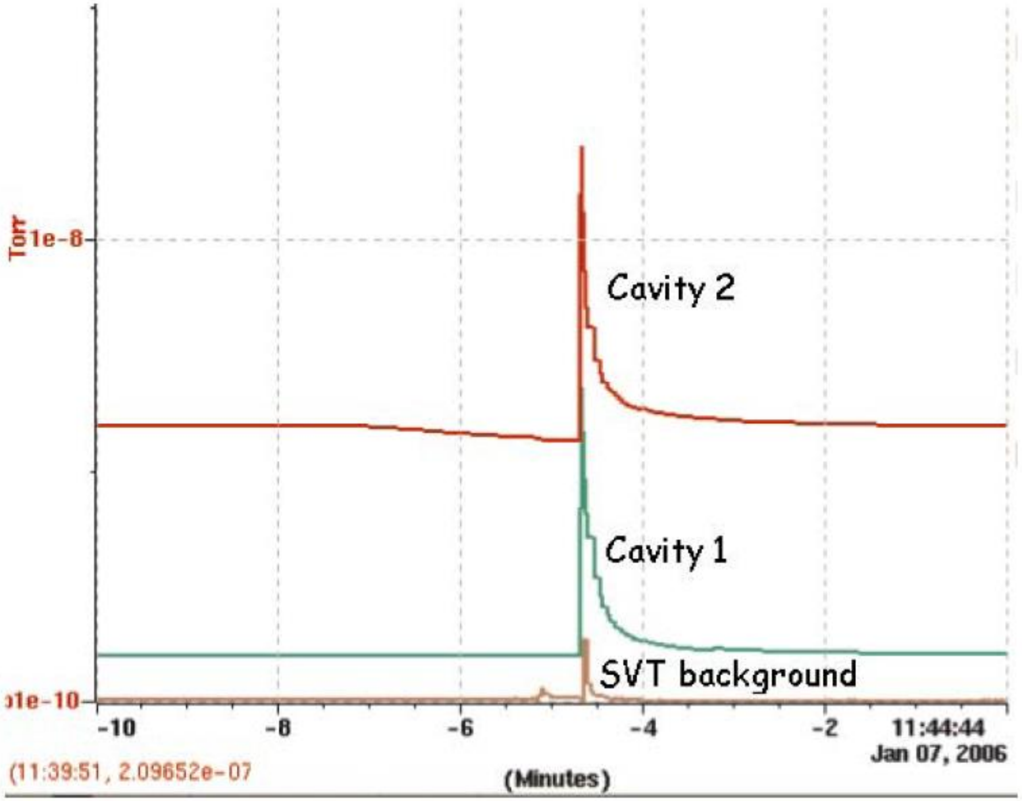

Figure 6: Spike in rf station 4-2 cavity vacuum pressure coincident with beam abort.

PEP-II HOM Measurements and RF Cavity Damage

HOM effect on RF cavity tuner

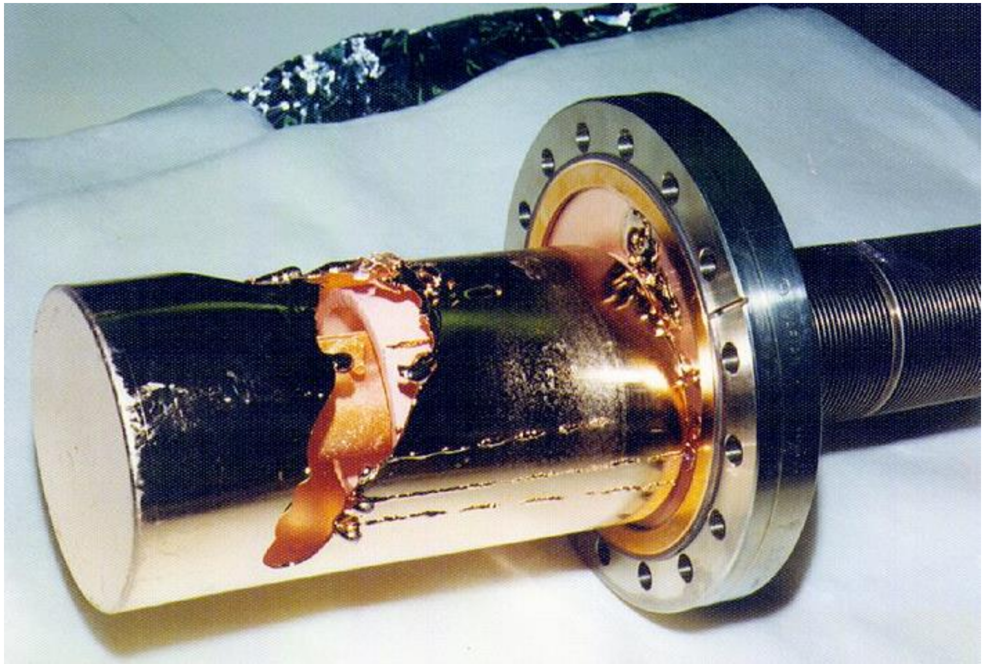

PEP-II longitudinal feedback system

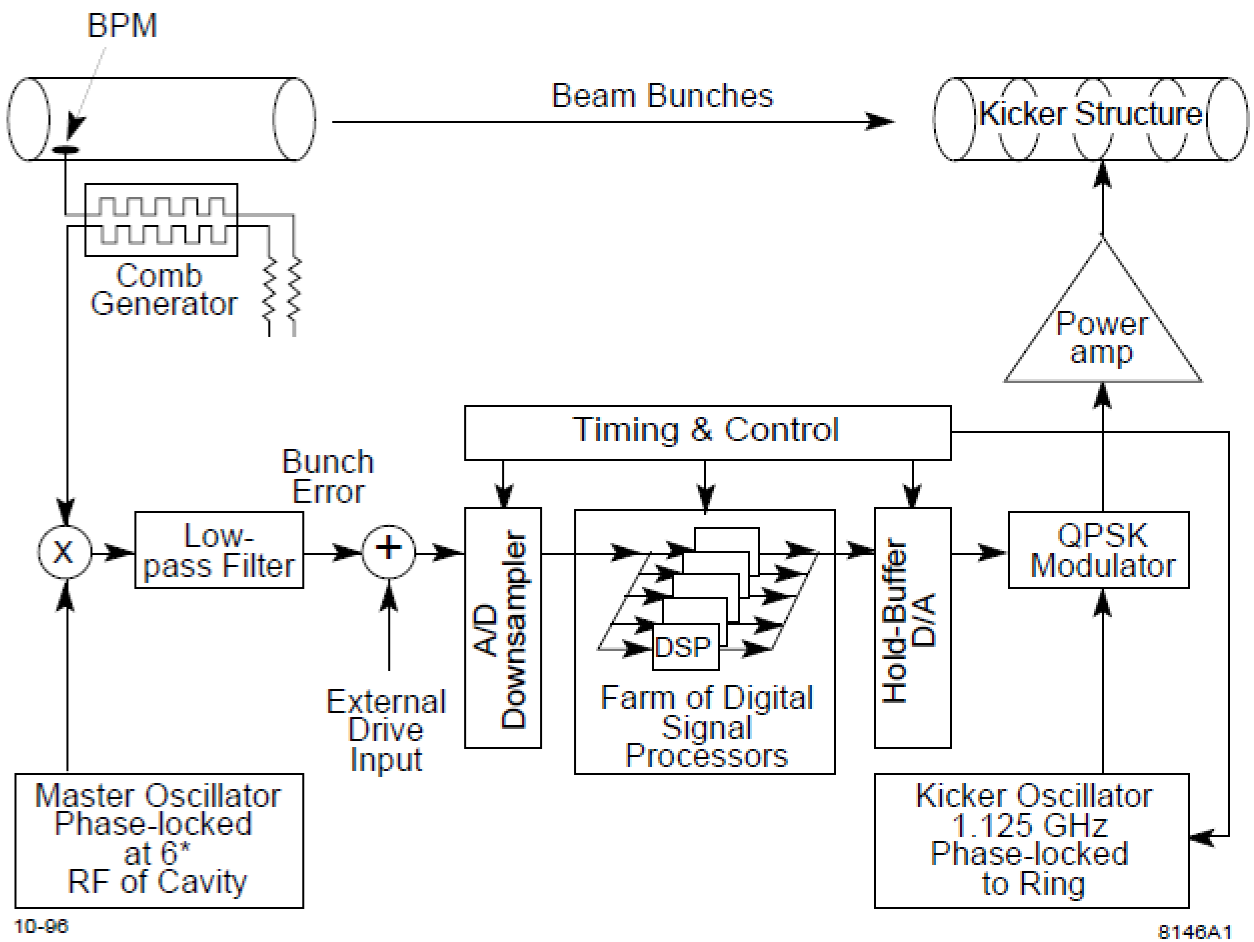

Figure 1: Longitudinal Feedback System.

Longitudinal Feedback Kicker Design

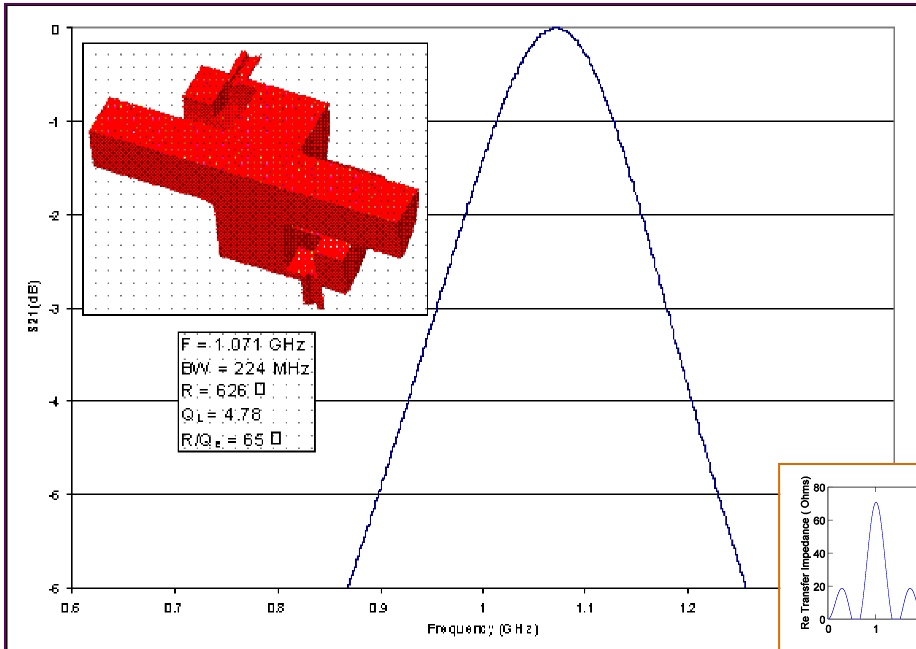

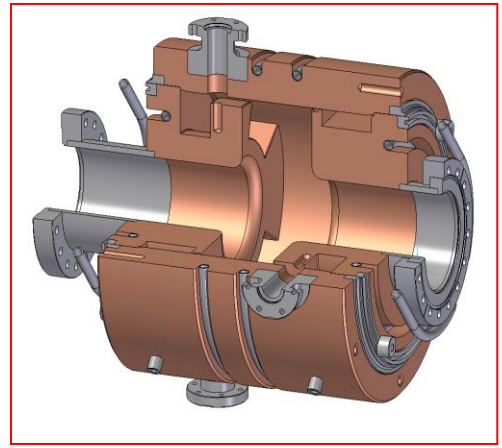

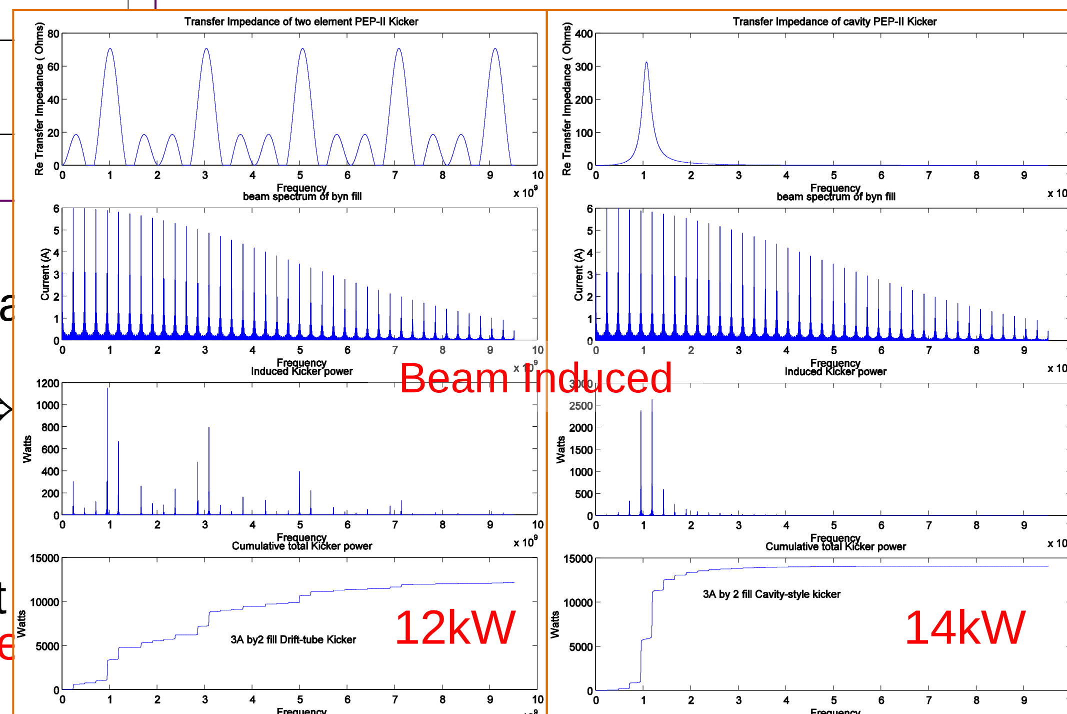

Existing drift-tube kickers have directivity ⇒ HOM power extracted via the 2 load ports

New cavity-kicker has no directivity ⇒ HOM power extracted via all 4 coupling ports, ∴ less power/feedthrough

New cavity-kicker has twice the shunt impedance of drift-tube kicker ⇒ more efficient!

RF System Upgrades - New LFB Kicker Feedthroughs

As V_{RF} in LER increased ⇒ bunch length reduces.
HOM heating ⇒ damage of LFB kicker feedthroughs and cables, which has limited LER currents:


In collaboration with INFN-Frascati and KEK, a new LFB cavity kicker has been designed and fabricated at SLAC.

A new high power, broadband feedthrough has also been designed at SLAC and manufactured by industry.

2 kickers will be installed in summer 2004.

New High Power RF Feedthrough

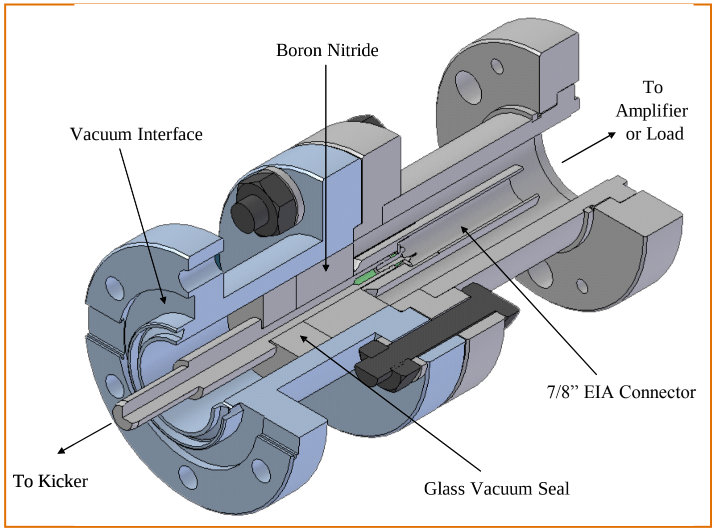

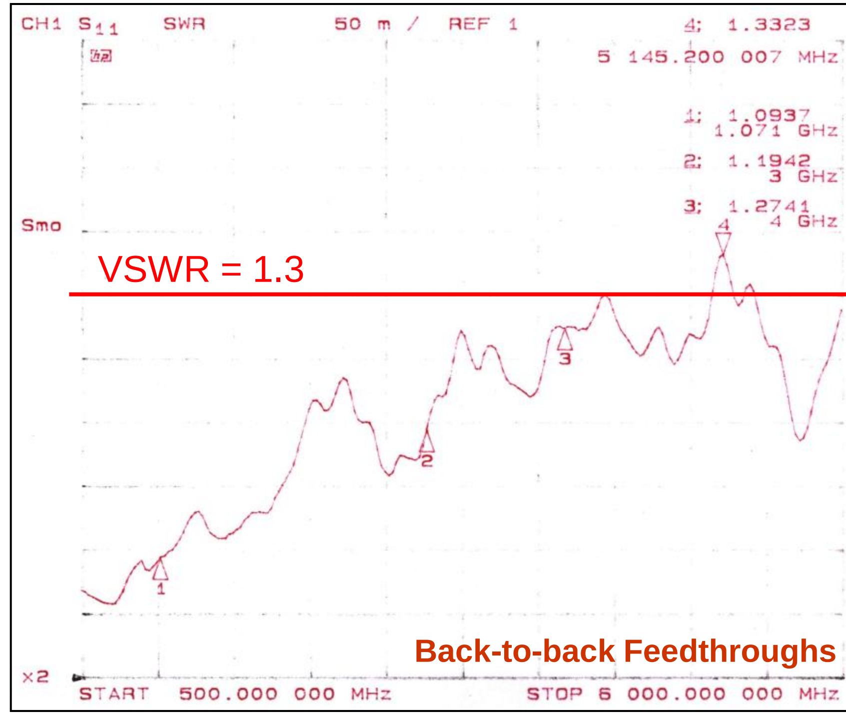

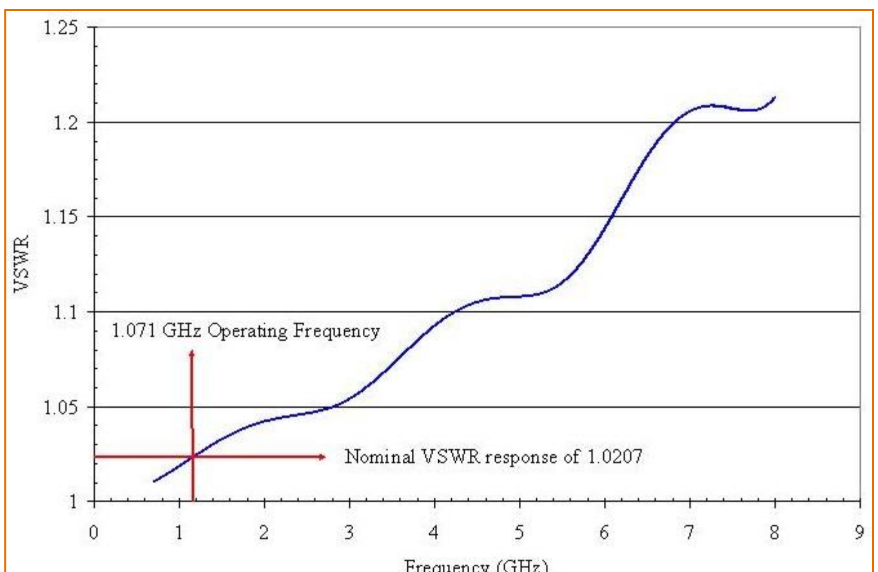

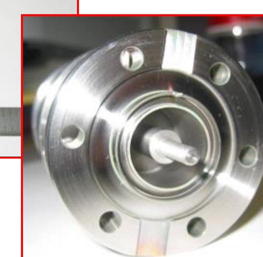

Interaction Region Chamber HOMs and Heating

Chamber geometry

Beam interaction

Chamber heating and temperature

Interaction Region Support Tube

Be chamber

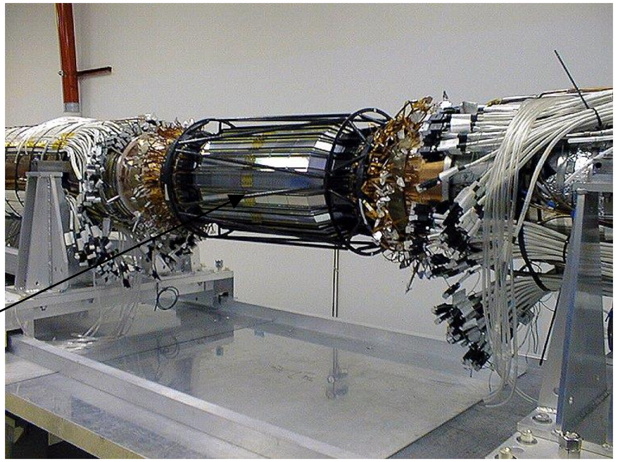

Silicon
Vertex
Tracker
SVT

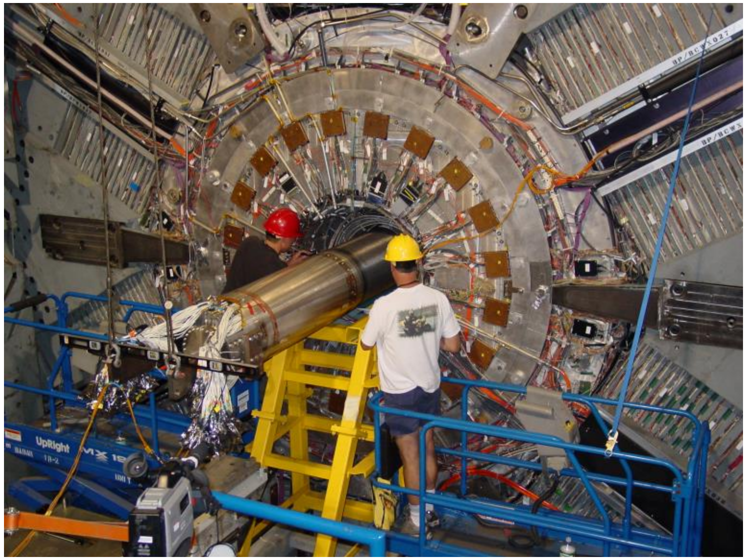

LER Forward Q4 Location

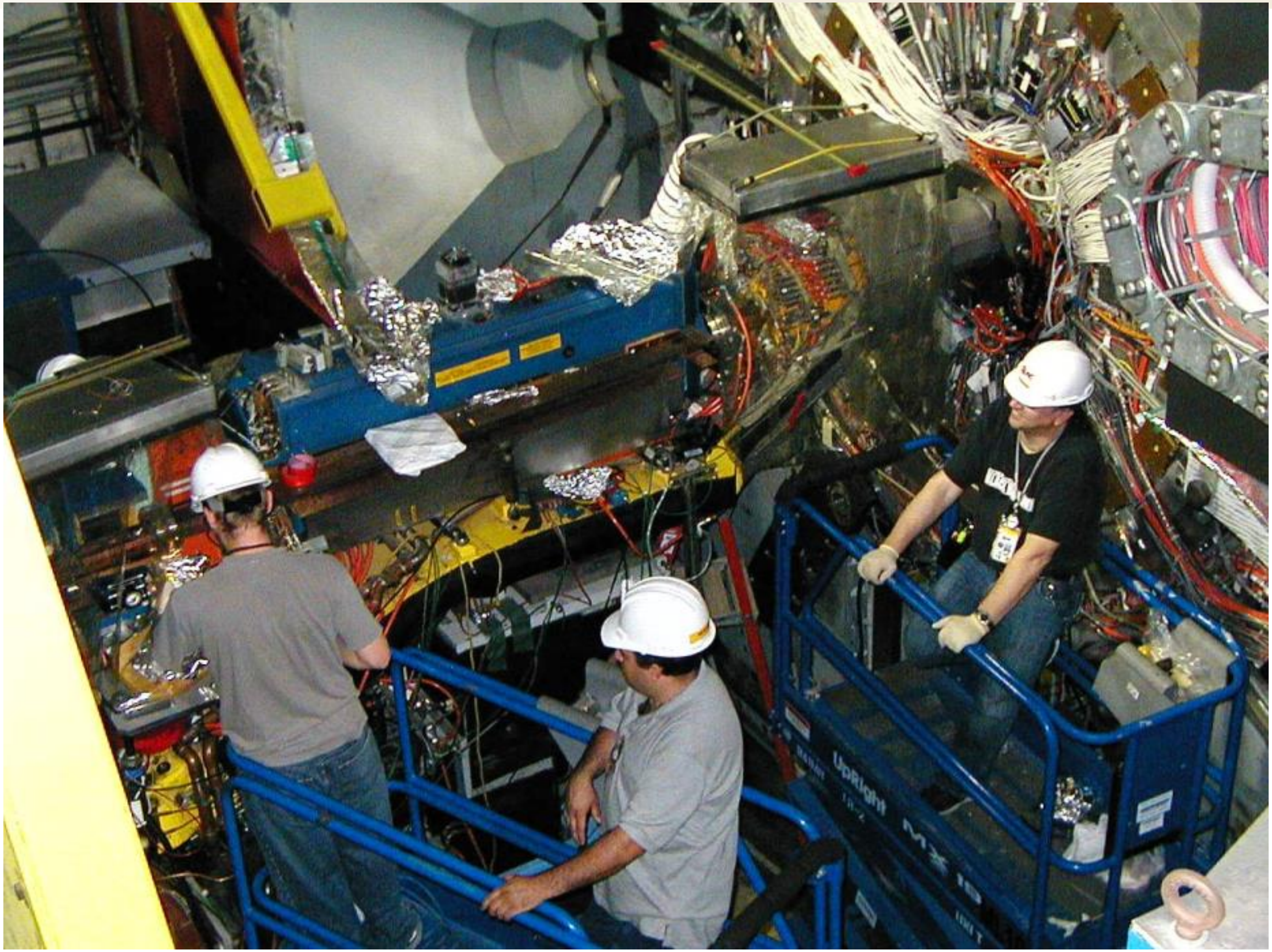

PEP-II and BaBar interaction region luminous region measurements

PEP-II vertex chamber and B1 dipoles

VTX Bellows Cooling Installation

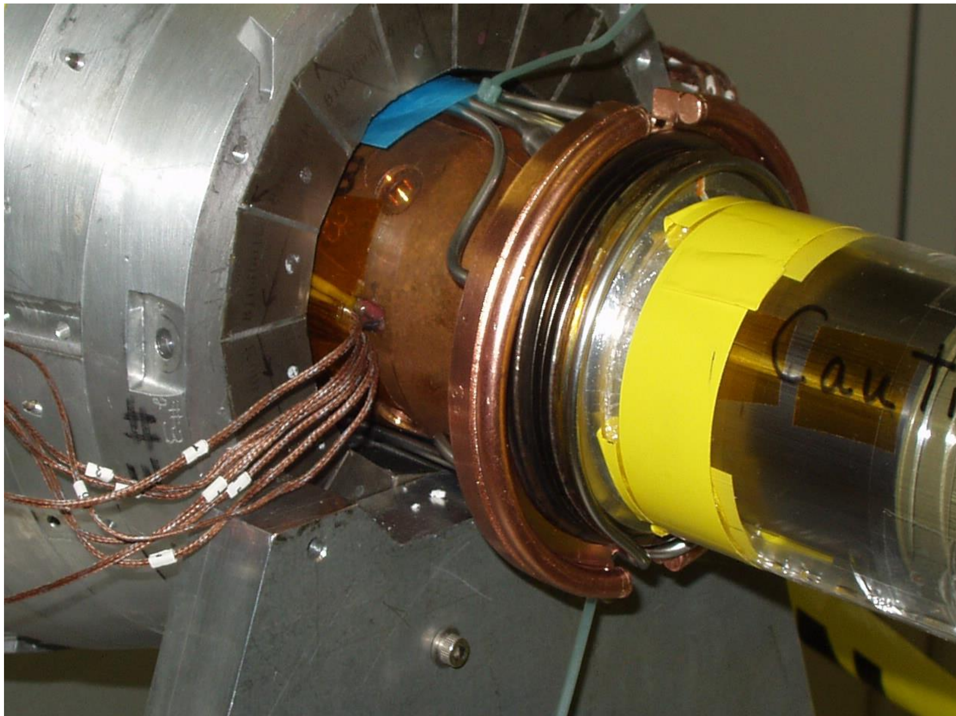

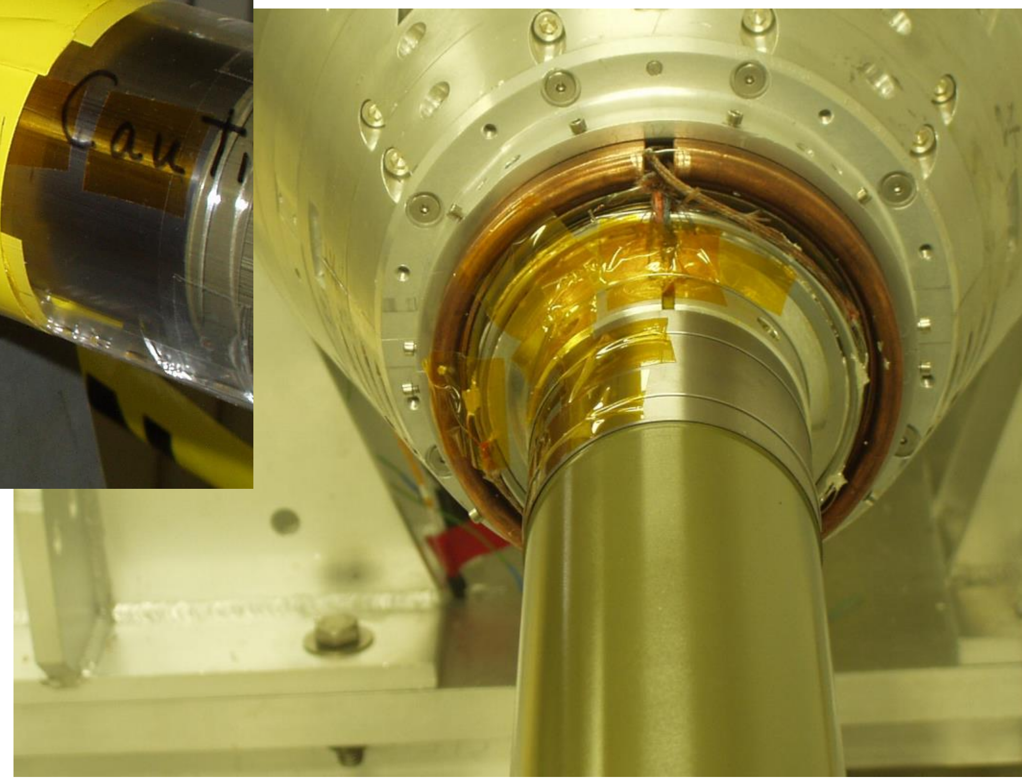

IR Vacuum Chambers

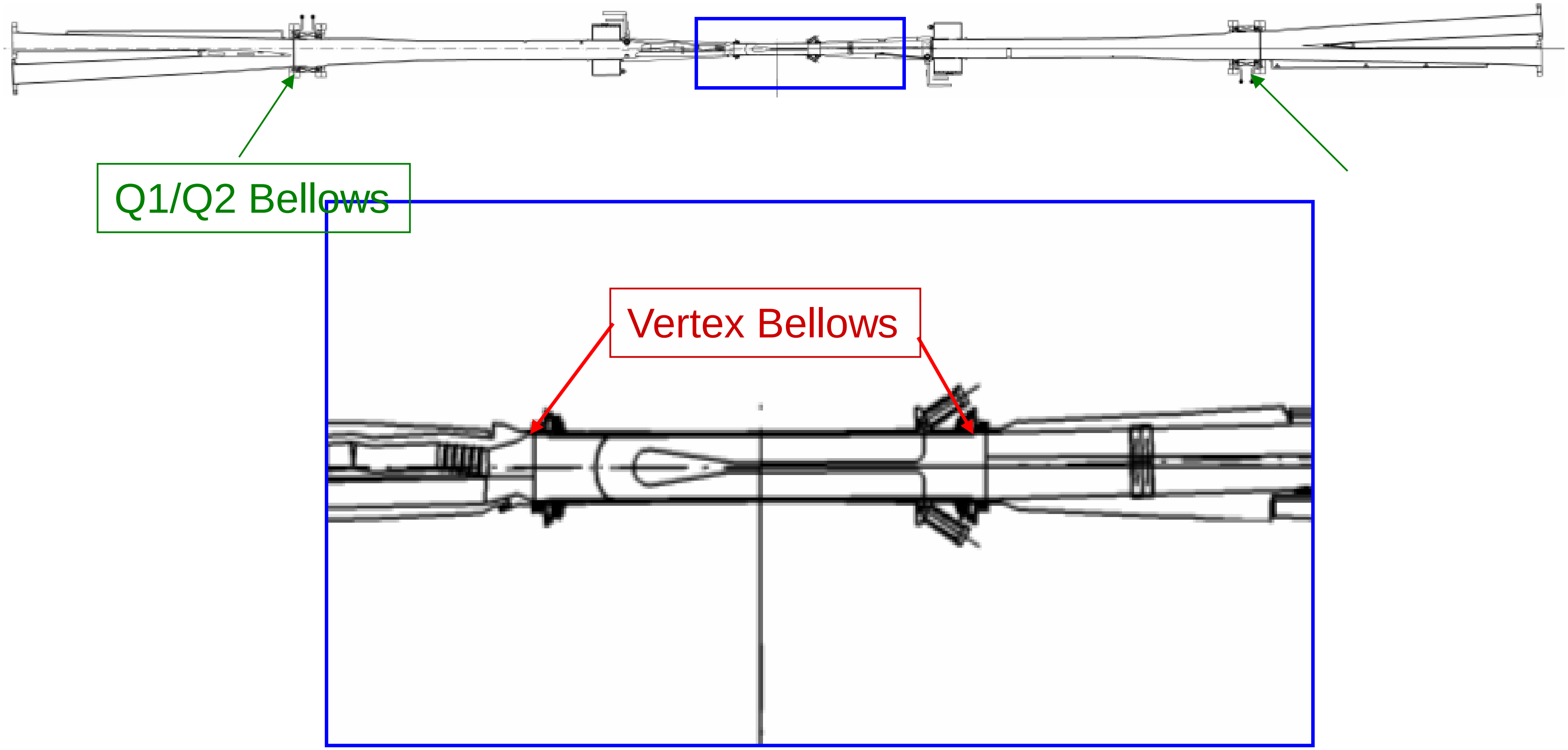

Forward Vertex Bellows – Before Cooling

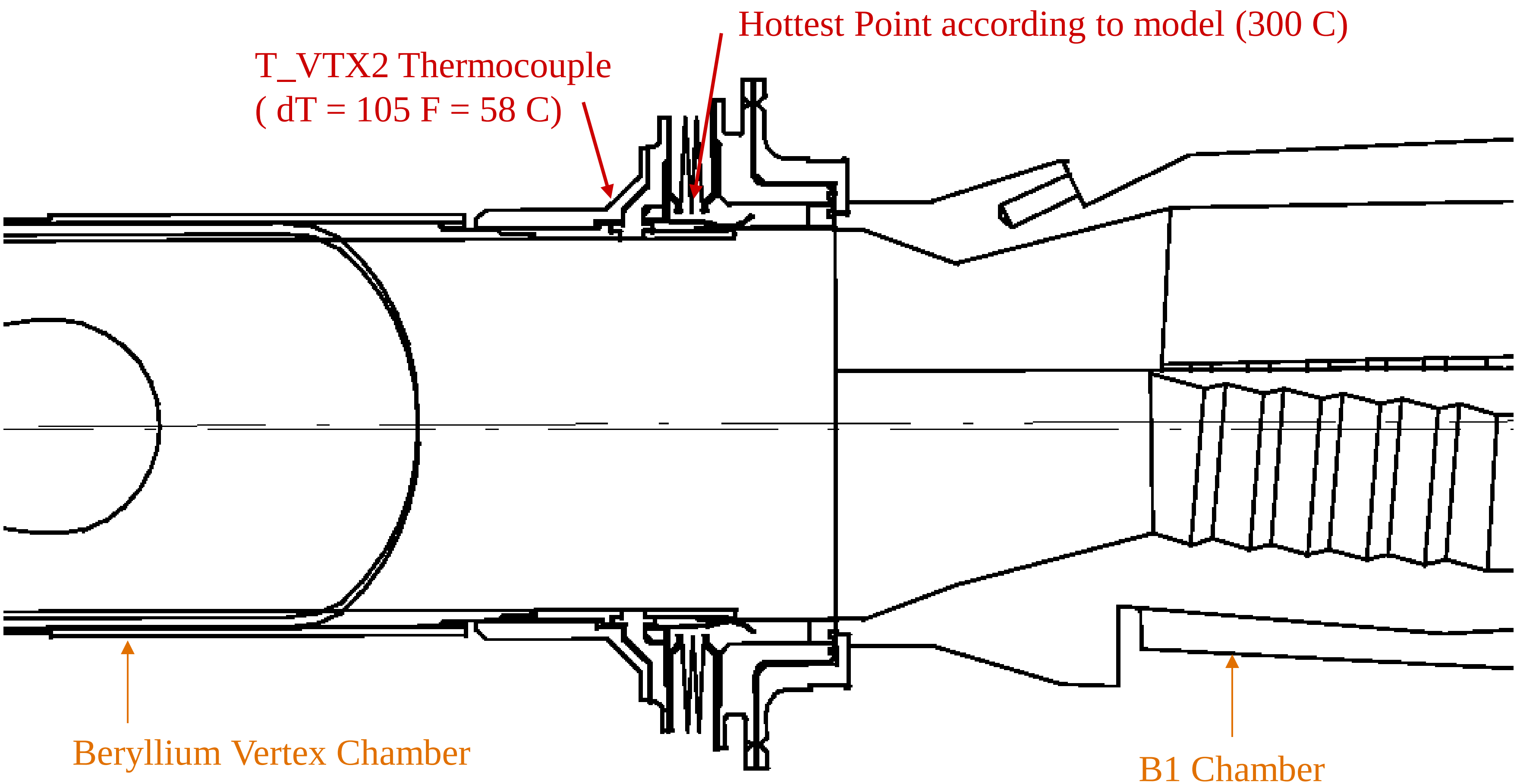

Forward VTX BLWS Cooling

Ecklund

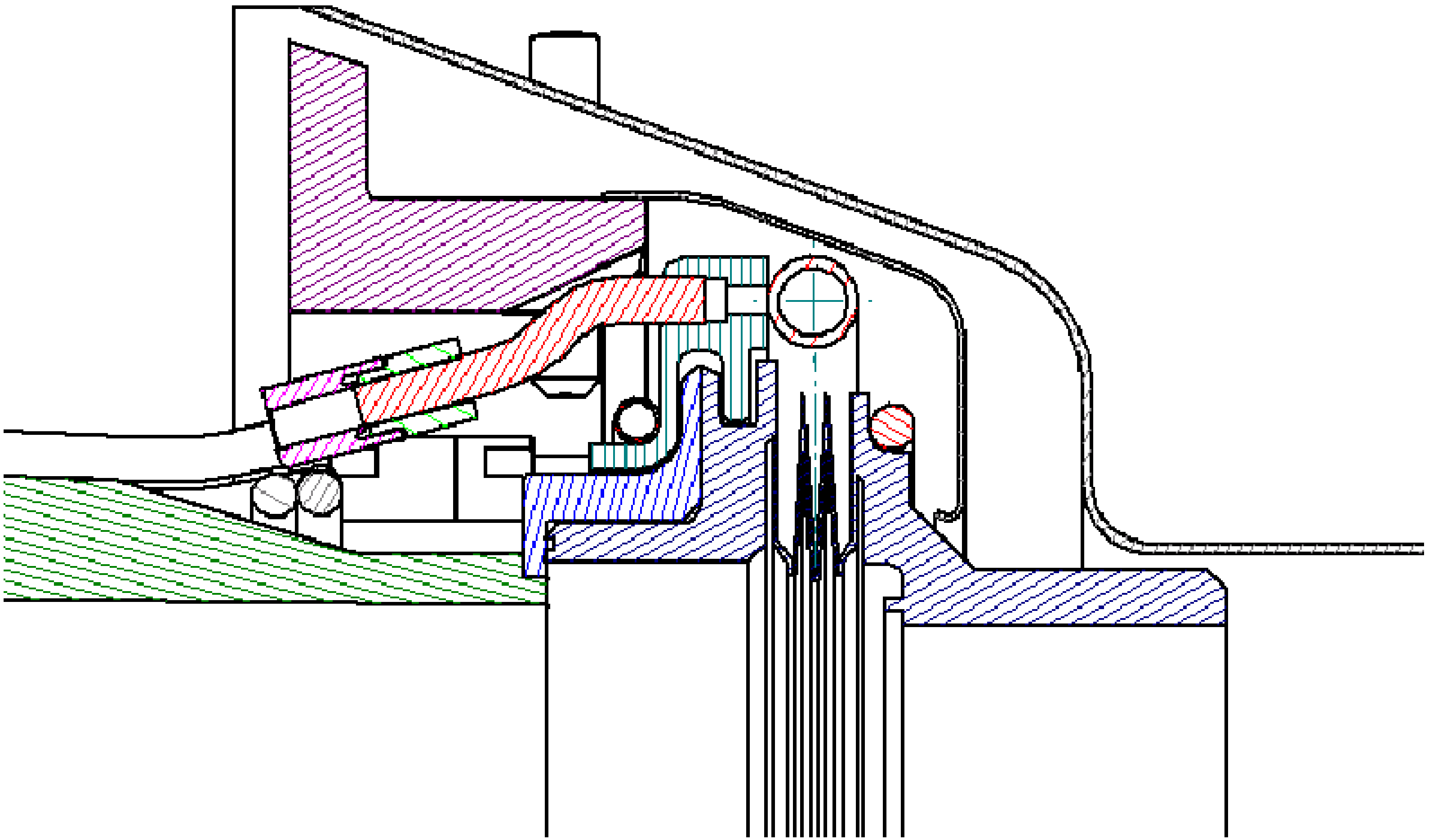

New Be bellows design

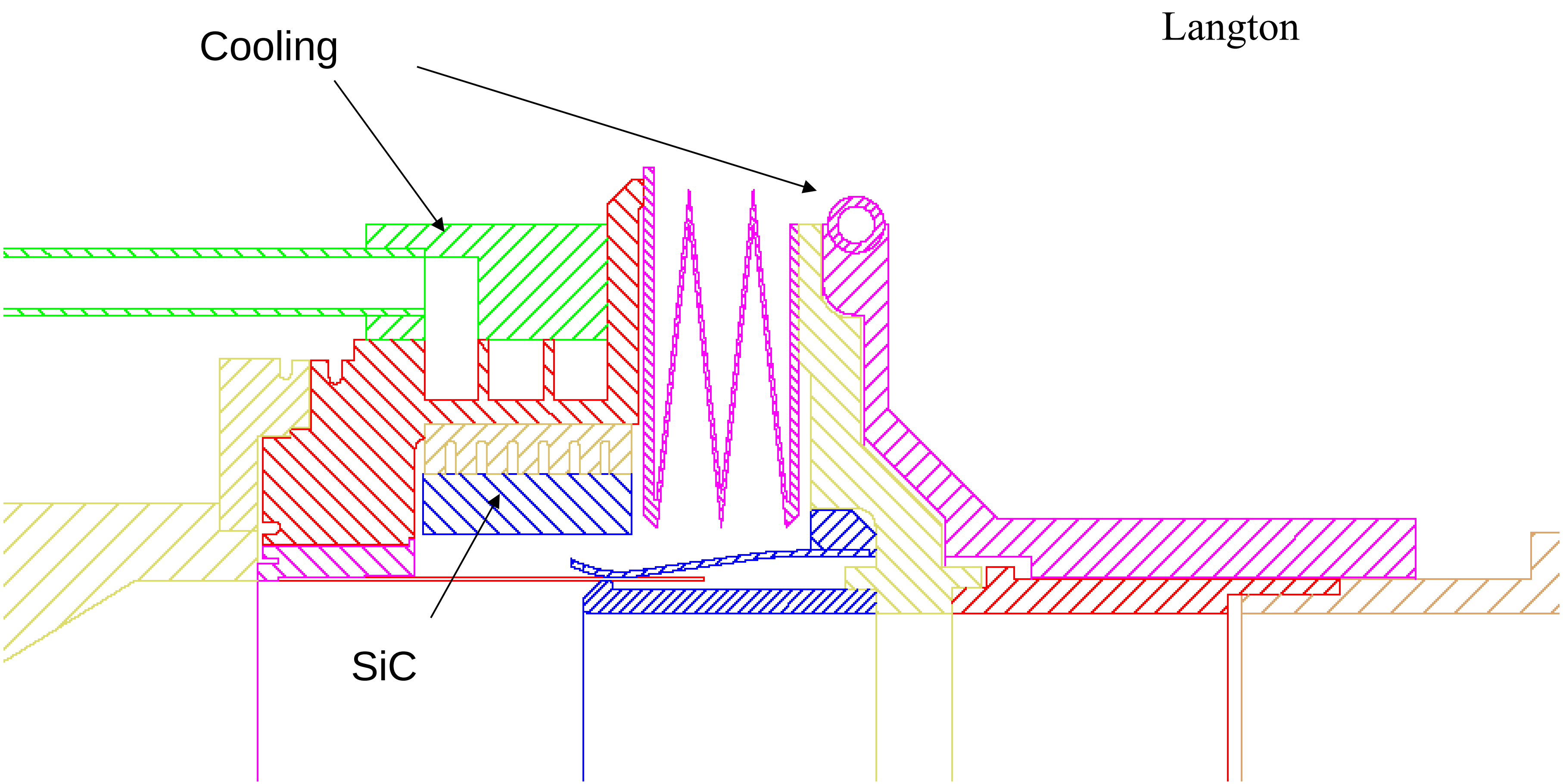

PEP-II IR bellow details

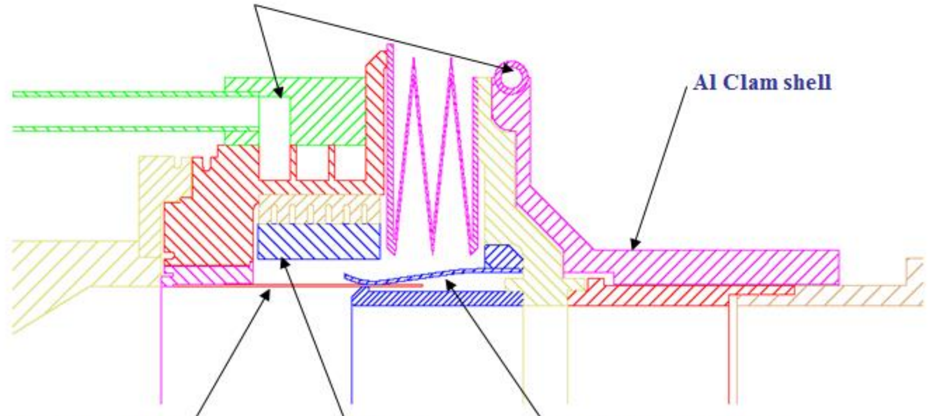

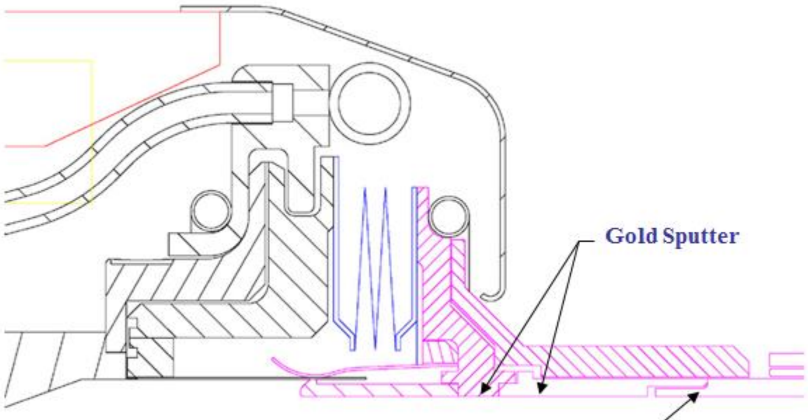

Thermo Model (May 2001) for 100 Watts Power input behind fingers.

Does not match data in detail.

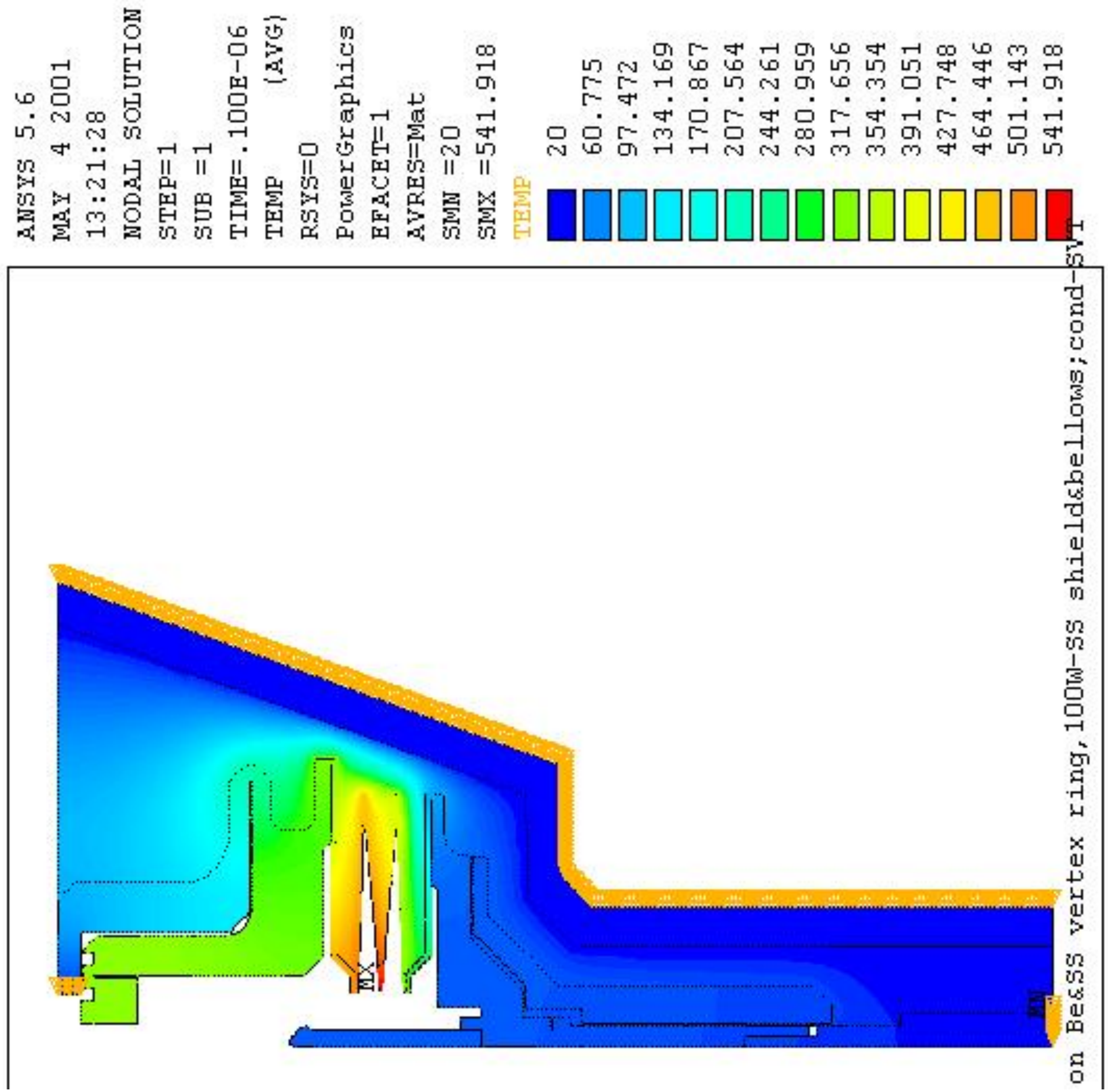

IP: Temperature monitoring

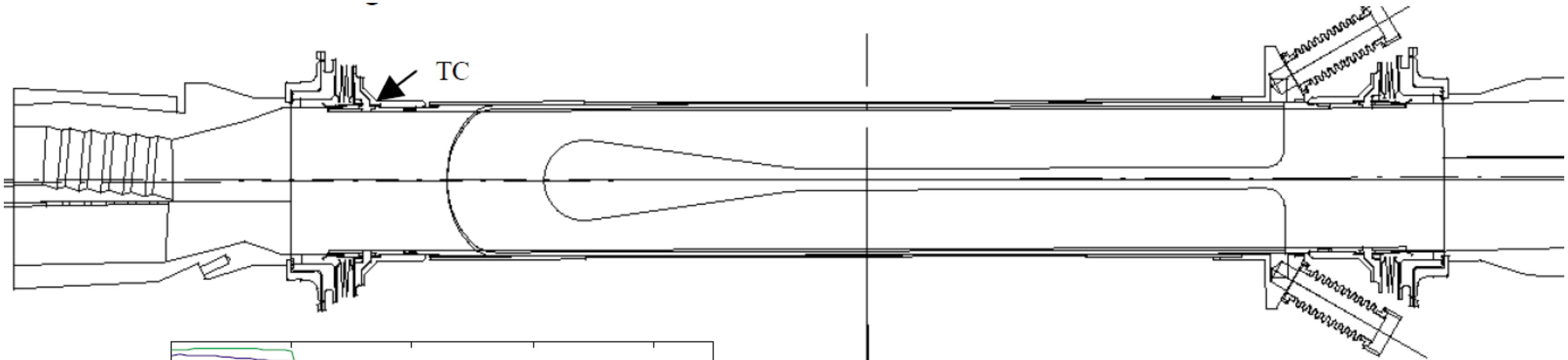

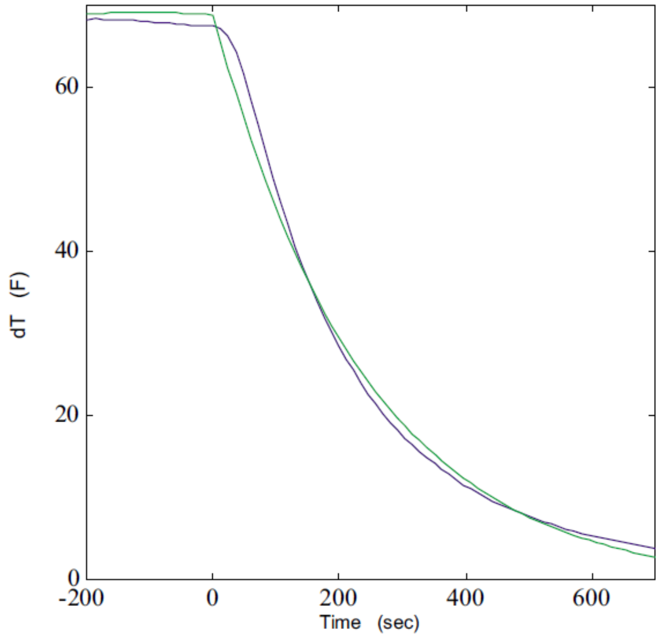

Figure 2: Response of thermocouple (blue) and exponential weighting from positron current (green) for a step change of -1.25 A.

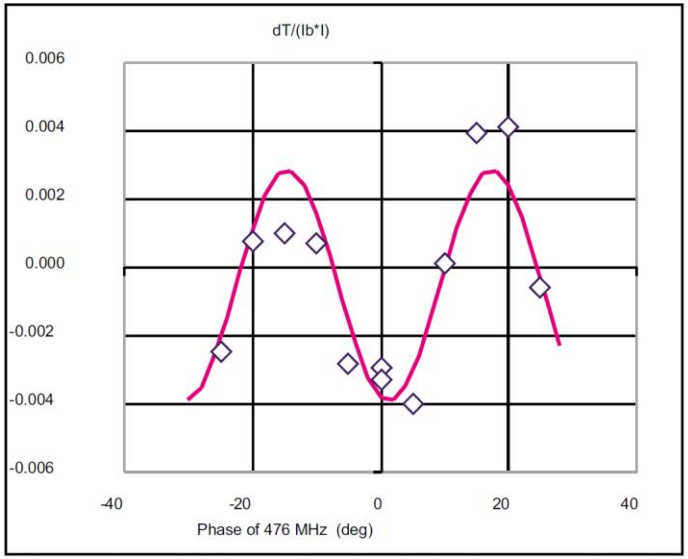

Figure 7: Modulation of heating by both beams changing the phase of the electron beam. The curve corresponds to 5.4 GHz

(Ecklund et al)

IP Temperature monitoring and modeling

SLAC

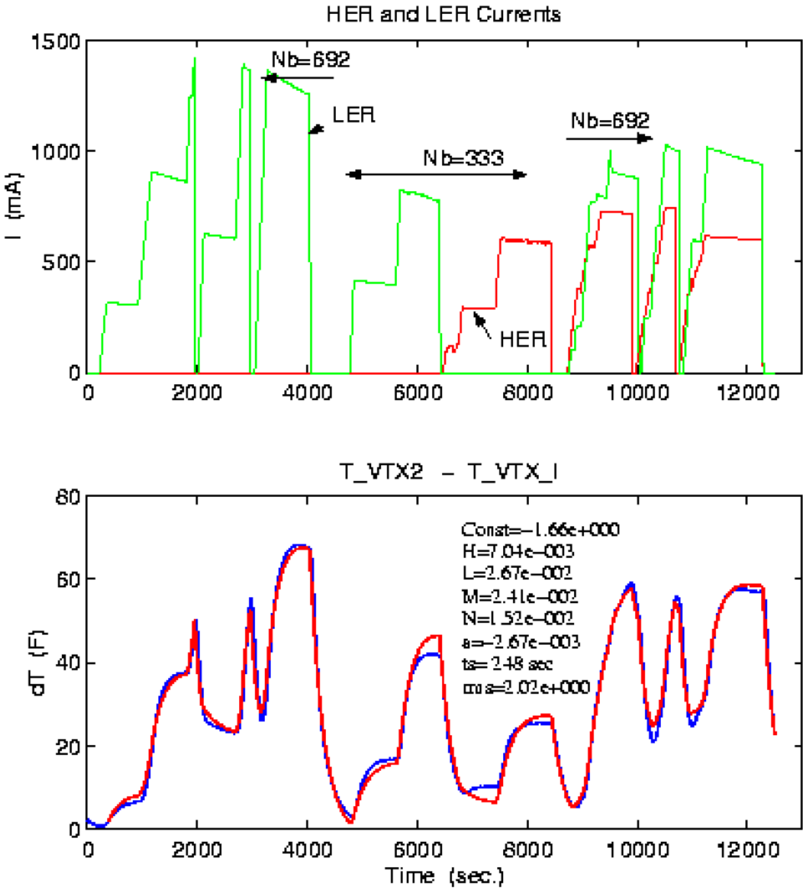

Figure 4: Data (blue) with changing electron and positron currents and fit (red).

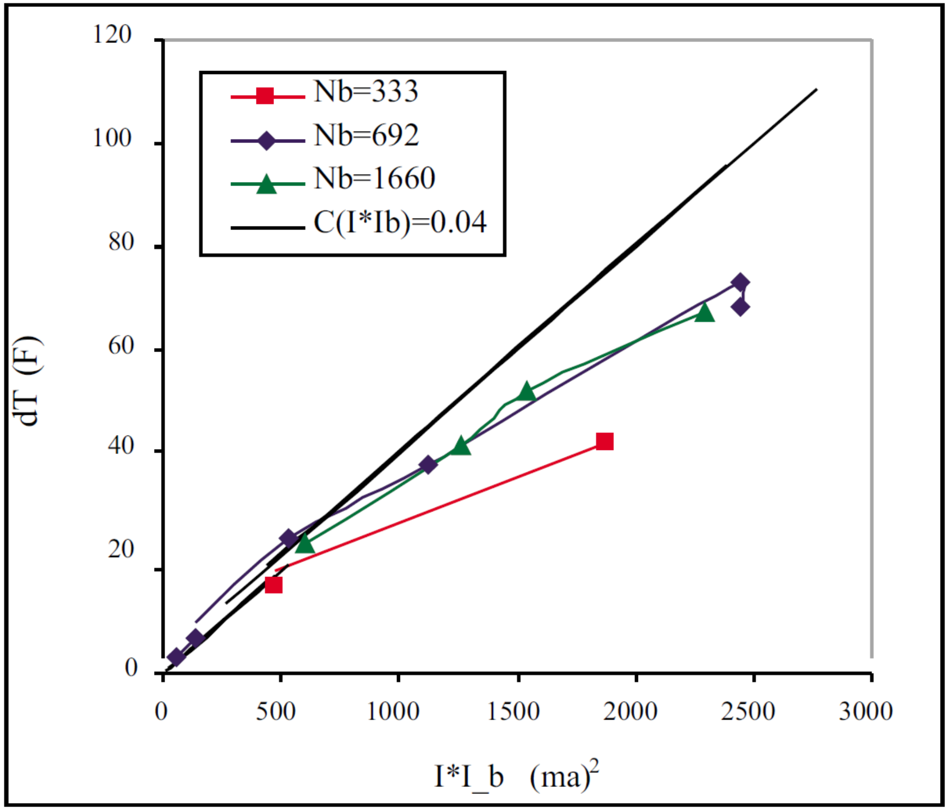

Figure 5: Temperature rise vs. product of bunch current times average current for various bunch fill patterns denoted by the number of populated bunches (Nb). The line shows the expected behavior from low currents.

(S. Ecklund et al)

Temperature: IR Q2 Bellows and Vertex Chamber Bellows

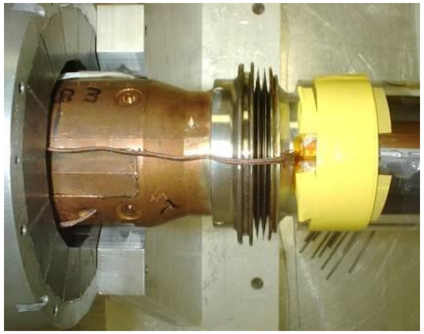

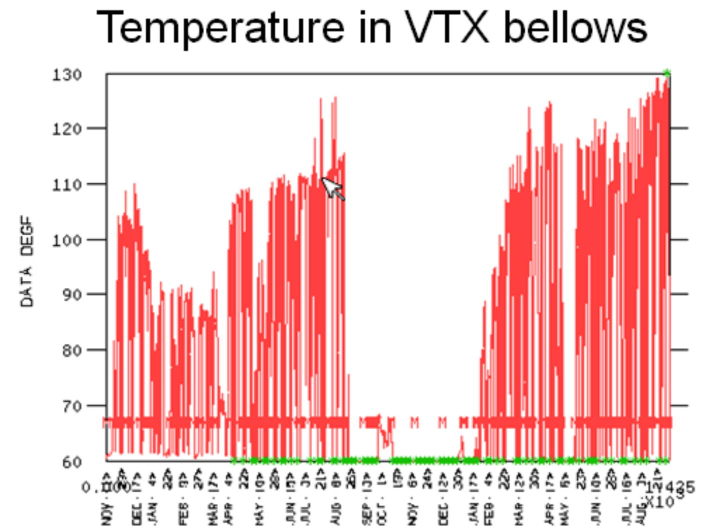

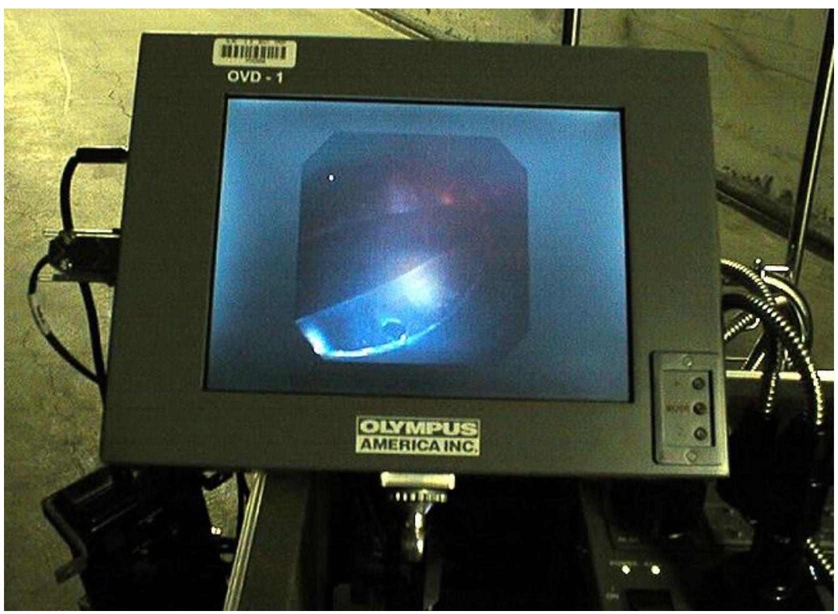

Borescope camera for vacuum chambers

LER Q5 Vacuum Chamber showing NEG Screen

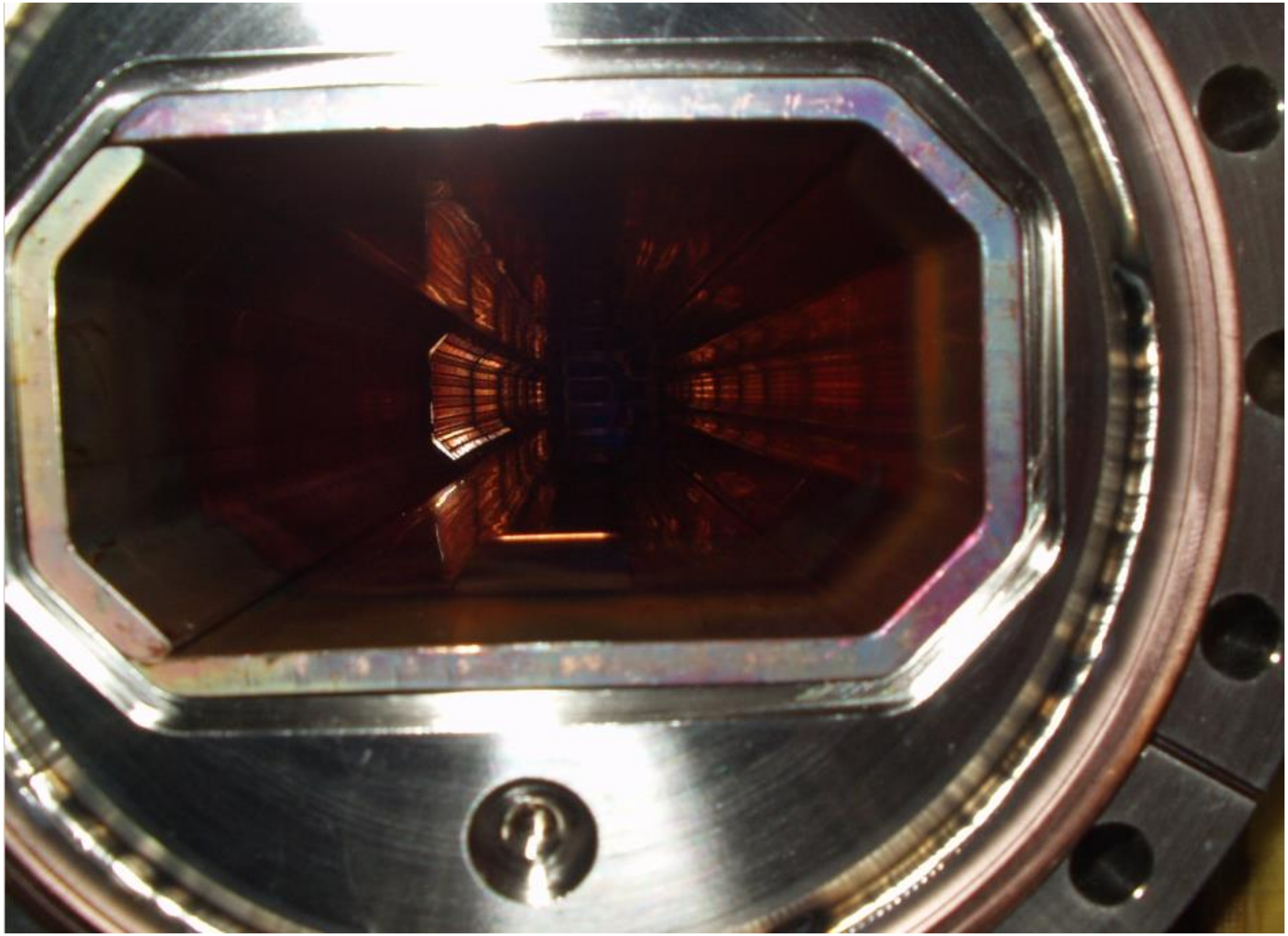

PEP-II high capacity NEG vacuum pumps

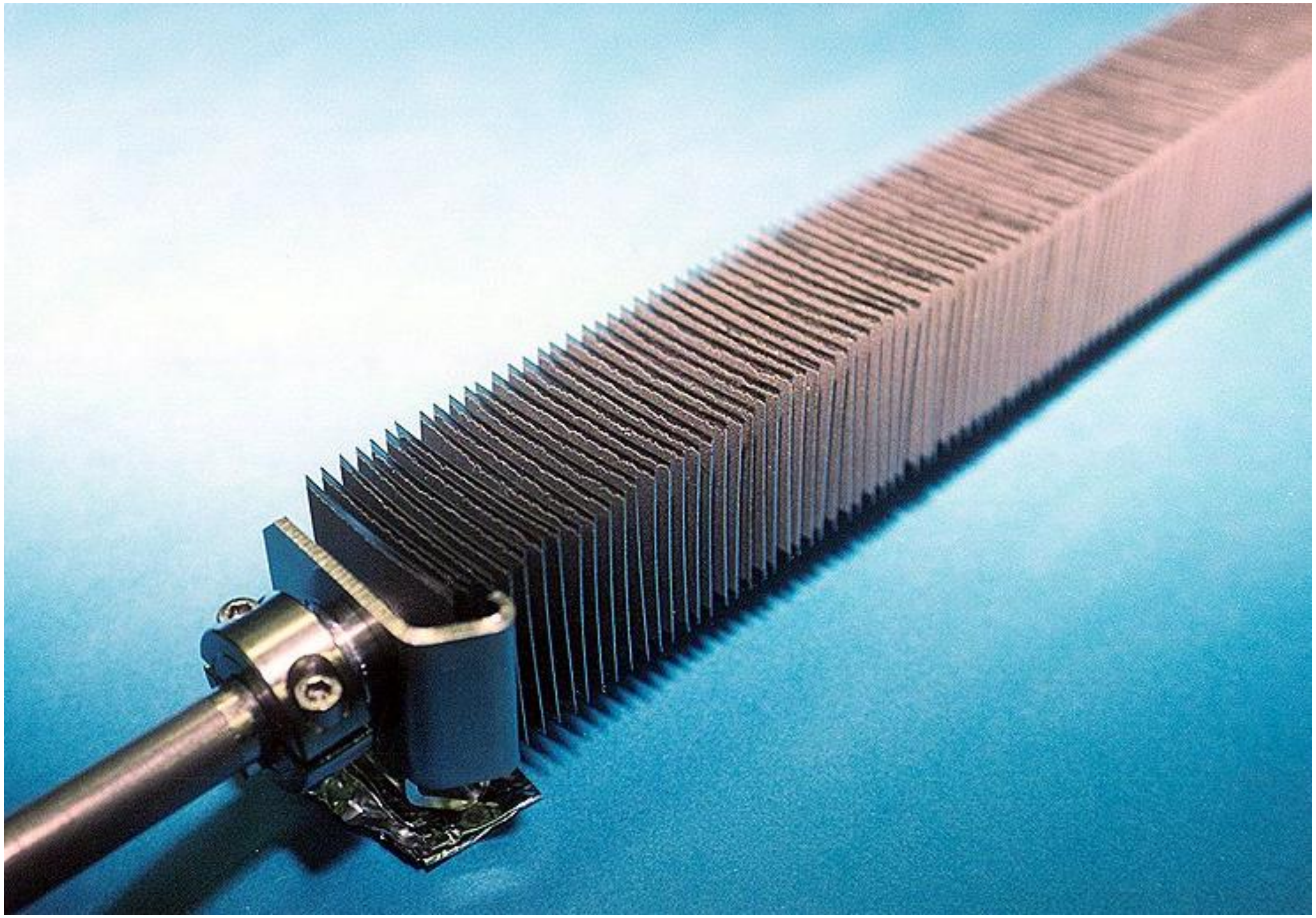

LER NEG
Test chamber

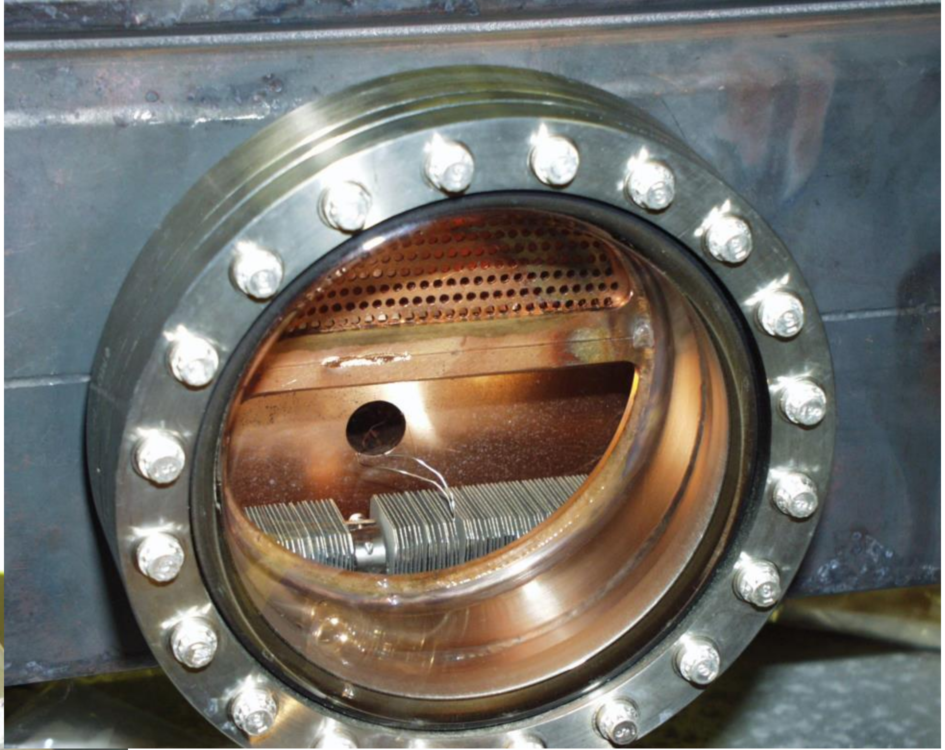

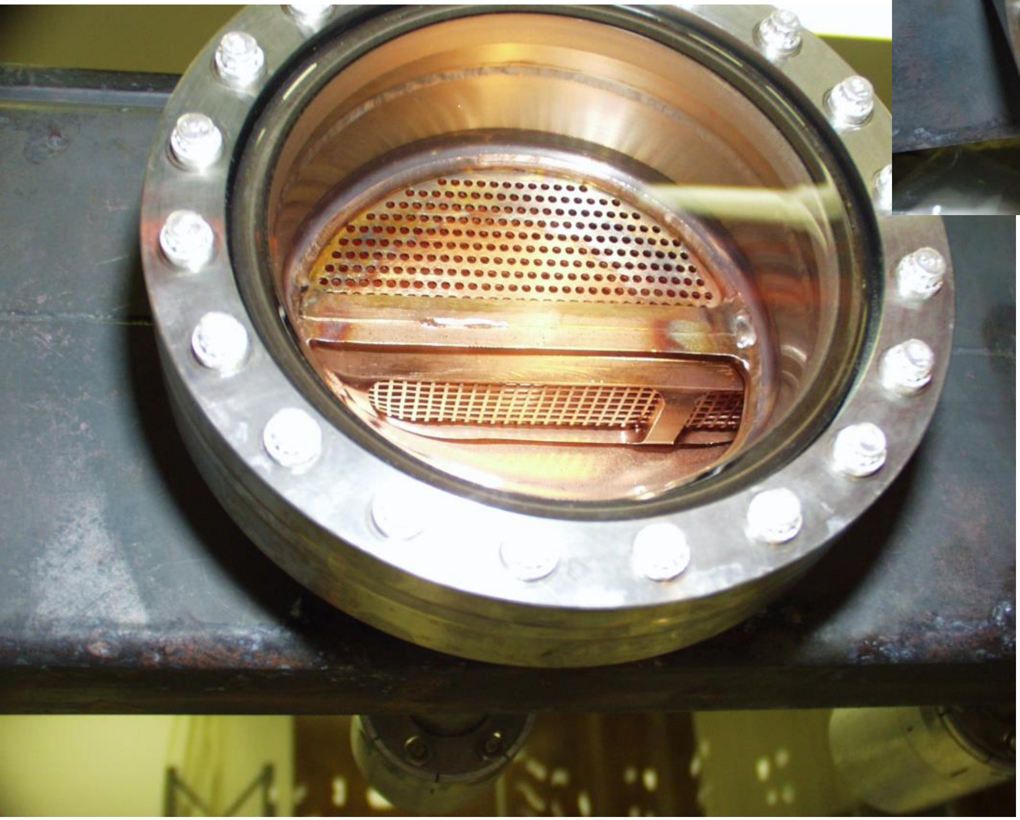

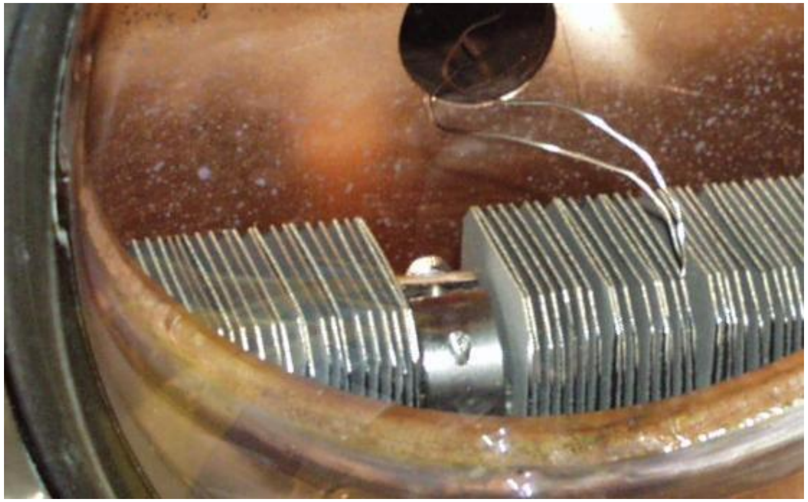

Beam loss rates (PMT with scintillators) (~200 around ring)

PMT loss monitors

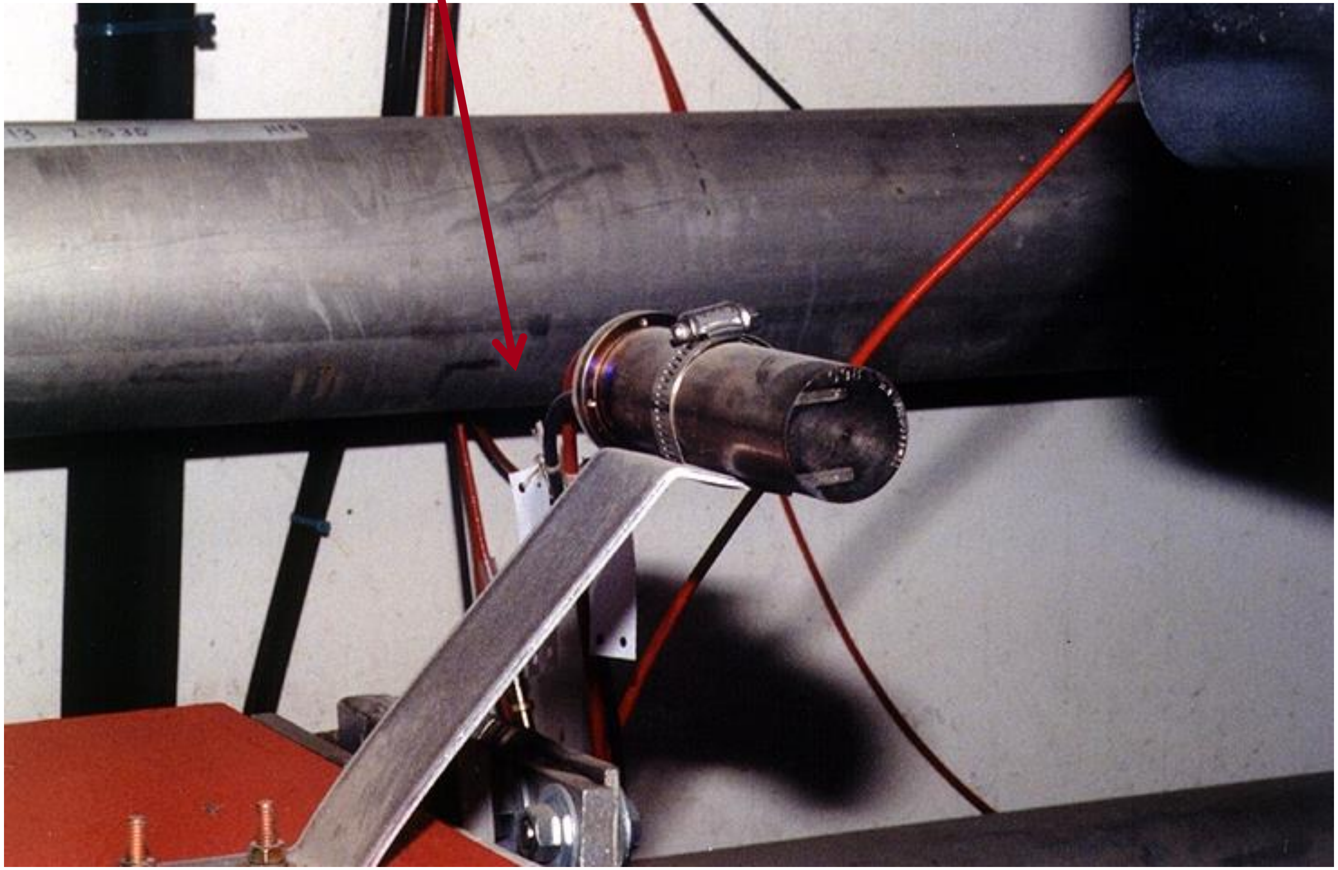

Lifetime versus collimator setting → beam profile in the tails

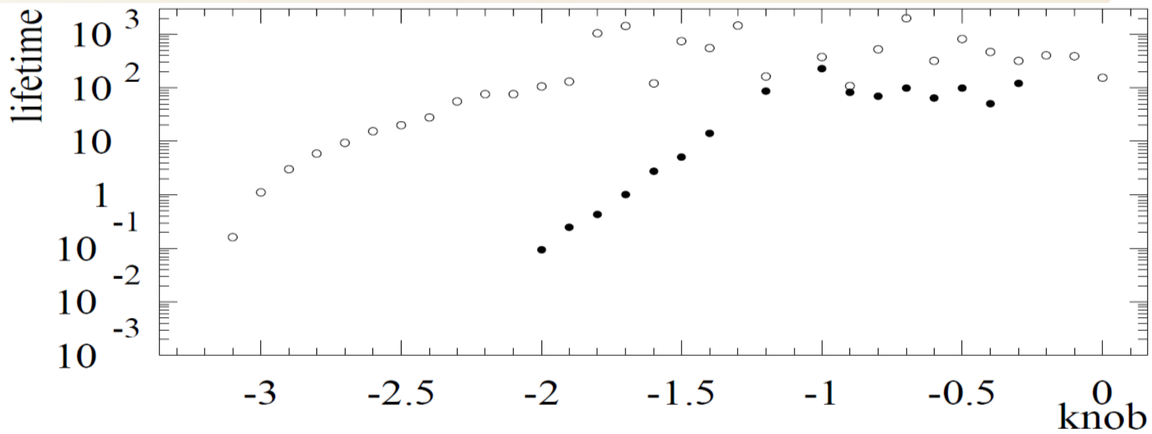

Figure 2: Results of vertical scraping measurements in the HER with colliding beams. Open circles are with high, bullets with low currents. The knob setting is given in mm at the collimator and the lifetime in minutes. Moving in the negative direction on the knob brings the beam closer to the collimator.

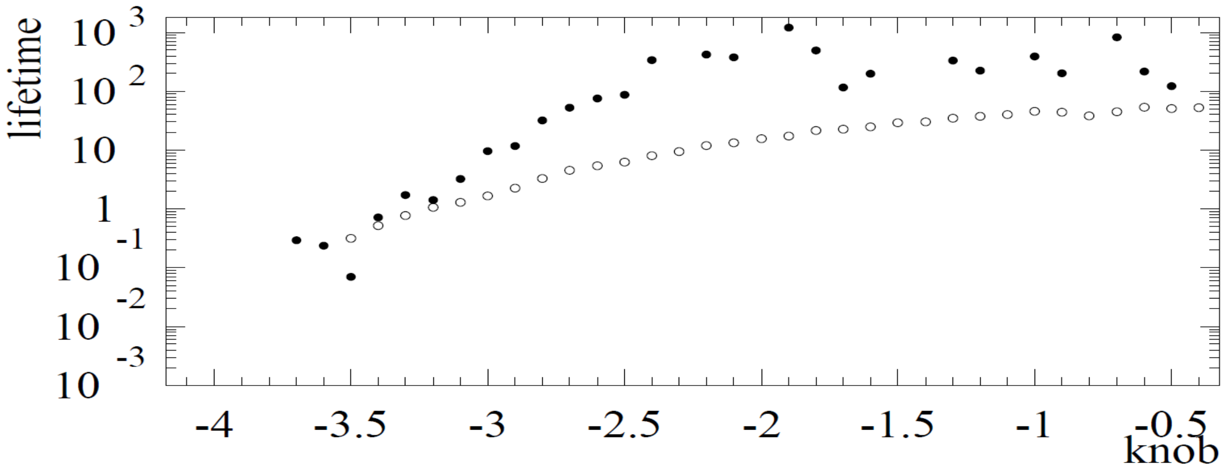

Figure 3: Results of horizontal scraping measurements in the LER with colliding beams. Open circles are with high, bullets with low currents. The knob setting is given in mm at the collimator and the lifetime in minutes. Moving in the negative direction on the knob brings the beam closer to the collimator.

Radiation tests of Coils and Undulator Magnets

KEK magnet coils

PETRA-II Undulators

APS Undulators

LCLS Undulators

Spring-8 Magnet Coils Radiation tests

SLAC

Proceedings of EPAC 2004, Lucerne, Switzerland

RADIATION DAMAGE OF MAGNET COILS DUE TO SYNCHROTRON RADIATION

K. Tsumaki, S. Matsui, M. Ohishi, T.Yorita, JASRI/SPring-8, Hyogo, Japan
T. Shibata, T. Tateishi, KOBELCO RESEARCH INSTITUTE, INC., Hyogo, Japan

We have measured the radiation damage done to magnet coils. Test pieces were irradiated with synchrotron radiation of 10^6 to 10^9 Gy. The insulator of the irradiated test pieces was carbonized and became more fragile with increasing radiation dose. However, the coil function did not deteriorate.

Spring-8: Coil irradiation Tests

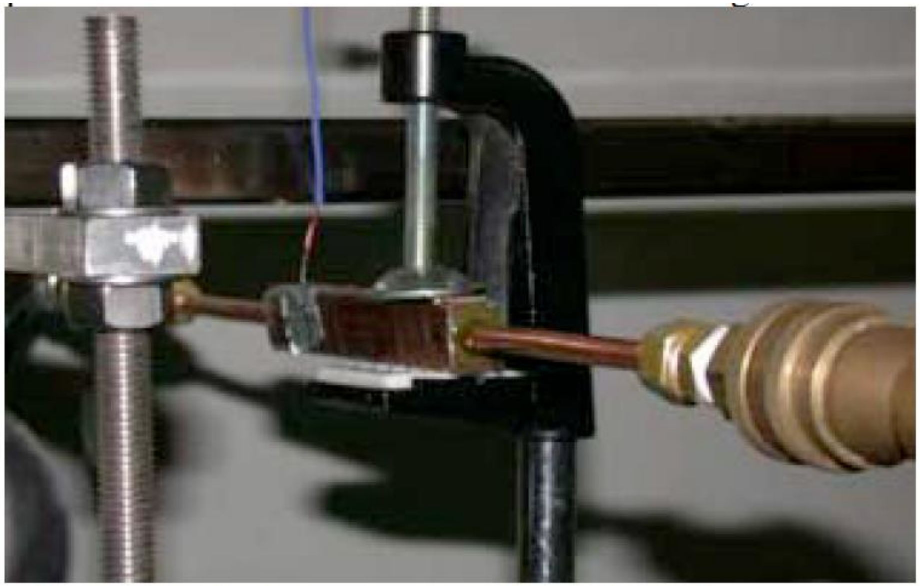

Figure 2: Test piece mounted on a beamline.

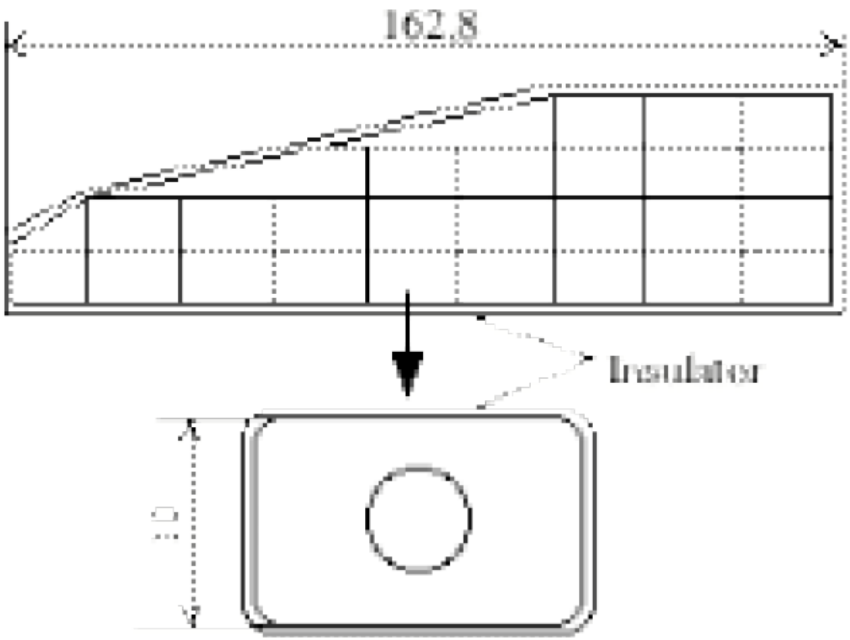

Figure 1: Cross section of a magnet coil.

Spring-8 Magnet coil tests

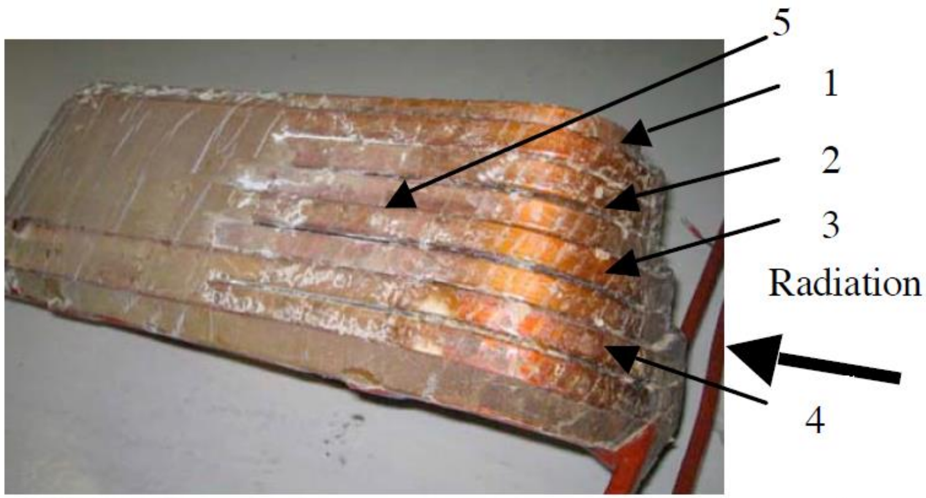

Figure 8: External view of the removed magnet coil.

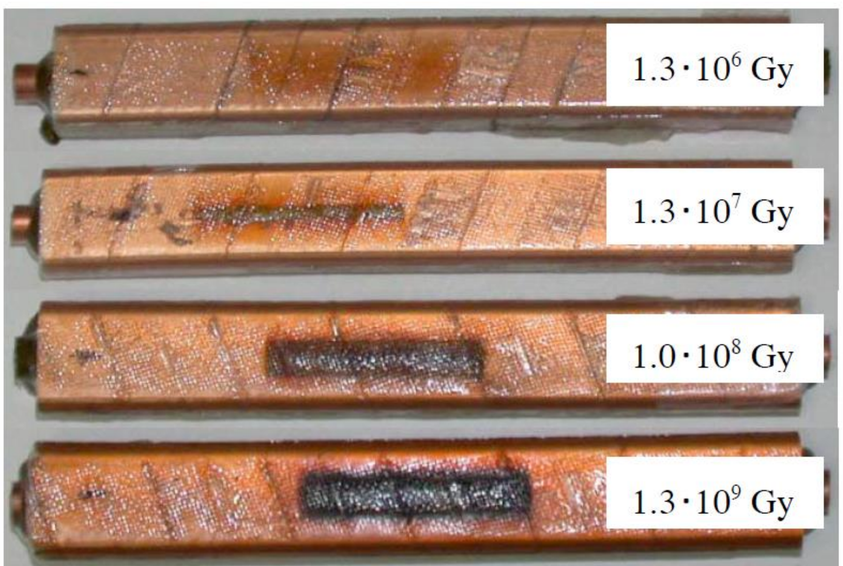

Figure 3: Test pieces after irradiation.

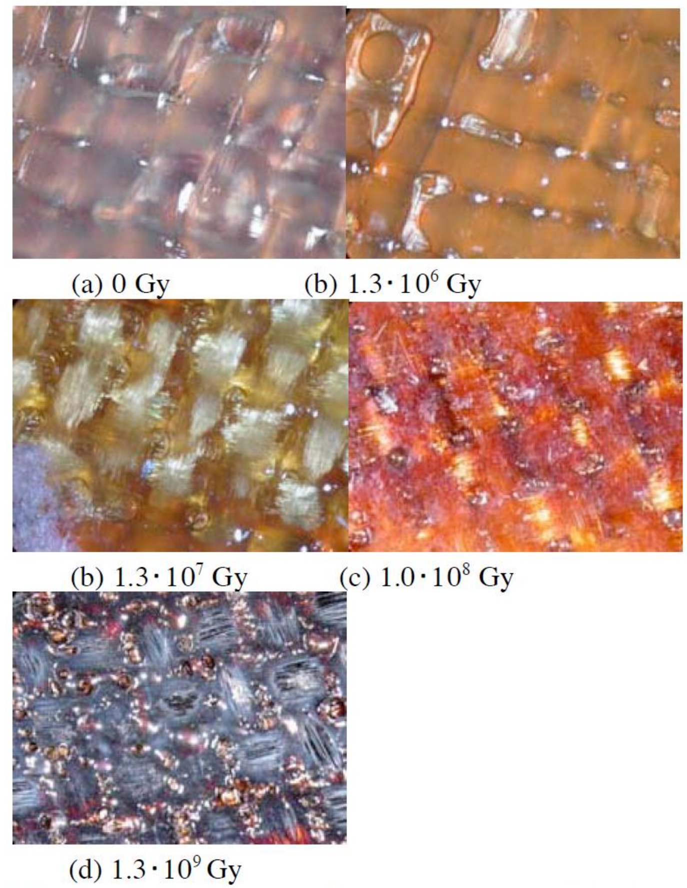

Figure 4: Test piece photographs magnified by a microscope.

Spring-8 coil insulation scratch test → damage test

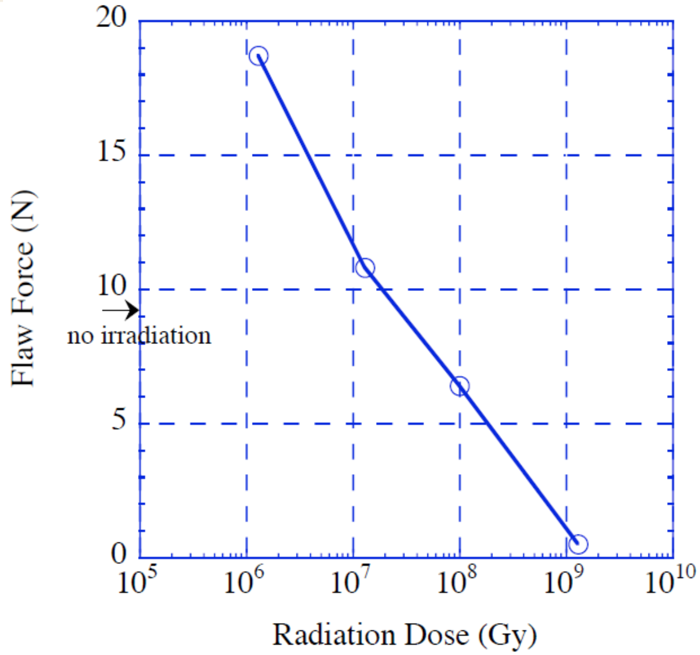

Figure 7: Relation between radiation dose and the flaw force.

When the force was applied, we saw that flaws appeared in the test pieces at certain levels of applied force. We refer to this force as the flaw force. The relation between the radiation dose and the flaw force is shown in Fig. 7. With 10^6 Gy irradiation, the glass prepreg hardened and the flaw force became higher than that for no irradiation.

Example: PEP-II IR Permanent Magnets

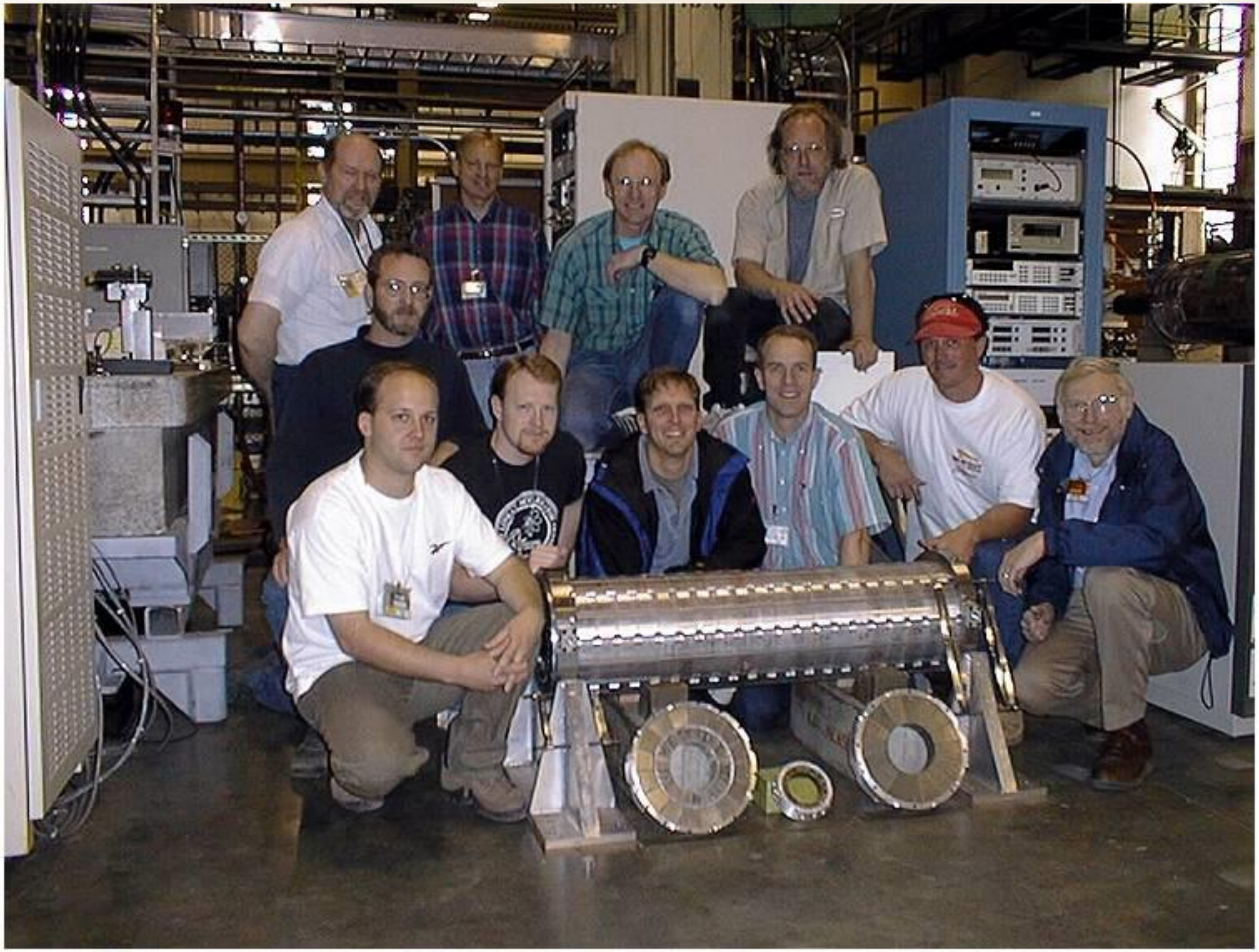

MS_044 Permanent Magnet Crew 04/09/98

INVESTIGATION OF RADIATION DAMAGE OF INSERTION DEVICES AT PETRA III (G. K. Sahoo et al. IPAC 2015)

PETRA III is a 3rd generation synchrotron light source dedicated to users at 14 beamlines with 30 instruments since 2009. The horizontal beam emittance is 1 nmrad while a coupling of 1% amounts to a vertical emittance of 10 pmrad. Some undulators and wiggler devices have accumulated total radiation doses of about 100 kGy.

PETRA-III

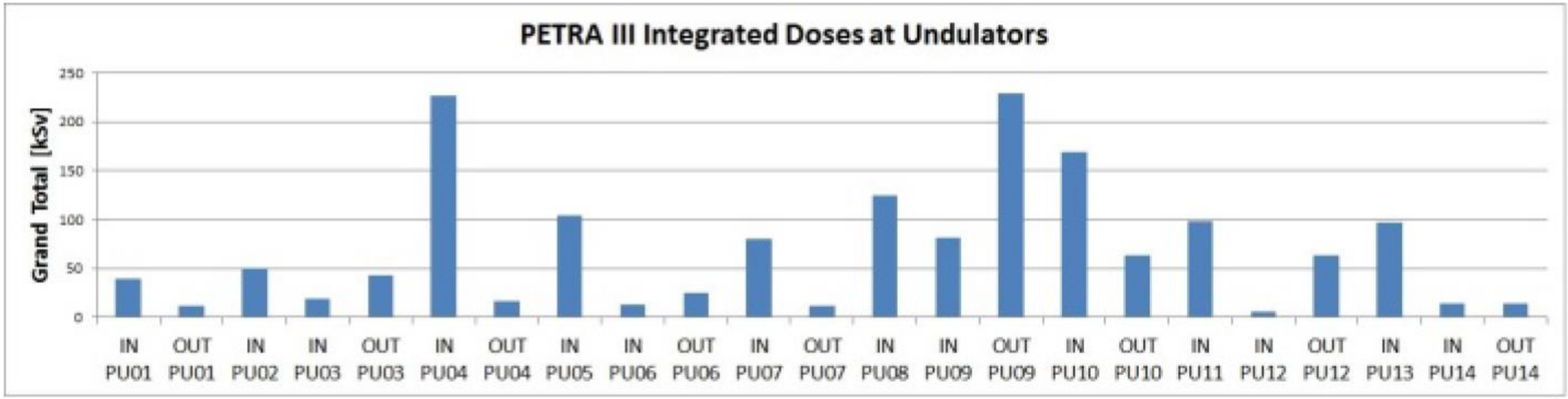

Figure 2: Integrated radiation dose accumulated at every insertion device from the first day of its installation as measured by TLDs.

Proceedings of IPAC2014, Dresden, Germany WEPRO035

RADIATION DAMAGE OF UNDULATORS AT PETRA III

P. Vagin*, O. Bilani, A. Schöps, S. Tripathi, T. Vielitz, M. Tischer, DESY, Hamburg, Germany

PETRA-III Undulator Radiation Damage

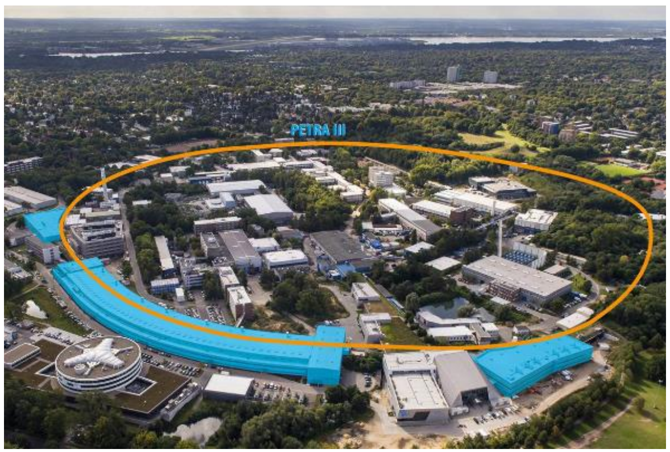

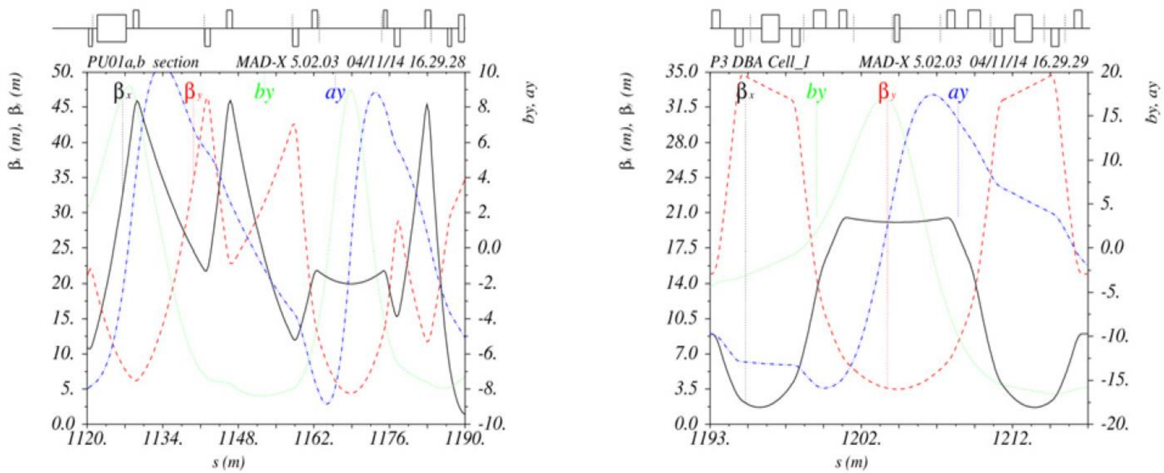

Figure 4: The computed values of a_y and b_y are plotted for the sections for sector (a) PU01 and (b) PU02. The a_y value is high at the upstream of PU01 and PU02; as well as downstream of PU01 and PU02.

PETRA-III

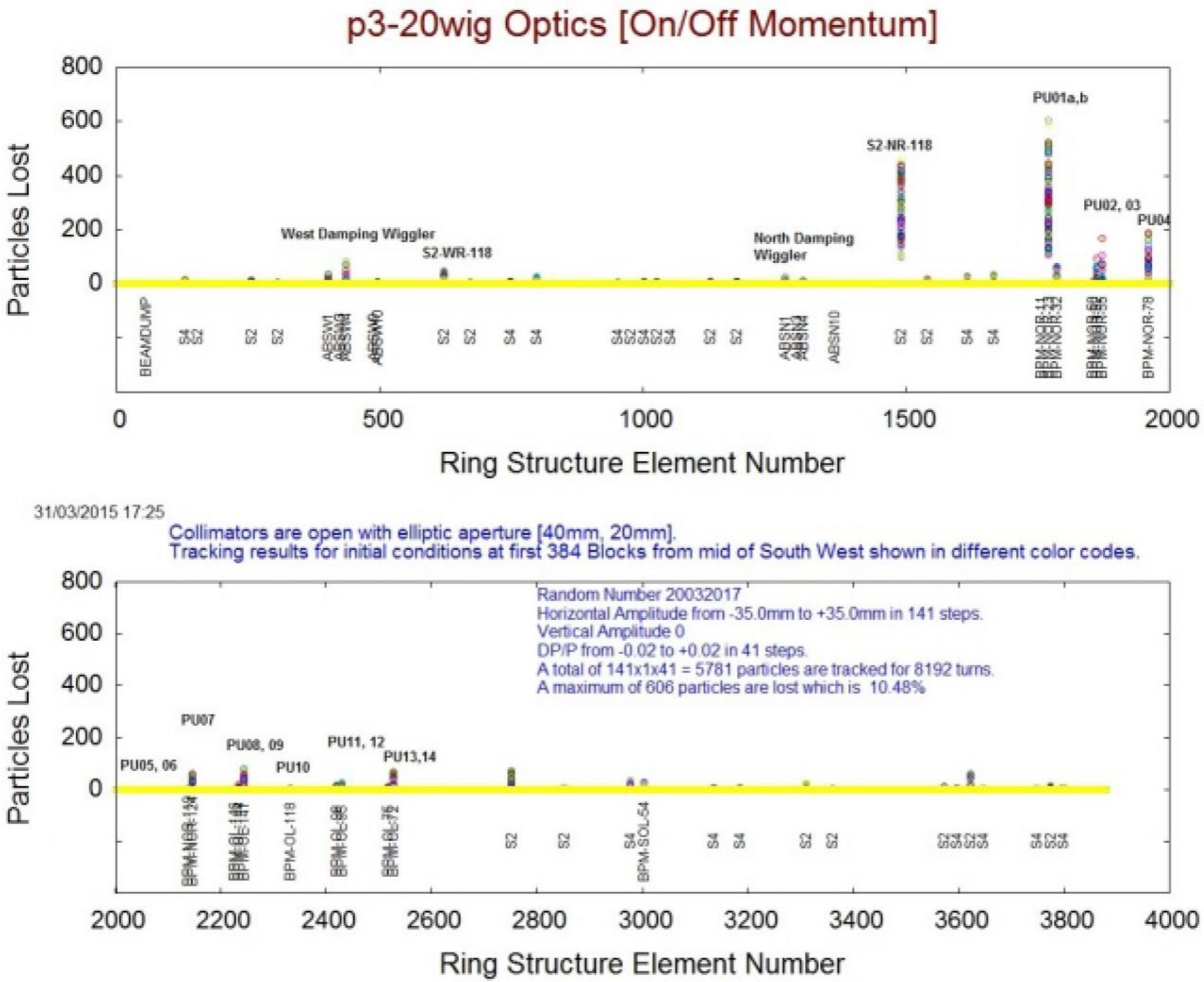

Figure 5: Tracking results for off momentum particles.

PETRA-III

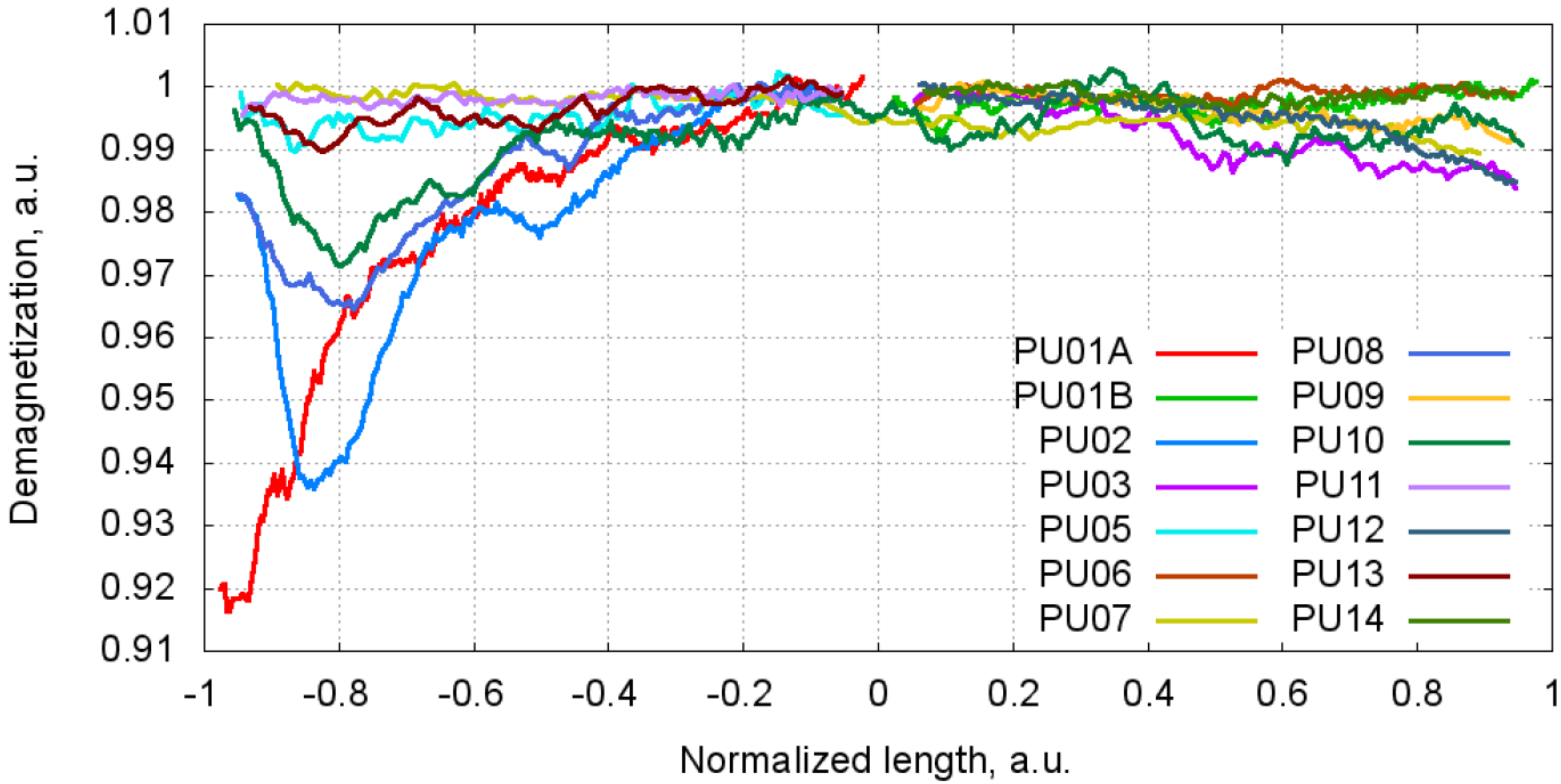

Figure 1: Demagnetization of PETRAIII undulators, horizontal axis is normalized to the length of a straight section.

PETRA-III

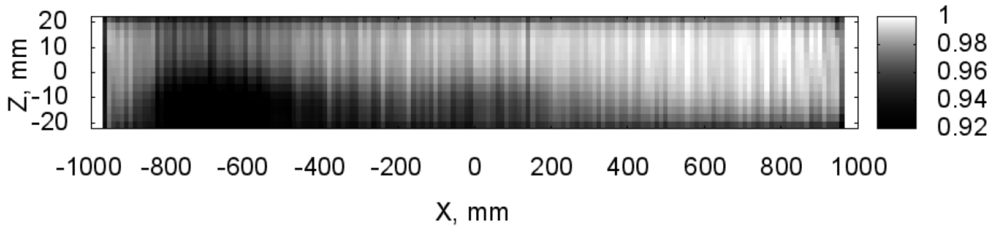

Figure 3: PU02 undulator demagnetization 2D fieldmap at closed gap=10mm, normalized to the initial field amplitude.

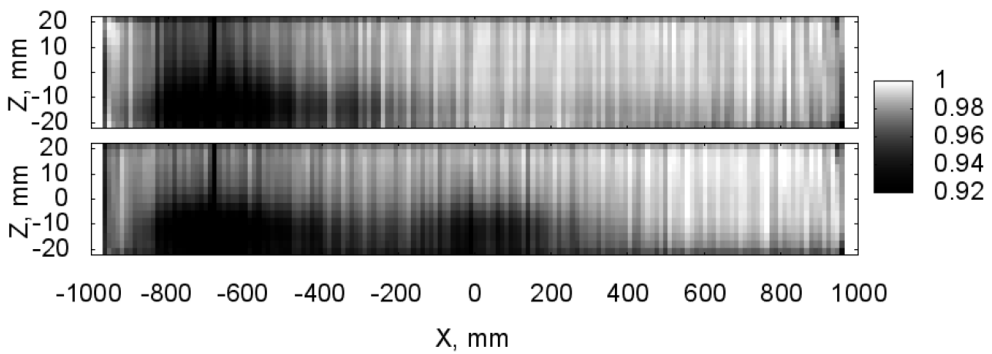

Figure 4: PU02 undulator demagnetization fieldmap measured for top and bottom modules separately at open gap.

PU02 UNDULATOR MEASUREMENTS

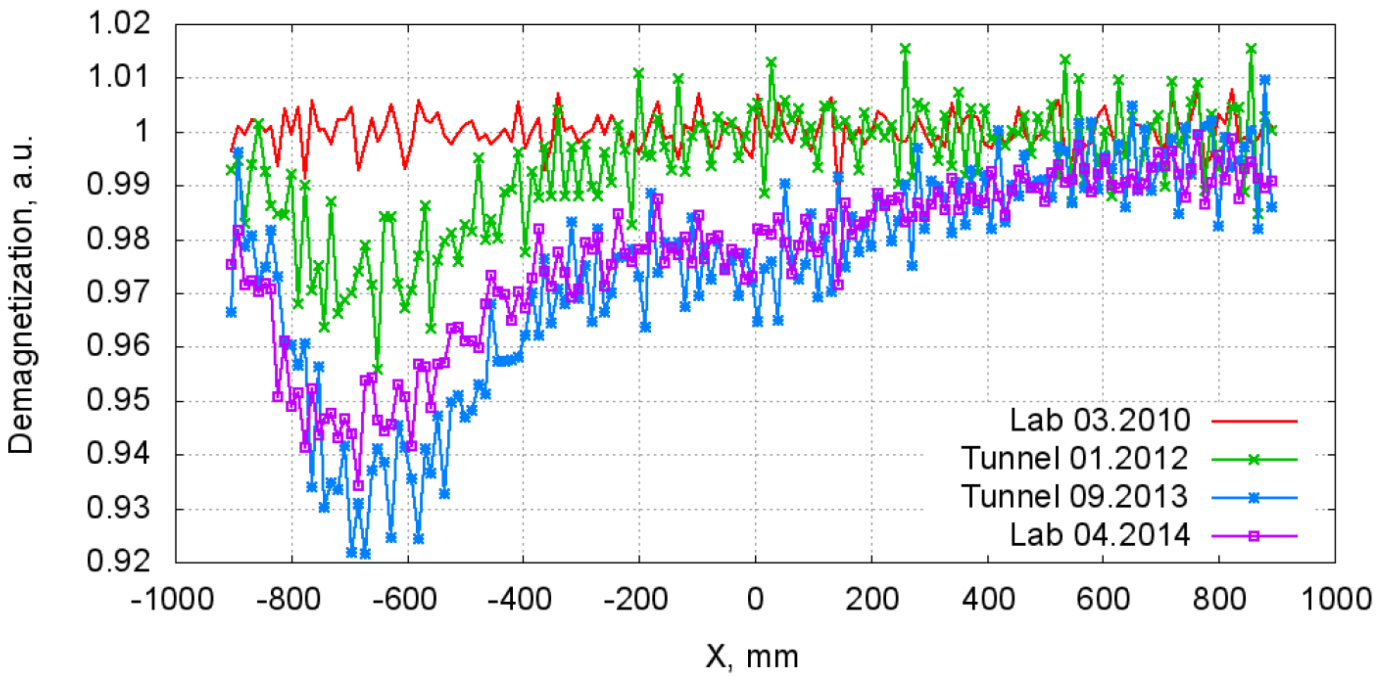

Figure 2: PU02 undulator demagnetization progress.

PETRA-III

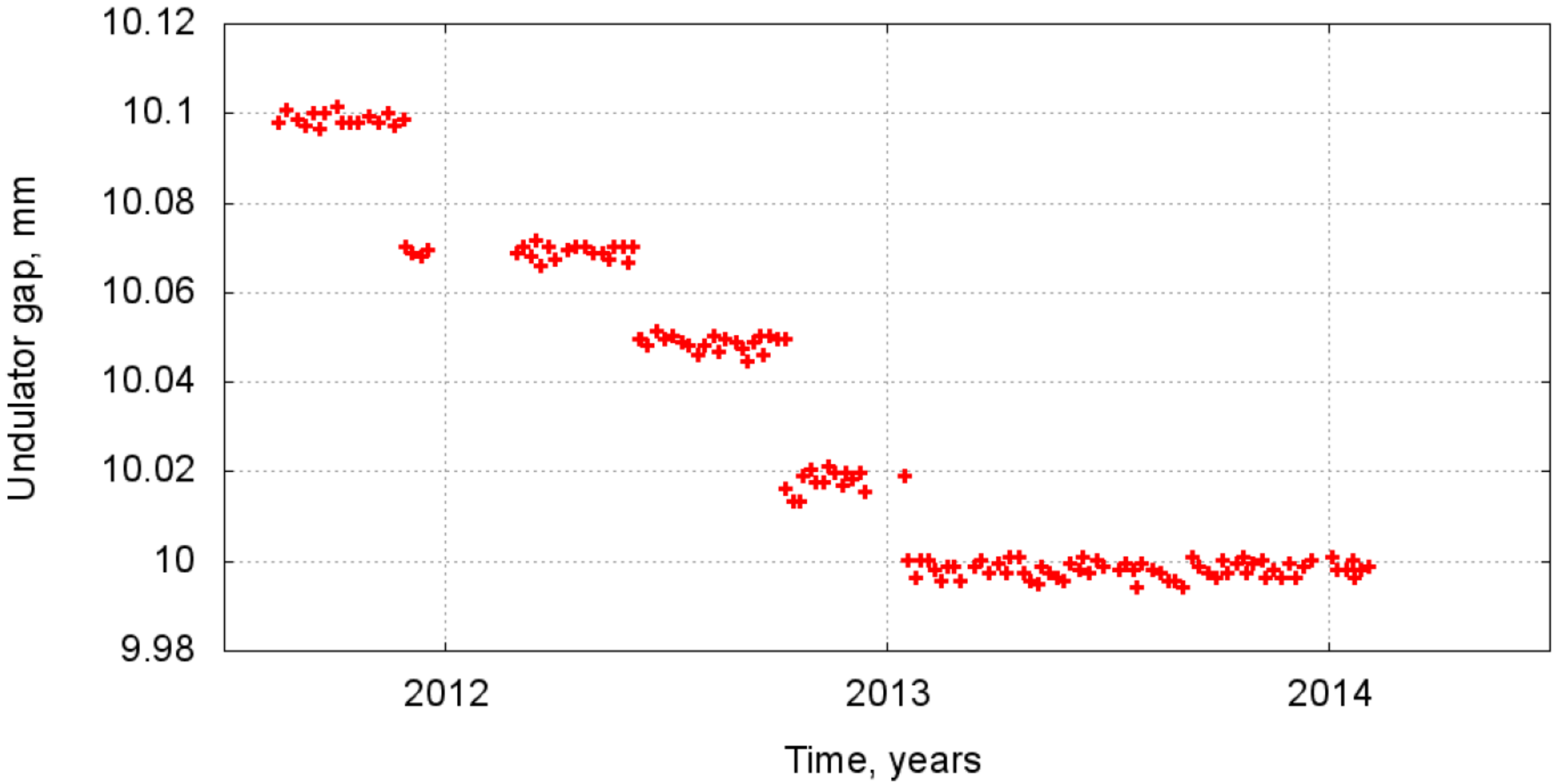

Figure 5: PU02 gap setting to reach 60keV on 7th harmonic is decreasing over time to compensate demagnetization, till it reaches minimum gap defined by vacuum chamber size.

PETRA-III

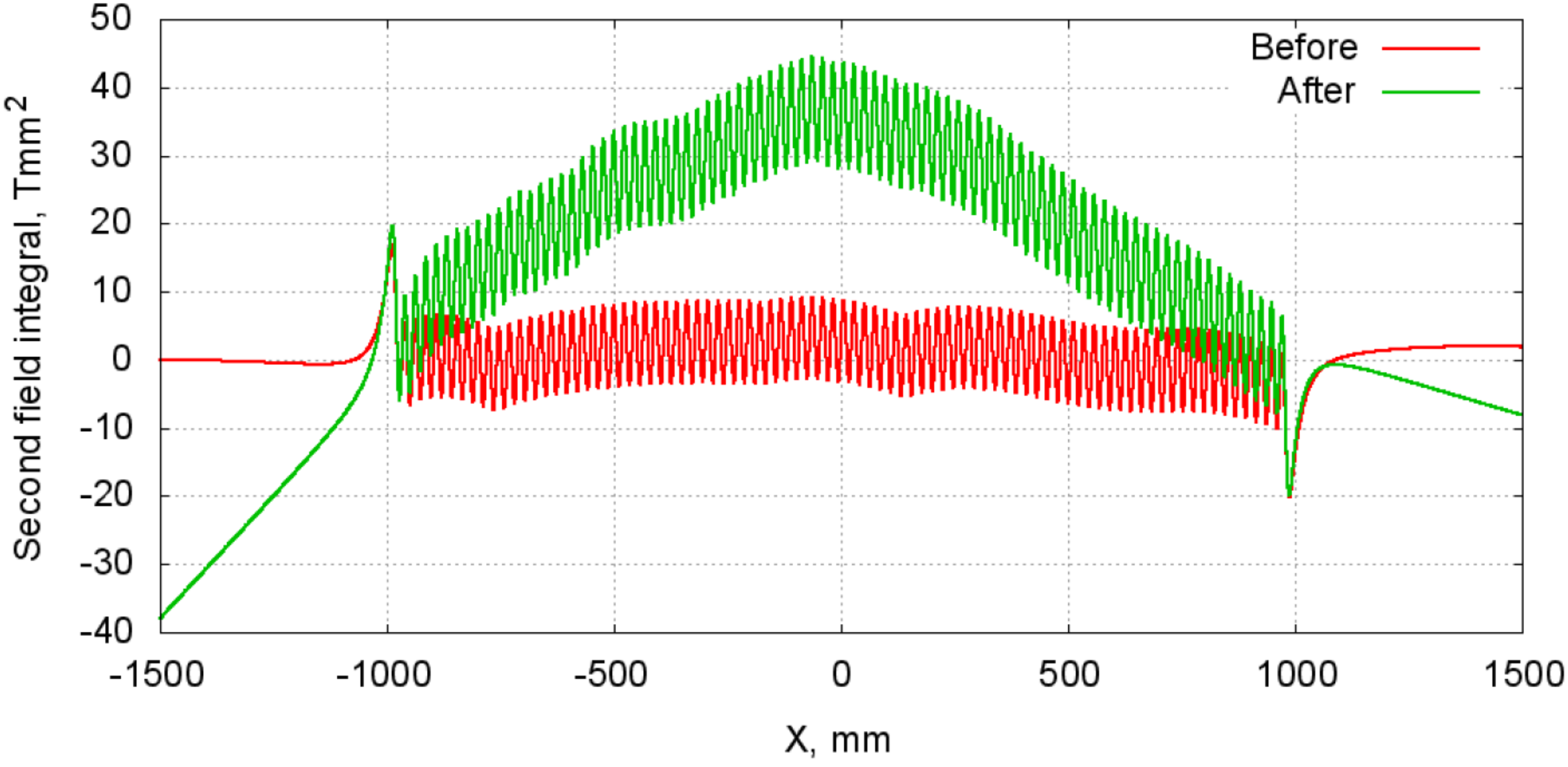

Figure 6: PU02 trajectory before and after demagnetizaton.

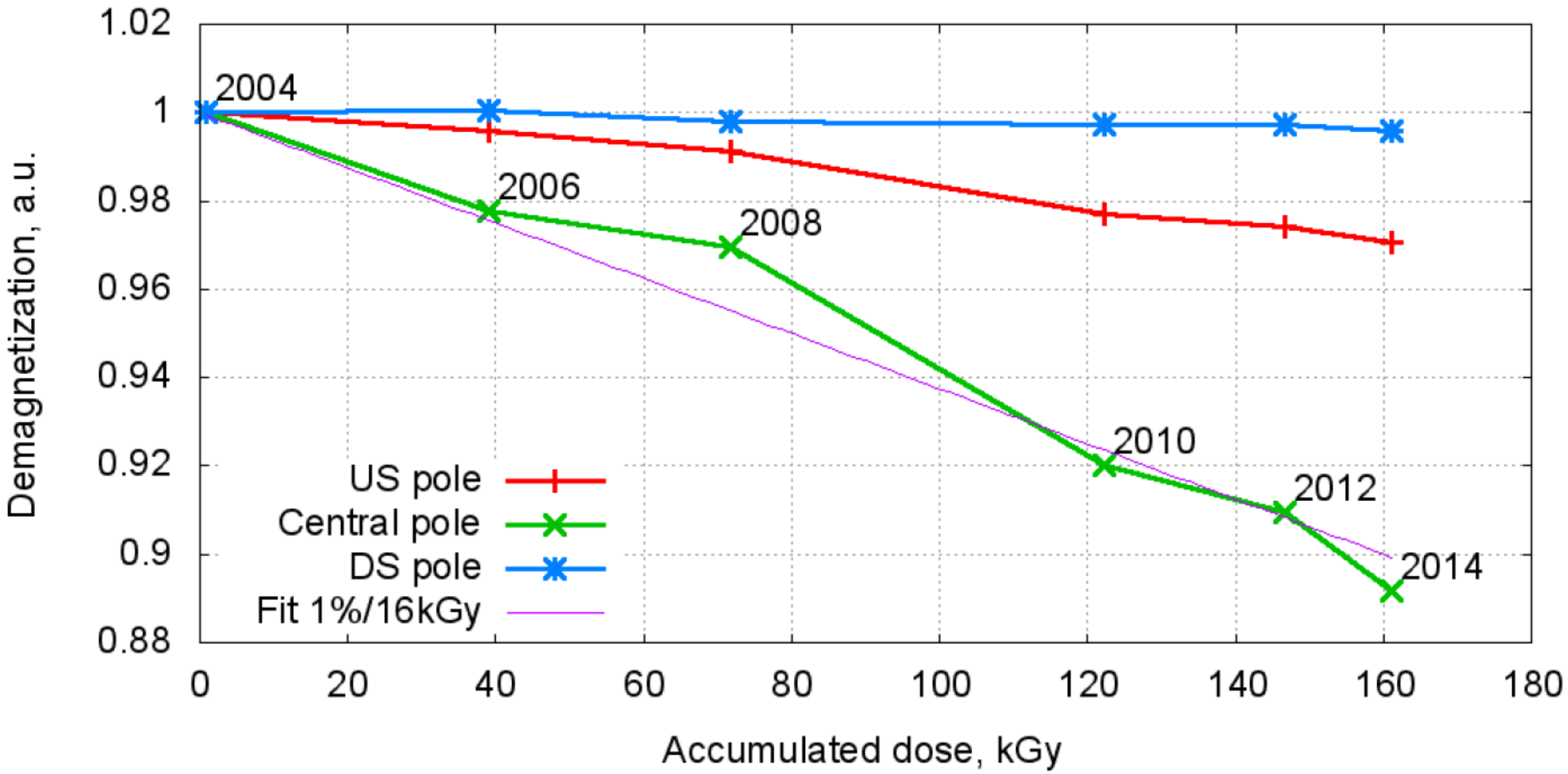

Figure 8: Sacrificial undulator demagnetization.

APS undulator radiation damage tests

Proceedings of 2005 Particle Accelerator Conference, Knoxville, Tennessee

RADIATION DAMAGE TO ADVANCED PHOTON SOURCE UNDULATORS*

Shigemi Sasaki, Maria Petra, Isaac B. Vasserman, Charles L. Doose, Elizabeth R. Moog, APS, Argonne National Laboratory, Argonne, IL 60439, U.S.A.
N. V. Mokhov, Fermi National Accelerator Laboratory, Batavia, IL 60510, U.S.A.

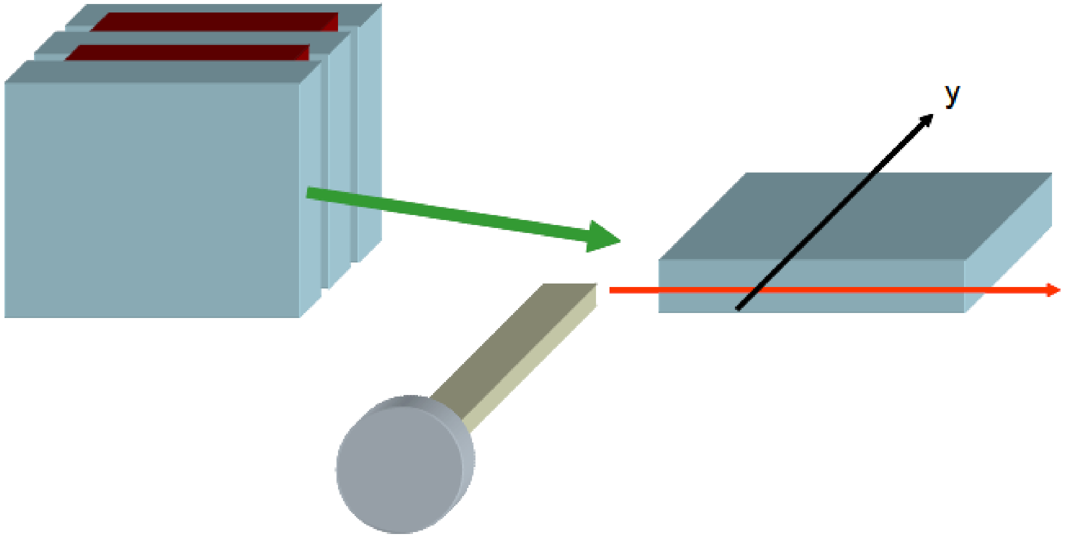

Fig. 2: Schematic of Hall probe measurement.

APS Undulator

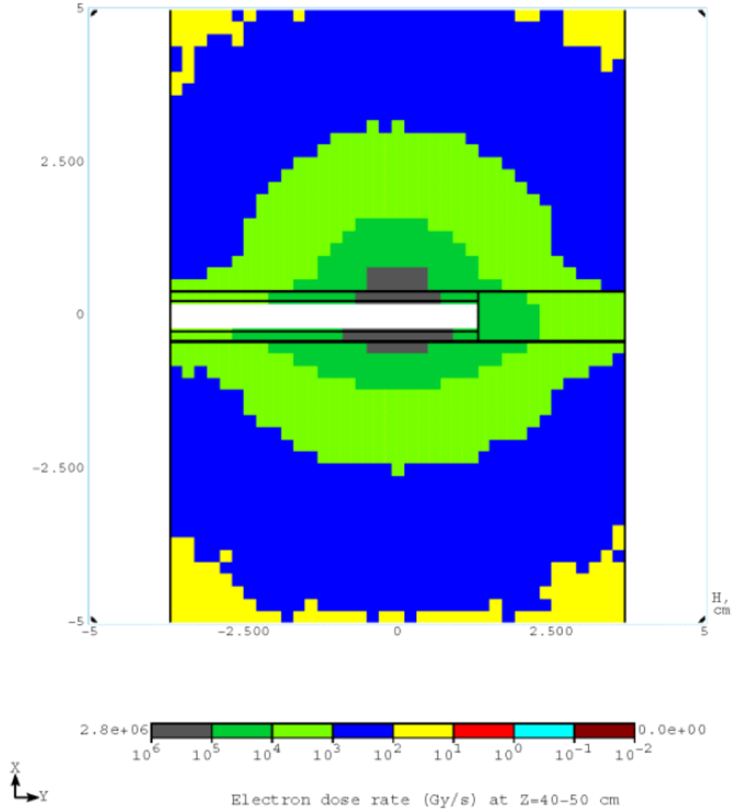

Fig. 5: Electron dose distribution in the undulator. 6.25×10^{14} e/s loss at 7 GeV was assumed for the simulation.

As can be clearly seen, the maximum dose rate is localized near the electron beam axis. Dose distributions from gamma-rays, charged hadrons, and muons all show

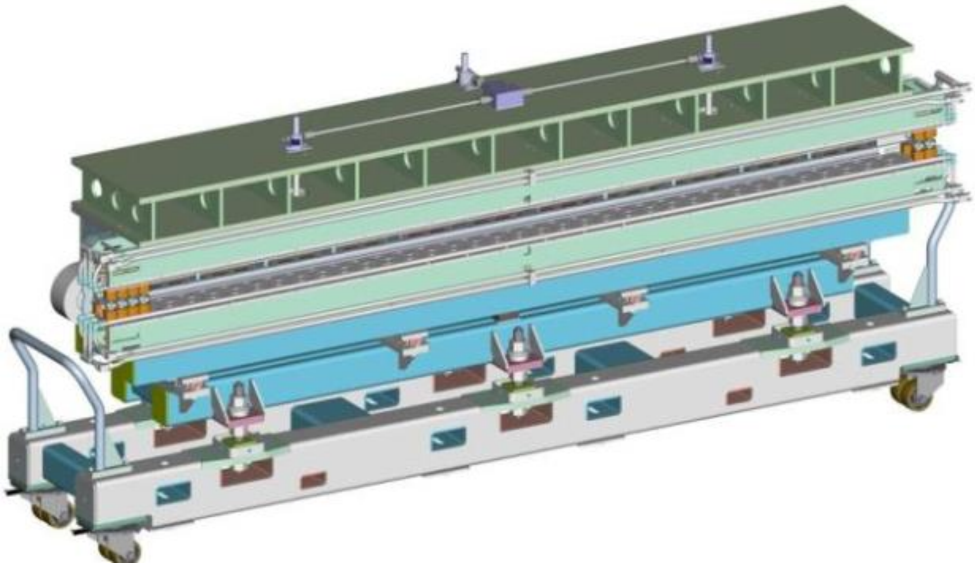

APS Undulators

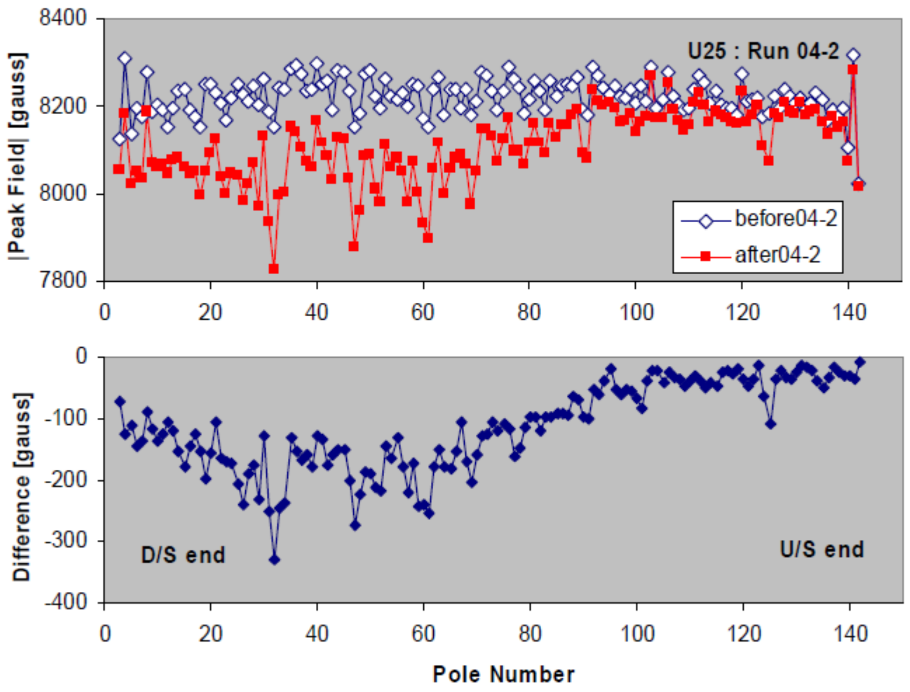

Fig. 1: Peak field comparison of the undulator before and after the May-August 2004 run. Bottom graph shows the difference before and after the run. Pole number is numbered from the downstream end. Open diamond: before user run, solid square: after user run.

LCLS (SLAC)

Proceedings of FEL2014, Basel, Switzerland MOP046

UNDULATOR RADIATION DAMAGE EXPERIENCE AT LCLS*

H.-D. Nuhn[#], R.C. Field, S. Mao, Y. Levashov, M. Santana, J.N. Welch, Z. Wolf
SLAC National Accelerator Laboratory, Menlo Park, CA 94025, U.S.A

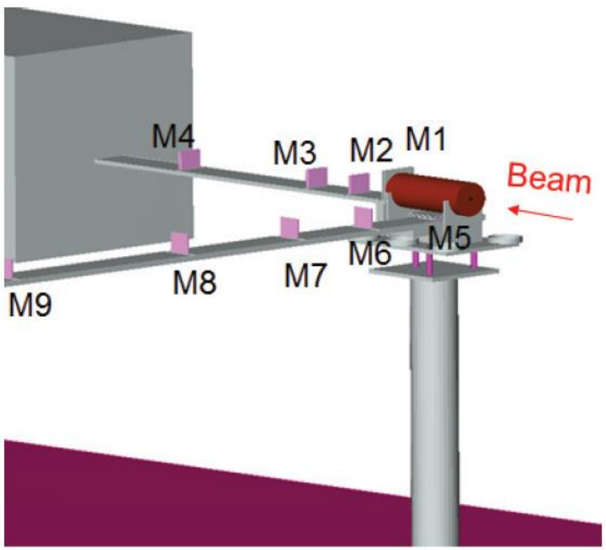

Figure 1: Layout of the SLAC End-Station A (ESA) undulator magnet block damage experiment. M1 to M9 indicate the placement of the individual magnet blocks relative to the copper cylinder. M5 is located underneath the copper cylinder.

LCLS has 33 magnet girders.

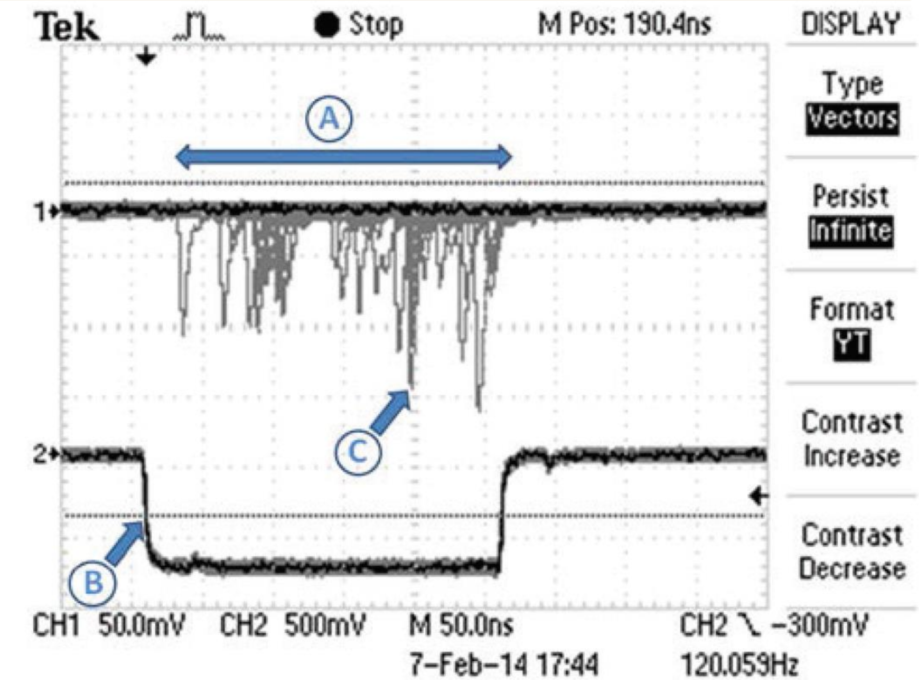

Figure 7: Lost particles from dark current pulses (A) and from the laser driven beam (C) observed at a position along the undulator by a beam loss detector (accumulated over about 500 beam pulses), showing the time spread loss events relative to the true beam time. The lower signal is the oscilloscope trigger from the accelerator timing system (B). The full width of the plot is 500 ns. The rf bucket separation is 0.3 ns.

LCLS

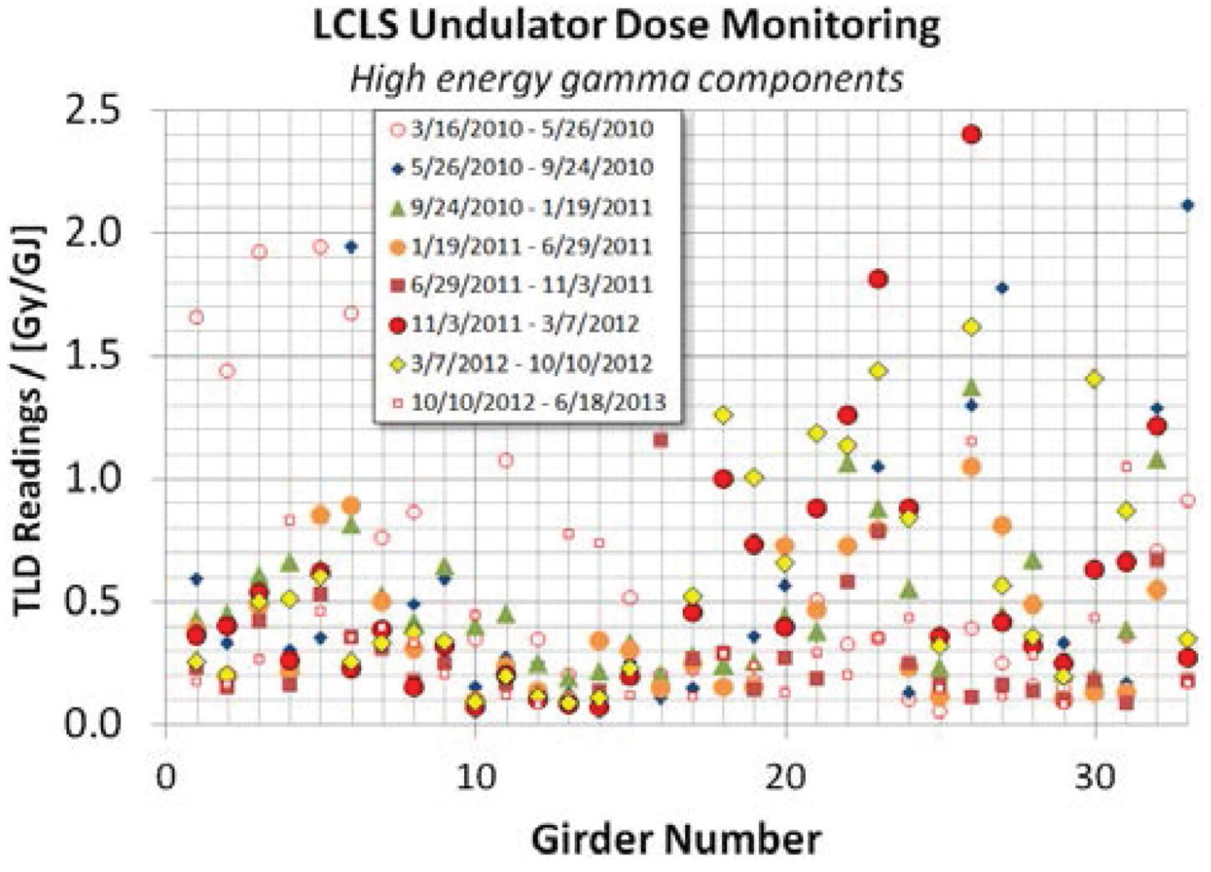

Figure 2: Radiation dose measurements by Pb-cased TLDs placed in front of each LCLS undulator segment. The readings are plotted against the beam energy passed through the undulator beam pipe during the same period.

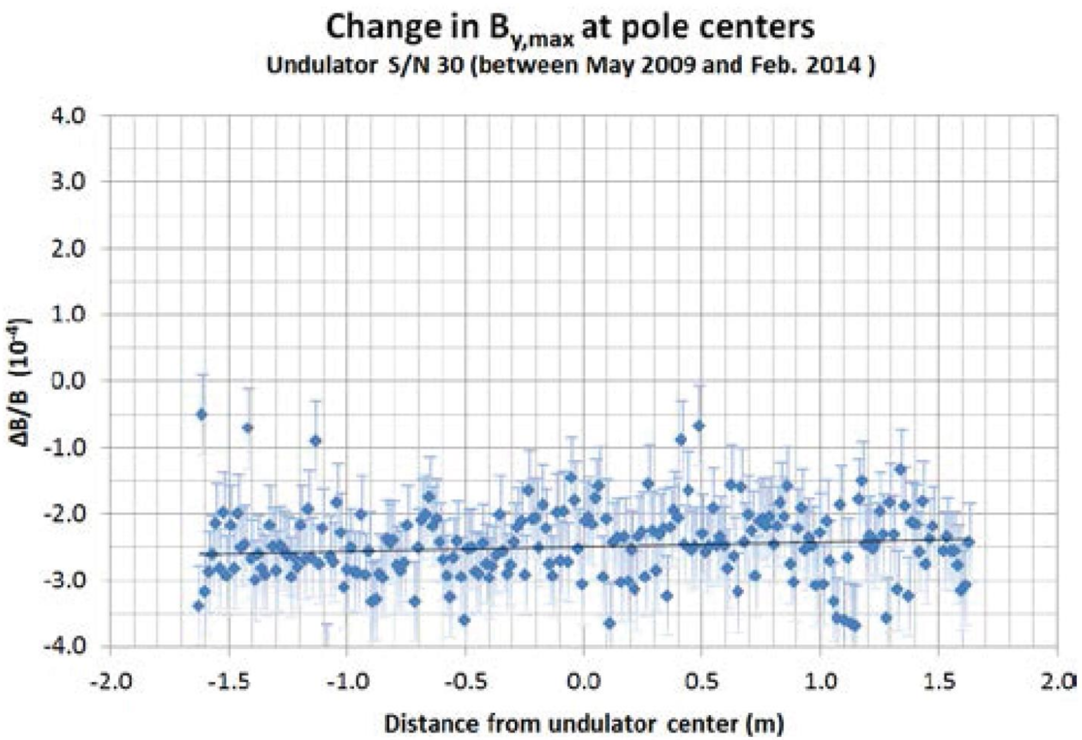

Figure 5: Magnetic field measurements shown in Figure 4 after correction by the CMM gap measurements shown in Figure 5. The remaining change in relative field amplitude is $-(2.5\pm0.5)\times10^{-4}$.

LCLS

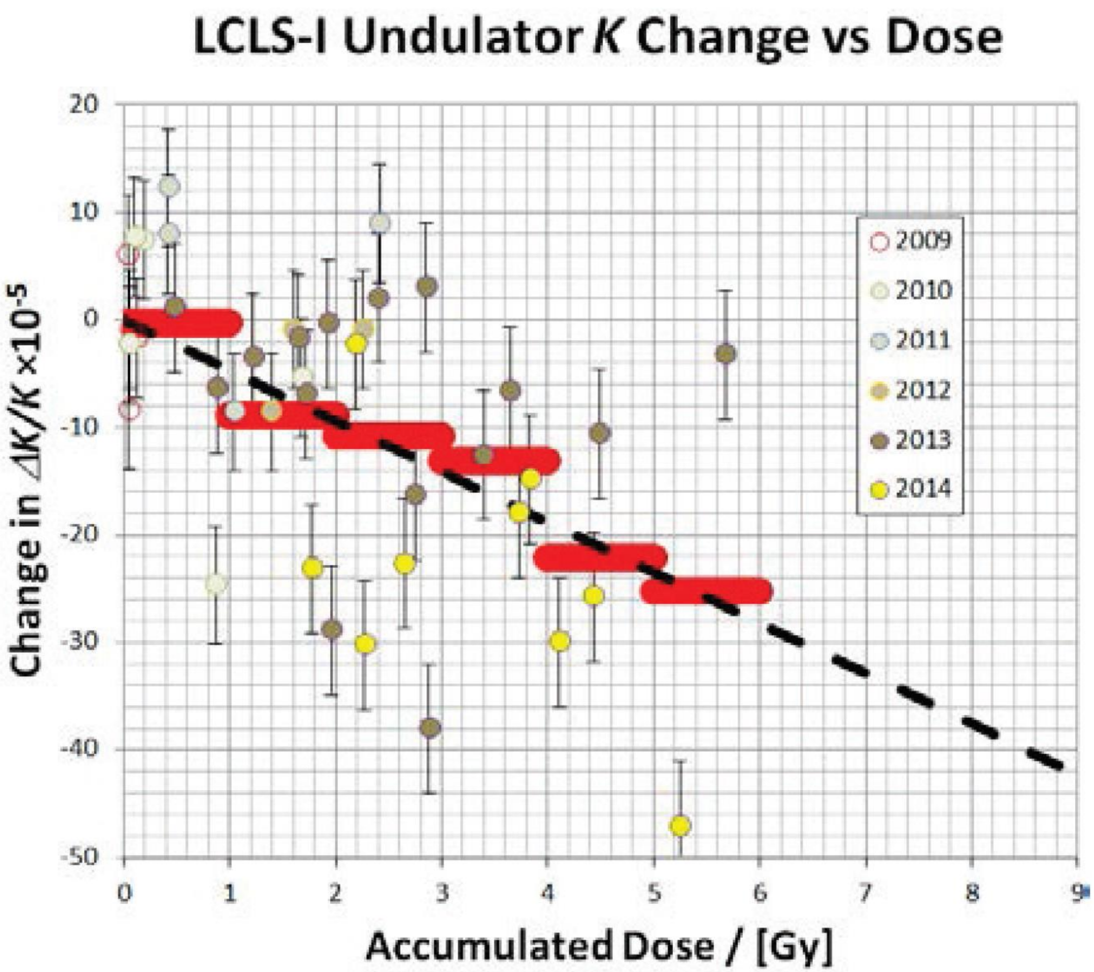

LCLS-I Undulator K Change vs Dose
Change in ΔK/K ×10-5
Accumulated Dose / [Gy]
20
10
0
-10
-20
-30
-40
-50
0
1
2
3
4
5
6
7
8
9
2009
2010
2011
2012
2013
2014

Power, HOM, and Radiation Conclusions

Many complicated designs, measurements, and operational techniques are needed in a high-power, high-current collider or light source.

Make a full plan for every lost watt that gets deposited.

Measure as many parameters and possible.

Many measurements relate to potential hardware damage to the accelerator.

Many measurements need to automated and computer monitored to make the accelerator operation safe and look at the past events.